Model-based Lifecycle Optimization of Well Locations and Production Settings in Petroleum Reservoirs

MODEL-BASED LIFECYCLE OPTIMIZATION OF WELL LOCATIONS AND PRODUCTION SETTINGS IN PETROLEUM RESERVOIRS

PROEFSCHRIFT

ter verkrijging van de graad van doctor
aan de Technische Universiteit Delft,
op gezag van de Rector Magnificus prof. dr. ir. J.T. Fokkema,
voorzitter van het College voor Promoties,
in het openbaar te verdedigen op

donderdag 17 april 2008 om 12:30 uur

door

Maarten Johan ZANDVLIET

werktuigkundig ingenieur
geboren te Washington, D.C., Verenigde Staten.

Dit proefschrift is goedgekeurd door de promotoren:

Prof. ir. O.H. Bosgra
Prof. dr. ir. J.D. Jansen

Samenstelling promotiecommisie:

Rector Magnificus,	voorzitter
Prof. ir. O.H. Bosgra,	Technische Universiteit Delft, promotor
Prof. dr. ir. J.D. Jansen,	Technische Universiteit Delft, promotor
Prof. dr. ir. P.M.J. Van den Hof,	Technische Universiteit Delft
Prof. dr. Y. Yortsos,	University of Southern California
Prof. dr. ing. B.A. Foss,	Norwegian Institute of Technology
Prof. dr. ir. A. Heemink,	Technische Universiteit Delft
Prof. dr. W.R. Rossen,	Technische Universiteit Delft
Prof. dr. P.L.J. Zitha,	Technische Universiteit Delft, reservelid

This dissertation has been completed in partial fulfillment of the requirements of the Dutch Institute of Systems and Control DISC for graduate study.

This research has been conducted in the framework of the "Integrated System Approach Petroleum Production" (ISAPP) programme. The knowledge center is a long-term co-operation of TNO, Shell and Delft University of Technology to increase hydrocarbon recovery through the application of innovative reservoir development and management technologies. Financial support has also been provided through the "Virtual Asset Learning and Understanding Environment" (VALUE) programme, which is sponsored by Shell and Senter/Novem.

ISBN: 978-90-9022987-4

Keywords: petroleum, reservoir engineering, systems and control, optimization

Printed in the Netherlands.

to Peet

Aknowledgements

Doing a PhD over the past four years has been fantastic thanks to the support of many people.

Paul, Okko and Jan-Dirk: thank you for your great supervision; I truly appreciate all your time and effort. Having three supervisors may not be the fastest way to publish, but it did inspire me to be thorough and approach a problem from different angles. I will miss our collaboration - most of all our lengthy research discussions in which one of us would often have a hard time convincing the rest about a certain point! You pointed me in the right directions at the right times, and I am very proud of our results. Thanks again for your guidance.

Special thanks to Gijs and Jorn for providing invaluable input into this thesis, and simply for being great colleagues and friends. Gijs and Martijn: it was a privilege to supervise your MSc theses, and as you can see your results have each resulted in a chapter of this book. At Shell I would like to thank Roald and Sippe for all the 'bakkies' during which you helped out with many a research difficulty, and Roald and Hans for helping out with MoReS and co-authoring several papers. In general I would like to thank the many present and former colleagues at DCSC and at Applied Earth Sciences (there are too many of you to mention) for providing a great place to work! John, Mathilde, Eric, Sarah and Stine: thanks for your constant interest and encouragement.

Jan, thanks for all the pleasant distractions. Finally, Peet: thanks for everything... "gewoon logisch blijven nadenken" is by far the best advice I've ever had!

Amsterdam, March 2008

Maarten Zandvliet

Contents

1 CHAPTER

Introduction

The coming years there is a need to increase production from petroleum reservoirs, and this thesis provides efficient tools to achieve this through model-based dynamic optimization of wells and their production settings. This chapter discusses some of the processes, problems and opportunities in the exploration and production industry, and provides the motivation for the research presented in this thesis.

1.1 Demand for hydrocarbons

According to the International Energy Outlook 2006, the coming decades there will be a significant growth in energy consumption as a result of robust economic growth - EIA (2006); see Figure 1.1.

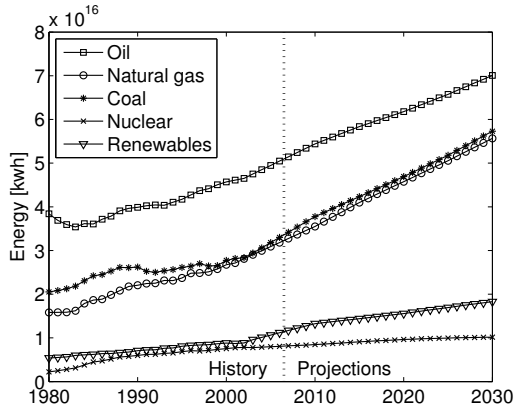

Figure 1.1: World marketed energy use by energy type, 1980-2030 (EIA (2006)).

While renewable energy sources become more economically competitive with fossil fuels (*i.e.* oil, natural gas, and coal), oil in particular will remain the dominant energy source until 2030. To meet the projected increase in world oil demand, total petroleum supply in 2030 will need to be around 40 million barrels per day higher than the 2003 level of 80 million barrels per day. The exploration and production (E&P) industry is struggling to keep up with this increasing demand, which has recently lead to a significant increase in crude oil prices - see Figure 1.2.

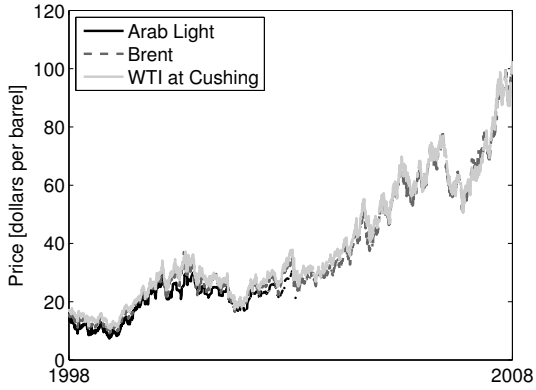

Figure 1.2: Prices of crude oil, February 1998 - March 2008.

In order to understand how the research presented in this thesis can contribute to increasing hydrocarbon production, the following sections discuss some of the processes, problems and opportunities in the E&P industry.

1.2 Exploration and production of oil and gas

1.2.1 Summary of E&P process

Origin of oil and gas

Oil and gas originate from the remains of prehistoric plants and animals deposited at the bottom of the oceans and swamps. Over millions of years, these layers gradually stacked up and the resulting pressure and heat converted them into oil and gas. Because oil and gas are less dense than water, they tend to migrate towards the surface and will only form an accumulation, or reservoir, if they are trapped by a layer of impermeable rock along the way. The subsurface is generally deformed over long periods of time, leading to folds, faults and fractures. Reservoirs therefore have spatially varying rock properties, and these property differences are referred to as heterogeneities.

Exploration phase

Finding oil and gas reservoirs is a major challenge, since they can be located at great depths (*e.g.* several kilometers) and in very inaccessible areas (*e.g.* the Arctic). By sending sound waves through the ground and measuring how long they take to bounce back off the different layers of rock, geoscientists create 3D maps of the subsurface (*i.e.* seismic imaging). If a certain area seems promising, exploration wells are drilled to verify whether oil or gas is indeed present. Core samples and logs from these wells can be combined with the previously mentioned seismic data to form models which can be used to roughly predict how field development decisions affect future production. A reservoir or field (*i.e.* a collection of reservoirs related to the same geological structure) will obviously only be developed if these predictions are promising enough.

Development phase

Developing a field essentially consists of drilling wells and connecting them to the surface facilities from which the produced oil and gas can be transported to refineries. The actual process of creating a well can be very complicated, and a well can cost between 1-100 million dollars. A well is created by drilling a hole and cementing a steel pipe (or casing) inside. Small holes (or perforations) are made in the part of the casing that passes through the reservoir to provide a path for the hydrocarbons to flow from the surrounding rock into the well. An example of a reservoir with several wells is depicted in Figure 1.3.

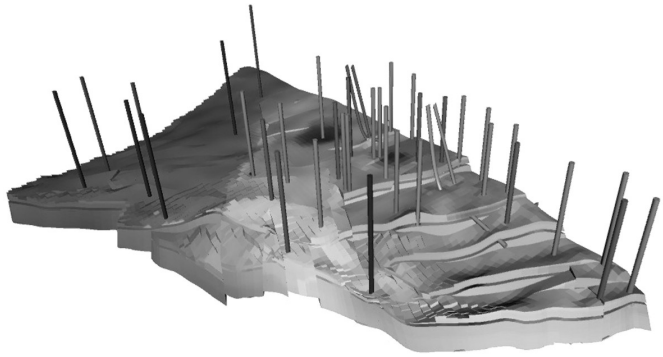

Figure 1.3: Reservoir with multiple wells. The shading indicates fluid saturations.

Production phase

The production lifecycle of a reservoir is usually in the order of tens of years, and can generally be divided into three stages. In the initial stage of production, the reservoir pressure is higher than the bottom-hole pressure inside the well. This natural pressure difference drives hydrocarbons toward the well, and this

process is referred to as primary recovery. During primary recovery only a small percentage of the initial hydrocarbons in place are usually produced. Referred to as the recovery factor, this is only around 10% for oil reservoirs. Because of production, however, the reservoir pressure declines and it may become necessary to inject fluids (*e.g.* water or gas) through injection wells to 'flood' the reservoir by driving the hydrocarbons to the production wells. This is referred to as secondary recovery, during which around 15-40% of the original oil in place is produced. Finally, tertiary recovery refers to techniques that alter the original properties of oil, for example using chemicals, CO_2 or steam.

Field development planning

When developing a field, the goal is often to maximize an economic criterion (*e.g.* oil and gas revenues minus field development costs). The choices that have to be made include the number, type, and location of wells, the type of surface facilities and the required infrastructure. These choices are referred to as inputs, and their effect can be measured through the produced volumetric flow rates of oil and gas and the pressures in wells, referred to as outputs. This is depicted as an open-loop process in Figure 1.4.

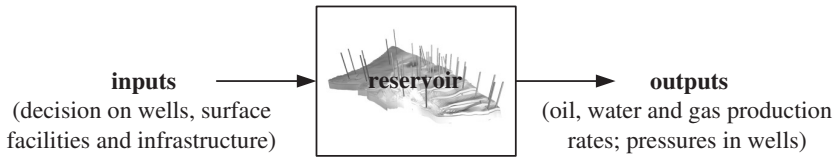

Figure 1.4: Field development planning. The decisions on wells, surface facilities and infrastructure determine hydrocarbon production.

Numerical reservoir simulation models, or reservoir models for short, often play an important role in field development planning. These models seek to describe the effect of decisions on hydrocarbon production (*i.e.* the 'reservoir' block in Figure 1.4), and are often based on physical conservation laws. The time-varying (dynamic) properties in reservoir models are generally the fluid pressures and saturations, and are referred to as states. The remaining fluid properties (*e.g.* viscosity or density, which can be functions of the state) and geological properties (*e.g.* permeability or porosity) are generally considered to be time-invariant (static), and are referred to as parameters[1]. Table 1.1 summarizes the terminology used throughout this thesis.

The governing equations for multi-phase flow through porous media are a set of mildly nonlinear parabolic (diffusion) equations, describing the rate of change of

[1] In the systems and control community a dynamical system with fixed parameters is formally called a *model*, while one with free parameters is called a *model structure*. Throughout this thesis, however, we only refer to *models* because it will be clear from the context whether the parameters are free or fixed.

Name	Description
inputs	decisions on wells, surface facilities, infrastructure
outputs	oil and gas production rates, pressures in wells
states	fluid pressures and saturations
parameters	fluid and geological properties

Table 1.1: Terminology.

pressures, coupled to a set of strongly nonlinear parabolic-hyperbolic (diffusion-convection) equations, describing the rate of change of fluid saturations - Ewing (1983), Jansen (2007); see also Chapter 2. The time constants of the pressure equation are typically in the order of hours to months, whereas the time constants of the saturation equation can be up to thousands of years. The fluid velocities are also usually much smaller than the propagation speeds of the pressure waves. Under some simplifying assumptions the equations may therefore be decoupled into a set of linear time-varying parabolic (diffusion) equations for pressures and a set of nonlinear hyperbolic (transport) equations for saturations.

As mentioned earlier, the geological properties within a reservoir can vary significantly over space. It is important to model the effect of these heterogeneities because they can lead to preferential flow paths outside of which significant quantities of oil can be bypassed and simply left behind. This is depicted in Figure 1.5, where water is injected through the injection well on the left in order to flood the reservoir by driving the oil to the production well on the right. The heterogeneities lead to an irregular-shaped oil-water front that, once it has reached the production well, will lead to a flow path through which most of the injected water will flow.

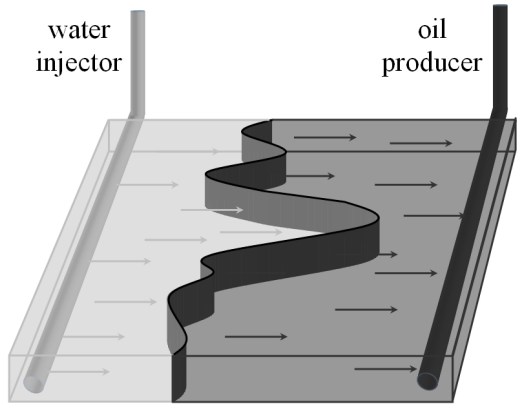

Figure 1.5: Process of water flooding using a horizontal injection and production well. The irregular-shaped oil-water front is a result of the reservoir heterogeneities (after Brouwer (2004) and van Essen et al. (2006a)).

Because reservoirs are generally heterogeneous, it is common in reservoir modeling to divide the reservoir into a finite number of grid blocks whose geological and fluid properties are assumed to be homogeneous. Unfortunately, adequately describing the heterogeneities throughout a reservoir requires a huge number of grid blocks, which in turn leads to a huge number of pressures and saturations (at least one pressure and saturation for each grid block). As a result, the number of parameters and states are generally in the order of $10^4 - 10^6$ and predicting the effect that field development decisions have on hydrocarbon production can take hours to simulate.

To make matters worse, the parameters and initial states can only be estimated to a very limited extent (*e.g.* through core samples and seismic data). In other words, not only are reservoir simulations computationally demanding, their predictions of oil and gas production are also very uncertain. For example, if the reservoir heterogeneities in Figure 1.5 are different from those used in the reservoir model, water may reach the producer much earlier than anticipated by reservoir simulations. When this happens, it can cease to be economically viable to keep producing from that particular well and it will consequently be shut-in. Had this water breakthrough been predicted accurately, the wells would have been drilled in a different location or else operated in a different fashion.

Reservoir management

Field data is therefore often gathered throughout the production lifecycle of a reservoir (*e.g.* in the form of pressure, temperature and production data at surface or in the wells) in a process called reservoir surveillance. These measurements can be assimilated in reservoir models in the hope of improving their predictive power, and thereby the robustness of the development decisions they serve. Unfortunately, this so-called history matching is generally very time-consuming. Consequently, measured data is often only incorporated into reservoir models when the underlying field is being considered for re-development: an exercise undertaken roughly every 5 years, whereby a series of new wells is drilled in order to increase production. This iterative closed-loop approach of reservoir surveillance and field (re)development is referred to as reservoir management.

Production operations

Where the decisions made in the reservoir management domain generally are taken every few years and concern an entire field, those taken in the so-called production operations domain involve a much shorter time and spatial scale. This division of the E&P process according to different time and spatial domains is depicted in Figure 1.6. Here, each domain provides objectives and constraints to the domain below it in the sequence, while it provides historic data and forecasts to the domain above it.

In production operations, available production data is used to manage day-to-day operations, for example to meet daily production targets. The to-be-taken decisions involve the individual well production settings, but also so-called workovers to repair an existing production well for the purpose of enhancing its production. These decisions are generally taken without the use of the previously discussed reservoir models. Instead, models describing the multi-phase flow through the wells and surface facilities are used, with the reservoir sometimes simply modeled as a tank.

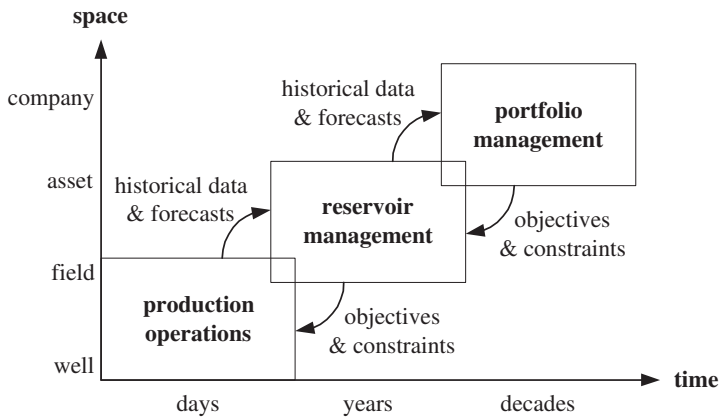

Figure 1.6: E&P process domains (after Jansen et al. (2005)).

1.2.2 Problems in the E&P industry

Technology

It is widely believed that the 'easy' producible reservoirs have been found, and to a large extent have been produced - Deffeyes (2001), Heinberg (2003), Simmons (2005), Voss and Patel (2007). This makes it harder for oil companies to meet the demand without undertaking more complicated and expensive projects. Fortunately, higher oil and gas prices in recent years have allowed the industry to invest heavily in advanced technology needed to develop resources from places before thought either impossible or not economically viable (*e.g.* the deepwater Gulf of Mexico, or the sub-Arctic conditions of Sakhalin). This is particularly true for commercial oil companies, who are finding it increasingly difficult to compete with national ones in projects where technology does not play a crucial role. In other words, commercial oil companies view technology not only as an enabler to pull off large and complicated projects, but increasingly as their main competitive advantage.

People

Reservoir management is a complex process, due to the large number of decisions that have to be made, the long simulation times of reservoir models required to predict the effect of these decisions, and the associated uncertainty. It is virtually impossible for a reservoir management team to determine a field development plan that maximizes an economic criterion or that is robust against model uncertainties in any meaningful sense within a acceptable time-frame. As a result, many decisions are made in a fragmented way for various pieces of a field.

To make matters worse, 40% of the E&P workforce is expected to retire within the coming decade - Parry et al. (2006). Referred to as 'the big crew change', it is the result of the close historical correlation between inflow of new personnel into the industry and oil price: very high immediately following the oil crises of the 1970s and 1980s, but quickly waning as prices dropped. To make matters worse, many oil and service companies economized on in-house training, research and development during the recent fall in prices in 1998-1999. Combined with the previously mentioned complexity in reservoir management, this loss of technological know-how clearly presents a huge challenge for an industry seeking to undertake larger and more challenging projects than ever before.

Processes

Besides being time-consuming, the essential processes in reservoir management (*i.e.* history matching and field development planning) and production operations suffer from a number of additional drawbacks. As discussed in Jansen et al. (2005), traditional history matching

- is usually only performed when a field is being considered for re-development, which is typically several years after the previous drilling campaign.
- The techniques are often ad-hoc and involve manual adjustment of model parameters.
- Uncertainties in the states, model parameters and measured data are usually not explicitly taken into account.
- The resulting history matched models often violate essential geological constraints.
- The updated model may show a perfect history match and yet have no predictive capacity because it has been over-fitted by adjusting a large number of unknown parameters using a much smaller number of measurements.

On the other hand, field development planning

- involves both discrete decisions variables (*e.g.* number of wells) as continuous ones (*e.g.* production settings). Even with significantly more time and resources, it is therefore still very difficult to determine a plan that is optimal in any meaningful sense.

- A field development plan is often based on a 'nominal' reservoir model, and its robustness is usually evaluated by applying it to a very limited number of other reservoir models (*e.g.* two: a 'high' and 'low' case) that have different parameter values than the nominal one. This ad-hoc way of taking uncertainty into account is again mainly driven by limited time and resources, and clearly provides no guarantees that future hydrocarbon production will not be less than predicted.

- The combination of uncertainty with significant investment make for a high incentive to earn back that investment as soon as possible, even though decisions based on short-term goals can have a detrimental effect on long-term ones, such as the recovery factor.

- Moreover, the field development planning and production operation tasks are often performed by separate teams within a single oil company. As a result, while fields are generally developed on a campaign basis according to long-term goals (*e.g.* the recovery factor), they are often operated on a daily basis according to short-term goals (*e.g.* daily production targets).

- There is a fundamental difference in the type of models used in the E&P industry to predict hydrocarbon production. Reservoir management teams generally use models describing the flow throughout the reservoir for long-term predictions, while production operations teams generally use models describing the flow through the wells and surface facilities for short-term predictions. This can lead to inconsistent decisions being made for developing the same field.

Summary

The easy oil has been found, new projects are becoming more challenging and the required expertise to undertake them is becoming more scarce. Furthermore, there are many drawbacks in the current reservoir management and production operation processes.

1.3 Opportunities to increase the recovery factor

Considering that the current recovery factor of petroleum reservoirs is relatively low (15-40%), there is enormous potential to increase production by increasing the recovery factor, and there are several opportunities to achieve this.

Technology

As mentioned earlier, higher oil and gas prices in recent years have allowed the industry to invest heavily in technology. Among the resulting developments are the following advances in hardware.

- Wells that are not only purely vertical, but have deviated or even horizontal sections, thereby increasing their contact area with the reservoir.
- Valves to remotely close off individual sections of a well, for example because they have experienced water breakthrough, referred to as Interval Control Valves (ICV's).
- Sensors to permanently measure pressure, temperature, flow rate or flow composition down-hole in the well. These sensors can gather a wealth of information on the processes in and around the wells in which they are installed.
- Seismic surveys that are repeated after a significant period of time (*e.g.* several years), also called time-lapse or 4D seismics, allowing for areal monitoring of the fluid flow throughout the reservoir.

Wells equipped with ICV's or sensors are often referred to as smart, intelligent or instrumented wells - see Figure 1.7.

The goal of these improvements in hardware is of course to increase the recovery factor, and this can be achieved along three different paths.

1. Making better field development and production operation decisions by using the extra freedom in well types and ICV's to better control the subsurface flow in petroleum reservoirs. For example, if the heterogeneities in Figure 1.5 are known and the wells are equipped with ICV's, their settings can be varied over time to reduce the bypassing of oil.
2. Reducing the effect of uncertainty, for example by installing ICV's to create the possibility to close off sections where there is earlier-than-foreseen water breakthrough.
3. Reducing the uncertainty itself, for example by installing sensors and incorporating the resulting measurements in reservoir models to make more accurate predictions, and ultimately a better and more robust development plan.

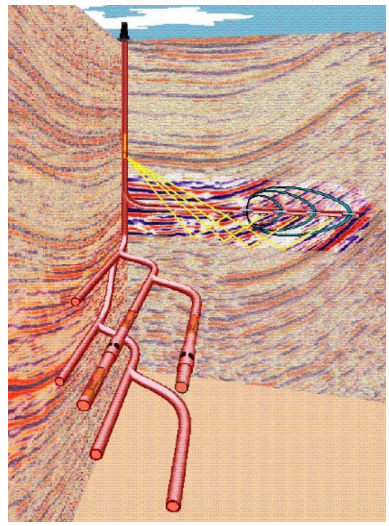

Figure 1.7: Artist impression of a futuristic smart well with multiple horizontal sections, Interval Control Valves and sensors (after Kapteijn and Muessig (2003)).

Although there are other ways to increase oil and gas production (*e.g.* by developing unconventional resources such as heavy oil or gas hydrates) and other ways to increase the recovery factor (*e.g.* by tertiary recovery techniques) this thesis focuses exclusively on increasing the recovery factor by the previously mentioned opportunities.

People

Attracting more personnel to work in the E&P industry and improving their technical expertise would arguably also lead to better decisions and thereby a higher recovery factor, however this is also not considered in this thesis.

Processes

Despite the previously mentioned advances in technology, actually making better decisions and reducing uncertainty is far from trivial because of the many drawbacks in reservoir management and production operation processes. Note that opportunities 1. and 2. involve optimization of inputs, and 3. the estimation of states and parameters. Optimization and estimation are *the* main topics in systems and control, and applying systems and control techniques is therefore a logical step to making better use of hardware to increase the recovery factor. The first step in this direction is to consider reservoir management and production operations as a model-based closed-loop controlled process, as depicted in Figure 1.8. Here, the open-loop relation from inputs to outputs from Figure 1.4 is closed by an estimation (*i.e.* history matching) and optimization (*i.e.* field development and

production operations) loop. The optimization process is model-based, because reservoir models are used to assess the effect of field development and production operation decisions on future hydrocarbon production.

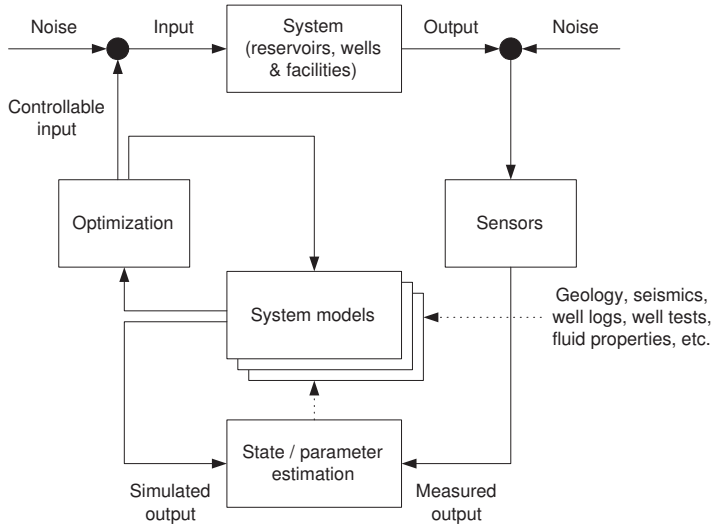

Figure 1.8: Reservoir management represented as a model-based closed-loop controlled process (after Jansen et al. (2005)).

Sometimes also referred to as real-time reservoir management, self-learning reservoir management, e-fields or smart fields, the concept of closed-loop reservoir management and production operations is not new - see Chierici (1992) and Nyhavn et al. (2000) with further references in Jansen et al. (2005). Indeed, Chierici (1992) stresses that a "continuous feedback process" is required throughout the lifecycle of a field in order to maximize its recovery factor, as opposed to the commonly applied campaign-based approach. In practice, however, this continuous feedback process is not feasible if its components (*i.e.* history matching, field development planning and production operations) are not made more efficient. After all, one of the main reasons why they are not continuously applied in the first place is that they are very time-consuming.

In other words, there is significant scope to increase the recovery factor of petroleum reservoirs by tailoring tools from the systems and control community to *efficiently* perform closed-loop reservoir management and production operations, in the sense that they lead to good decisions while requiring limited time from the user.

1.4 Literature overview

1.4.1 Introduction

There are many promising optimization and estimation techniques available in the systems and control literature, but their applicability is highly dependent on the type of model under consideration. It is important to note that reservoir models are typically

- physics-based (white-box),
- large-scale, (*e.g.* $10^4 - 10^6$ states and $10^4 - 10^6$ parameters),
- MIMO (*e.g.* $10^1 - 10^2$ inputs and $10^1 - 10^2$ outputs),
- nonlinear,
- uncertain, and
- take hours to simulate.

Not surprisingly, many systems and control techniques cannot directly be applied to reservoir models because of these properties. This section describes some of the tools that are applicable, which of these have already been applied in the literature, and some of the related open problems.

1.4.2 Model-based optimization

Optimal control of production settings

Given a correct reservoir model and a certain configuration of wells[2], finding the time-varying production settings over the lifecycle of a reservoir that maximize the recovery factor can be posed as an optimal control problem. With the exception of certain specific situations, it is generally very difficult to find analytical solutions to such problems. For example, optimal control problems involving quadratic performance measures of the state and input trajectories of a linear system (*i.e.* so-called LQ problems) do have an analytical solution. Moreover, the solution can be implemented by a linear state-feedback controller, which makes it particularly suitable for online implementation as it allows for disturbance rejection and robustness to model uncertainties - Athans (1971). Unfortunately, a reservoir's recovery factor cannot be written as a quadratic performance measure (see Chapter 3) and a reservoir's dynamics are generally described by equations that are linear in the control, but nonlinear in the state (see Chapter 2). Although it is theoretically possible to transform such a nonlinear system into a linear one

[2]Determining the number, trajectory and location of wells that maximize the recovery factor - clearly also very important decision factors in a field development plan - involves integer optimization, and is discussed later in this section.

by means of a nonlinear feedback control law (see Isidori (1983)), this so-called feedback linearization requires higher order partial derivatives of the nonlinear equations with respect to the state which, for reservoir models, are too tedious to derive.

There are, however, several methods to compute solutions to optimal control problems involving nonlinear systems and non-quadratic performance measures, such as the gradient, simultaneous, shooting or dynamic programming method - Bryson and Ho (1975), Srinivasan et al. (2002b). Of these, only the gradient method is applicable due to the extremely large number of reservoir model states. The main idea is to iteratively improve upon an initial guess of the optimal control using a gradient-based method until a local optimal solution is reached. The difficulty lies in effectively obtaining the required gradients. Conceptually, the easiest approach is to approximate each individual component of the gradient by finite differences, but this is computationally too demanding since each approximation requires an evaluation of the performance measure (*e.g.* the recovery factor) which in turn requires a reservoir simulation. The only viable approach is therefore to compute the gradient using a so-called adjoint model - see Kirk (1970), Stengel (1986). Adjoint models are discussed in Chapter 3.

There have been numerous applications of adjoint-based optimization of production settings in the petroleum engineering literature. Some of the earliest ones are by Ramirez and co-workers, summarized in Ramirez (1987), who considered tertiary recovery techniques. This was quickly followed by Asheim (1987), Asheim (1988), Virnovsky (1991), Zakirov et al. (1996), and Sudaryanto and Yortsos (2000) who considered secondary recovery techniques. Although the type of production settings differ (*e.g.* from concentrations of injected chemicals to water injection rates), they are all applications of the same technique: gradient-based optimization with gradients computed using an adjoint model. In this respect it is interesting that the method only received significant attention after Brouwer (2004) and Brouwer and Jansen (2004) demonstrated the possibility to significantly increase the recovery factor using smart wells. There have been numerous applications since, several of which involve the particularly difficult problem of including state constraints - see Sarma et al. (2006a), de Montleau et al. (2006), and Kraaijevanger et al. (2007). Since state constraints (*e.g.* bounds on the reservoir pressure or the amount of produced water) are particularly important in production operations, state constraint handling is a topic of ongoing research. Another relevant open issue is the shape of optimal solutions: Sudaryanto and Yortsos (2000) and Sudaryanto and Yortsos (2001) state that these will sometimes be of the bang-bang (*i.e.* on-off) type, having the obvious advantage over smooth solutions in that they can be implemented with simple on-off valves. Interestingly, this statement is supported by some, but not all, applications in Brouwer (2004) and Brouwer and Jansen (2004). In other words, it is unclear why and under what conditions optimal production setting problems can be expected to have bang-bang optimal solutions. This is important, because variable-setting valves are much more expensive than simple on-off ones.

Integer optimization of wells

During the modeling process, reservoirs are essentially divided into a finite number of 'grid blocks', the properties of which are assumed to be homogeneous. Wells are then simply source or sink terms (depending on whether they produce or inject fluids) into or from certain of these grid blocks. Optimization of the well trajectory and its location is thereby an integer problem - Kosmidis et al. (2005), Bangerth et al. (2006). For example, if a single well is to be placed in 1 out of N grid blocks, the problem clearly involves N discrete possible choices. Determining the number of wells is also clearly an integer problem, and the combination with the optimization of production settings leads to a mixed-integer nonlinear problem, or MINLP.

MINLP's also frequently arise in the chemical process industry, and there are several methods to deal with them - see Kallrath (2000). Most of these methods, however, require far too many evaluations of the performance measure to be applicable to reservoir models. In practice, well optimization is therefore mostly done manually, although there are several publications on automatic well optimization. These applications can be broadly classified into local, or global optimization methods. Local optimization methods try to iteratively improve upon an initial well configuration, much as in the previous optimization of production settings, until a local optimal solution is reached. The main challenge in this application, again as in the optimization of production settings, is to effectively find improving directions[3] in which to alter the well configuration. Global methods, on the other hand, will sometimes tolerate lower performance measures in the hope of finding the global, as opposed to local, optimal solution.

There are many applications of global methods to the well optimization problem: Beckner and Song (1995) applied simulated annealing, Centilmen et al. (1999) neural networks, Bittencourt and Horne (1997), Montes et al. (2001) and Aitokhuehi et al. (2004) genetic algorithms, and Yeten (2003) a combination of the latter two. Although these applications have the virtue of simplicity (a global optimization algorithm of choice is coupled with a reservoir simulator to evaluate the performance measure), they generally require many reservoir simulations to converge to an adequate solution.

Bangerth et al. (2006) compares two local methods for optimizing the location of vertical wells in a 2D reservoir model. The first one is the Finite Difference Gradient (FDG) method, which as the name suggests tries to find improving directions by perturbing each well location by one grid block in each direction. This has the obvious drawback of requiring $2m + 1$ reservoir simulations to compute an improving direction of m to-be-placed wells. The second method is the simultaneous perturbation stochastic approximation (SPSA) method of Spall (1992), which basically chooses a random direction in which to alter the wells and, if this does not yield an improvement in the performance measure, assumes that the opposite

[3]Being an integer problem, the gradient is of course not defined.

direction will. The obvious advantage is that an improving direction is almost always found in at most 2 reservoir simulations, with the disadvantage that this direction is generally far from the 'steepest' one. In other words, an efficient method to find (almost) steepest improving directions using a limited number of reservoir simulations is currently lacking.

Robust control

It is possible to estimate each individual uncertain reservoir model parameter (*e.g.* the permeability in a specific grid block) within a certain continuous range of values. For example in the case of one parameter, say permeability in a certain grid block, this could be the interval $[1, 1000]$ mDarcy. This naturally leads to the possibility for robust optimization, where the goal is to optimize a so-called robust performance measure that represents the performance over the entire uncertainty range (*e.g.* the worst case, or lowest recovery factor). In order to implement robust optimization methods, however, we have to somehow propagate the probability distribution of the uncertain parameters to the states in order to ultimately determine what the effect will be on the performance.

In the systems and control literature, robust control is often associated with designing a feedback controller for an uncertain linear system such that the resulting closed-loop performance is robust against (or acceptable for) all possible uncertainties within a certain class. As with LQ problems, certain robust control problems also have an analytic solution (*e.g.* so-called $\mathcal{H}_\infty$ control, see Zhou et al. (1996)). Moreover, for these problems it is possible to analytically determine the worst-case effect of the uncertainty on the performance measure.

For large-scale nonlinear systems, however, determining the effect of uncertainty on the performance measure is often only possible by sampling the uncertainty space. This is a common approach in the optimization of batch processes in the chemical process industry - see Terwiesch et al. (1994), Ruppen et al. (1995) Terwiesch et al. (1998) and Srinivasan et al. (2002a). In field development planning a similar approach is often adopted, where the uncertain parameters are lumped into a single vector $\boldsymbol{\theta}$, which is subsequently assumed to take on only a limited number of values - Narayanan et al. (2003). Sometimes as few as three cases are considered and given labels 'low', 'medium' and 'high' (meaning $\boldsymbol{\theta} \in \{\boldsymbol{\theta}_{\mathrm{low}}, \boldsymbol{\theta}_{\mathrm{medium}}, \boldsymbol{\theta}_{\mathrm{high}}\}$). The variation in predictions of the resulting three reservoir models is then assumed to be representable for the entire continuous uncertainty range. The expected value is an example of a robust performance measure that is sometimes used in field development planning, although there are many others - see Samsatli et al. (1998) for an overview. Note that in this respect the expected value is mostly used for analyzing the robustness of a particular field development plan against model uncertainty, and not maximized using an optimization procedure (*e.g.* as with the previously mentioned applications to batch processes in the chemical process industry). However, there are a few applications of robust

optimization in the petroleum engineering literature.

Yeten et al. (2004) maximized a robust performance measure (5 realizations of the subsurface heterogeneity and risk of ICV failure) by varying the production settings, and subsequently decided on wether or not to deploy these ICV's using a decision-tree analysis. Guyaguler and Horne (2004) maximized a robust performance measure (23 realizations of the subsurface heterogeneity) by varying the well locations using a hybrid genetic algorithm. Aitokhuehi et al. (2004) maximized a robust performance measure (2 realizations of the subsurface heterogeneity) by varying the well type, location and trajectory using a genetic algorithm. In these applications, the robustness of the outcome is never validated against a different set of possible reservoir models. In this sense it must still be demonstrated that robust optimization can reduce the effect of a continuous range of uncertainties, as opposed to the representation of uncertainty by a limited number of models. Also, it is unclear how to generate a minimal set of models that in some sense is representative of the entire uncertainty range.

1.4.3 Model reduction

Reservoir engineers prefer to work with the physically interpretable states of current reservoir models (*e.g.* pressures and saturations). Since model reduction often involves transforming original states into physically non-interpretable ones (*e.g.* through projection), the main motivation for applying model reduction is to reduce the computation time of the corresponding simulations. There are several nonlinear model reduction techniques, but very few of them are suited for large-scale applications - Antoulas (2005). Moreover, the techniques that are applicable often destroy any sparsity that the original model structure may have, and therefore do not lead to a reduction in computation time - van den Berg (2005).

There are a few applications of model reduction in the petroleum engineering literature. Markovinovic et al. (2002), Heijn et al. (2004) and later Gildin et al. (2006) successfully applied several standard model reduction techniques (*e.g.* modal decomposition and balanced truncation) to a reservoir model that, under certain simplifying conditions, has linear dynamics. They also applied proper orthogonal decomposition (POD) to a nonlinear reservoir model, and this was further exploited in Van Doren et al. (2006) to reduce the computation time required to find optimal production settings by 35%. The fact that these early attempts at model reduction were successful indicates that reservoir models are controllable and / or observable to a very limited extent, and that the relevant reservoir dynamics are therefore less complex than they seem. Controllability and observability of reservoir models is, however, still largely an unexplored issue.

1.4.4 State estimation and parameter identification

Before discussing state estimation and parameter identification techniques, it is important to note that

- the saturation dynamics in reservoir models are governed by strongly nonlinear equations,
- the saturation dynamics in reservoir models can have time constants of up to thousands of years, and
- depleting a reservoir is essentially a single-batch process since it cannot be repeated.

Inferring the values of states and parameters based on measured data thereby becomes a combined state - parameter estimation problem. Unfortunately, most techniques in the systems and control literature focus on either one or the other - Evensen (2007).

Parameter identification

In the systems and control literature, building mathematical models based on measured data is generally referred to as system identification, and the theory for linear time-invariant systems is very mature - see Ljung (1999). The resulting models are called black-box if they rely purely on the measured data and the identified parameters have no physical interpretation. However, if the resulting models also rely on physical considerations in the system and the parameters do have a physical interpretation, they are called gray-box. The latter approach is commonly adopted in petroleum engineering and is generally called history matching, for obvious reasons. Unfortunately, the theory for system identification of large-scale nonlinear systems is much less mature than for linear time-invariant ones.

In practice, the problem of estimating the physical parameters in reservoir models based on measured data is often approached by defining a cost function (typically the weighted squared difference between predicted and measured data), and minimizing it over all possible parameter values. The cost function is then minimized using a gradient-based optimization procedure where, as in the optimization of production settings, the gradients are computed using the adjoint method from optimal control theory - see Jacquard and Jain (1965), Carter et al. (1974), Chavent (1975), Reynolds et al. (1996), Li et al. (2003) and Gao and Reynolds (2006). Another approach which has recently received significant attention is the so-called Ensemble Kalman Filter. However, since it is based on the Kalman Filter used for state estimation, it is discussed in the following subsection.

Given the number of to-be-estimated parameters in reservoir models, it is not surprising that a major difficulty in this particular application is that it does not have

a unique solution, meaning there are many combinations of parameter values that yield the same minimum value of the cost function. In other words, reservoir model parameters are not uniquely identifiable. Unfortunately, two different combinations of model parameters that give the same minimum value of the cost function may lead to completely different predictions - Tavassoli et al. (2004).

Many authors have therefore attempted to regularize the problem (*i.e.* render it 'less' ill-posed). One approach is to redefine the cost function by including the squared difference between initial and final estimated parameter values. By weighting the data and prior mismatch terms, the resulting problem can, under certain conditions, be interpreted as finding the maximum a posteriori estimate - Tarantola (2005). This is often referred to as the Bayesian estimation approach to history matching - see Gavalas et al. (1976), Zhang and Reynolds (2002), Li et al. (2003) and Zhang et al. (2005). The so-called Representer Method, originally developed by Bennett for oceanographic applications and described in Bennett (2002), is essentially a Gauss-Newton implementation to minimize the previously mentioned cost function. It has been used to estimate the permeability in reservoir models in Rommelse et al. (2006).

Another regularization method is to re-parameterize the high number of physical model parameters by a much smaller number of non-physical ones. Some of the re-parameterization techniques applied in history matching to achieve this include zonation (Jacquard and Jain (1965), Jahns (1966)), adapted versions thereof (Grimstad et al. (2003), Berre et al. (2007)), grad zones (Bissell (1994), Bissell et al. (1994), Brun et al. (2004)), spectral decomposition and subspace methods (Shah et al. (1978), Reynolds et al. (1996), Abacioglu et al. (2001)), kernel principle component analysis (Sarma et al. (2007)) and the discrete cosine transform (Jafarpour and McLaughlin (2007a), Jafarpour and McLaughlin (2007b)). Despite all of these applications, it is not clear how many parameters can be uniquely identified for any particular reservoir model.

State estimation

The most common state estimation technique for linear systems is by far the Kalman Filter. Under the condition that the system is linear and that the only source of model uncertainty is Gaussian noise on the states and measurements, the Kalman Filter provides the linear estimate of the state minimizing the mean square estimation error - see Kalman (1960), Anderson and Moore (1979). The reason for its wide-spread use is its optimality at low computational cost: the optimal estimate and corresponding error covariance is computed recursively using simple matrix multiplications.

There are several state estimation methods for nonlinear systems, such as the Extended Kalman Filter (EKF), the Unscented Kalman Filter (UKF), particle filters, the Moving Horizon Estimator (MHE) and the Ensemble Kalman Filter (EnKF) -

see Bos (2006) for an overview. The EKF uses linearizations of the original nonlinear model equations to recursively compute an estimate and corresponding error covariance, but it does not perform well when the nonlinearities are very large as in reservoir models. The UKF is more capable of dealing with nonlinearities, but requires two simulations per state element to compute an estimate and corresponding error covariance. Similarly particle filters, which try to compute the entire probability density function of the state using a Monte Carlo approach, also require too many simulations to be applicable to reservoir applications. The MHE is essentially a least-squares approach to state estimation as has been discussed in the previous section on parameter identification, and is therefore not reconsidered here. The EnKF, originally developed by Evensen for oceanographic applications and described in detail in Evensen (2007), uses a Monte-Carlo approach to compute the error covariance through an ensemble of prior model estimates. As with the least-squares approach, it has been successfully applied to various large-scale problems.

The EnKF has been applied to history matching of reservoir models, among others in Naevdal et al. (2005), Rommelse et al. (2006) and Reynolds et al. (2006). In these applications the state vector is extended with the to-be-identified parameters, yielding surprisingly good results with as few as 50 reservoir models in the Monte-Carlo approach. As with model reduction, this could possibly be explained by the limited controllability and observability of reservoir models.

1.4.5 Closed-loop control

Many processes are controlled by sequentially applying an estimation and optimization technique, where the former computes an improved estimate of the system's state and parameters every time measurements become available, and the latter computes a new optimal control based on this improved estimate. Usually called closed-loop control in the systems and control literature, it is also known as Model Predictive Control (MPC) in the chemical process industry. In many MPC applications the performance measure is defined in terms of a reference or set-point[4] (*e.g.* a desired temperature, or end-product concentration). Two different types of MPC are generally distinguished, depending on the time interval over which the performance measure is defined. If the performance measure is defined over a fixed time interval (*e.g.* 1 hour in the future) one generally refers to moving or receding horizon MPC, as opposed to shrinking horizon when it is defined up to a fixed terminal time (*e.g.* 10:00 am today). MPC is widely applied in the chemical process industry because of its ability to handle constraints - Mayne et al. (2000). Indeed, in the case of a linear model, a quadratic performance measure and linear inequality constraints on the inputs and states, the optimization subproblem can be written as quadratic program for which the global optimal solution can be efficiently found - Garcia et al. (1989), Maciejowski (2002). Not surprisingly, this no longer holds for problems involving nonlinear models and

[4]When the reference is also a degree of freedom, the term Dynamic Optimization is sometimes used instead of MPC.

non-quadratic performance measures (see also the previous discussion on optimal control of production settings) and for these problems it is particularly difficult to analyze the closed-loop performance - van Hessem (2004).

Due to the nonlinearity and large number of equations governing flow through porous media, closed-loop control of reservoirs as depicted in Figure 1.8 is often simply the combination of an estimation and optimization technique of choice, and the resulting closed-loop performance is usually evaluated by numerical simulation. Nevertheless, the results of these simulations are sometimes surprisingly good. Brouwer et al. (2004), Jansen et al. (2005), Naevdal et al. (2006) and Sarma et al. (2006b) consider the combination of the EnKF with adjoint-based optimization of the production settings in a shrinking horizon framework with large uncertainty in the reservoir permeability. These applications are very successful in that the results are often marginally worse than those obtained without model uncertainty. Apparently, the models resulting from the EnKF's state and parameter estimates have sufficient predictive power for the adjoint-based optimization procedure. Again, this could possibly be explained by the limited controllability and observability of reservoir models.

Several other shrinking horizon applications are reported in Nikolaou et al. (2006), however these involve global optimization methods (*e.g.* genetic algorithms) and perform worse than the optimal production settings obtained by gradient-based optimization using the previously discussed adjoint method. A moving horizon MPC application is reported in Saputelli et al. (2006), where a performance measure defined over 2200 days is maximized using a horizon of 30 days by varying the production settings of wells. Although the MPC results are better when compared to an uncontrolled case, no comparison is made to optimal production settings obtained by the adjoint method.

Finally, we remark that there are deeper control-theoretical problems involved with closed-loop control of petroleum reservoirs. For example, well optimization becomes more complicated in closed-loop, since new wells offer the possibility to obtain measurements in previously inaccessible areas of the reservoir. This new information can be used to reduce uncertainty, although it is not always clear how to value this information - see Ozdogan and Horne (2006) for some first results in this direction. Similarly, production settings that are good for maximizing the recovery factor are not necessarily good for reducing model uncertainty (*i.e.* the certainty equivalence principle does not hold because reservoir models are nonlinear). This so-called dual control problem (after Fel'dbaum (1965)) in production setting optimization is difficult because, again, it is not clear how to quantify the value of information.

1.4.6 Discussion

We have seen that there are many systems and control techniques that, in theory, could be applied to efficiently perform closed-loop reservoir management and production operations, but that in practice this is severely limited by the properties of reservoir models. As a result, there are still many open problems in reservoir management and production operations processes.

Some of the open problems in field development planning and production operations are as follows.

- How can we automatically determine the number, trajectory, and location of wells using a limited number of reservoir simulations?
- How can we reduce the gap between the models (*i.e.* reservoir vs. wells and surface) and goals (*i.e.* long-term vs. short-term) used in reservoir management and production operations?
- How can we efficiently handle state constraints when optimizing production settings during field development planning?
- When and why are optimal production settings sometimes smooth as opposed to bang-bang (*i.e.* when should we choose variable setting control valves over simple on-off ones)?
- Can robust optimization reduce the negative effect of a continuous range of uncertainties?
- Can we significantly reduce the currently long reservoir simulations times through the application of model reduction techniques?

Some of the open problems in history matching are as follows.

- Which state and parameter estimation technique is the most reliable?
- How can we determine the number of parameters that can be reliably estimated through measured data?
- What are the controllability, observability and identifiability properties of reservoir models?
- How can we generate a discrete set of models that in some sense is representative of the entire uncertainty range?
- How can we determine the value of information?

1.5 Problem formulation

1.5.1 Research objective

Following the discussion on open problems concerning the processes reservoir management and production operations, the main research objective of this thesis is as follows.

-Research objective-
Develop efficient tools for dynamic optimization of well locations and their production settings to maximize the recovery factor of petroleum reservoirs based on uncertain reservoir models.

The motivation for the various elements of this research objective is as follows. First of all, **maximize the recovery factor of petroleum reservoirs** relates to the desire to increase the cumulative production in order to meet increasing global demand. **Well locations and their production settings** relates to the degrees of freedom considered in this thesis. Although there are numerous other factors that can contribute to increasing the recovery factor, these fall outside the scope of this work. **Dynamic optimization** relates to optimization of the recovery factor by considering a dynamic system, in this case a petroleum reservoir, as opposed to static optimization. This optimization should be **based on reservoir models**, as opposed to model-free optimization. The **uncertainty** in these reservoir models should explicitly be taken into account by reducing its effect as well as reducing the uncertainty itself. Finally, as discussed in the previous section, there are many open issues in this field. By **developing efficient tools**, in the sense that they lead to good decisions while requiring limited time from the user, closed-loop reservoir management and production operations can evolve from concept to reality.

1.5.2 Solution directions

Because there are too many open problems to be treated in one thesis, the previously stated research objective is tackled along four main solution directions.

D1. Shape of optimal solutions
Investigate the structural properties of optimal production settings. In particular, find out why and under what conditions production setting optimization problems can be expected to have bang-bang (on-off) optimal solutions.

D2. Robust optimization
Investigate the possibilities for robust optimization of production settings to reduce the negative effect of model uncertainty. In particular, find out if robust optimization can be used to find production settings that are robust

against a continuous range of uncertainties, and not just its representation by a limited number of models.

D3. Well placement optimization
Investigate how we can effectively find optimal well locations. In particular, find out if the gradients used in production setting optimization - efficiently derived using adjoint models - can also be used in well location optimization.

D4. Controllability, observability and identifiability of reservoir models
Analyze and interpret the controllability and observability of single-phase flow reservoir models, and how these are affected by well locations, heterogeneity and fluid properties. In particular, investigate if better understanding of a reservoir's controllability, observability and identifiability properties can be used to increase the recovery factor or reduce the uncertainty of the outcome.

1.5.3 Outline of thesis

The outline of this thesis is as follows. Reservoir models, productions constraints and the sources and effects of model uncertainty are discussed in Chapter 2. The shape of optimal production settings is treated in Chapter 3, and is based on Zandvliet et al. (2006) and Zandvliet et al. (2007). Reducing the negative effect of model uncertainty by means of robust optimization is treated in Chapter 4, and is based on van Essen et al. (2006a) and van Essen et al. (2006b). How to effectively find optimal well locations using adjoint models is shown in Chapter 5, and is based on Handels et al. (2007) and Zandvliet et al. (2008a). The controllability and observability of reservoir models is analyzed in Chapter 6, and is based on Zandvliet et al. (2008b). How the analysis of Chapter 6 can help in identifying reservoir parameters is discussed in Chapter 7, and is also based on Zandvliet et al. (2008b). Finally, the conclusions and recommendations are given in Chapter 8.

2 CHAPTER

Reservoir Modeling

This chapter presents the notation, the reservoir models and the production constraints used throughout this thesis, and as such forms the basis of all the chapters that follow. Particular attention is paid to the sources, effects and representation of uncertainty in reservoir models.

2.1 Black oil formulation

2.1.1 Introduction

Petroleum reservoirs always contain both hydrocarbons and water. The former consists of many chemical components which, theoretically, should each be considered individually in the modeling process. Computationally, however, this is too demanding. Moreover, reservoir engineers are often mainly interested in predictions of future hydrocarbon production. Most reservoir models are therefore based on a so-called black oil formulation, which only considers three phases: oil, water and gas.

In this section we make further simplifications in considering only oil and water and ignoring several important physical aspects such as gravity, capillary pressures and the presence of an aquifer. Gravity effects, however, are included in the applications that follow in later chapters, but are omitted here to economize on the derivation length. For more details on black oil models the reader is referred to the textbooks Peaceman (1977) and Aziz and Settari (1979), on which this chapter is largely based.

2.1.2 Derivation of PDE's

The mass balances for oil (o) and water (w) are[1]

$$\frac{\partial}{\partial t}\left(\phi \rho_i S_i\right) \quad = \quad -\nabla \cdot \left(\rho_i \bar{u}_i\right) + q_i, \quad i \in \{\mathrm{o}, \mathrm{w}\} \tag{2.1}$$

where t is time, $\nabla\cdot$ the divergence operator, ϕ the porosity, ρ_i the density of the phase i, $\bar{u}_i$ the superficial velocity, and S_i the saturation. It is assumed that there is no flow across the boundaries of the reservoir geometry over which (2.1) is defined, other than through the source/sink terms q_o and q_w (*i.e.* so-called Neumann boundary conditions). How we can indirectly control these source/sink terms through the production settings of wells is discussed later.

Conservation of momentum is governed by the Navier-Stokes equations, but is normally simplified for low velocity flow through porous media to be described by the semi-empirical Darcy's equation - Muskat (1937), Hubbert (1956):

$$\bar{u}_i \quad = \quad -k\frac{k_{\mathrm{r}i}}{\mu_i}\nabla p_i, \quad i \in \{\mathrm{o}, \mathrm{w}\} \tag{2.2}$$

where p_i is the pressure of phase i, ∇ the gradient operator, k the permeability, $k_{\mathrm{r}i}$ the relative permeability, and μ_i the viscosity of phase i. The relative permeabilities are generally highly dependent on the water saturation S_w in that they can vary between 0 and a value smaller or equal to 1, and thus form a major source of nonlinearity. Figure 2.1 depicts typical curves for k_{rw} and k_{ro}.

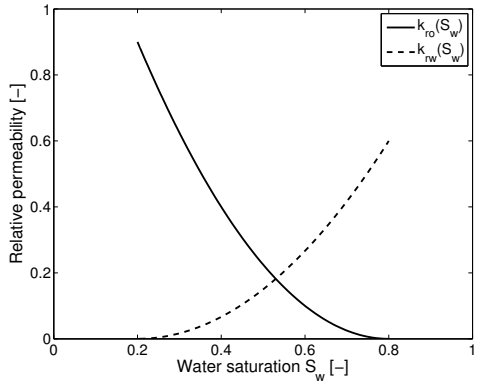

Figure 2.1: Typical relative permeability curves.

Substituting (2.2) into (2.1) leads to two flow equations with four dynamic unknowns: p_o, p_w, S_o and S_w. Two additional equations are required to complete the

[1]To be precise we would have to include spatial coordinates, such as Cartesian ones (x, y, z). For notational convenience, however, all of the dependent arguments are omitted, (*e.g.* we write $\bar{u}_i$ instead of $\bar{u}_i(t, x, y, z)$ and ϕ instead of $\phi(x, y, z)$).

system description. The first is the closure equation requiring that the sum of the phase saturations equals one:

$$S_{\mathrm{o}} + S_{\mathrm{w}} \quad = \quad 1. \tag{2.3}$$

Secondly, the difference between the individual phase pressures is given by the capillary pressure, which is assumed to be a function of water saturation. As mentioned earlier, however, we will ignore these capillary effects, and can therefore write

$$p_{\mathrm{w}} \quad = \quad p_{\mathrm{o}}. \tag{2.4}$$

Common practice in reservoir simulation is to substitute (2.3) and (2.4) into the flow equations by taking the oil pressure and water saturation (for notational convenience now symbolized by p and S) as state variables, leading to the following partial differential equations (PDE's)

$$\frac{\partial}{\partial t}\left(\phi\rho_{\mathrm{o}}\left[1-S\right]\right) \quad = \quad \nabla\cdot\left(k\frac{k_{\mathrm{ro}}}{\mu_{\mathrm{o}}}\rho_{\mathrm{o}}\nabla p\right) + q_{\mathrm{o}} \tag{2.5}$$

$$\frac{\partial}{\partial t}\left(\phi\rho_{\mathrm{w}}S\right) \quad = \quad \nabla\cdot\left(k\frac{k_{\mathrm{rw}}}{\mu_{\mathrm{w}}}\rho_{\mathrm{w}}\nabla p\right) + q_{\mathrm{w}} \tag{2.6}$$

The variables ϕ, k, μ_i and ρ_i are, generally speaking, dependent on pressure. However, for simplicity we assume the pressure dependency of ϕ, k and μ_i to be so small that it can be ignored.

2.1.3 State-space formulation

Because oil and gas reservoirs are generally heterogeneous (their geological properties vary significantly over space), (2.5)-(2.6) cannot be solved analytically, but must be evaluated numerically. The first step in this numerical evaluation is spatial discretization, where the reservoir is divided into a finite number of grid blocks whose geological properties are assumed to be homogeneous.

Each grid block j now relates to two states: oil pressure p^j and water saturation s^j. Let us stack all of these states into a vector $\mathbf{x}$ as follows

$$\mathbf{p} \quad := \quad \left[\begin{array}{ccc} p^1 & \ldots & p^N \end{array}\right]^T, \tag{2.7}$$

$$\mathbf{s} \quad := \quad \left[\begin{array}{ccc} s^1 & \ldots & s^N \end{array}\right]^T, \tag{2.8}$$

$$\mathbf{x} \quad := \quad \left[\begin{array}{cc} \mathbf{p}^T & \mathbf{s}^T \end{array}\right]^T. \tag{2.9}$$

Because a reservoir has evolved over millions of years, it is generally initially in equilibrium. In other words, the fluids in a reservoir only start to flow once wells are drilled.

If an injector well is perforated in grid block j, then we can directly control the source terms $q_{\rm o}^j$ and $q_{\rm w}^j$, which are in [kg/m^{3}s]. Only water (and not oil) is injected to keep the pressure in the reservoir above a certain level, and we can write

$$q_{\rm o}^j = 0, \tag{2.10}$$

$$q_{\rm w}^j = \frac{\rho_{\rm w}(p^j)}{v^j}\, q^j, \quad j \in \mathcal{N}_{\rm inj} \tag{2.11}$$

where v^j is the volume of grid block j, q^j is the rate of injected fluid in [m^3/s] and $\mathcal{N}_{\rm inj}$ is the set of grid block indices in which an injector well is perforated.

If a producer well is perforated in grid block j, then we can only indirectly control the source terms $q_{\rm o}^j$ and $q_{\rm w}^j$ since the produced liquid is a combination of oil and water:

$$f_{\rm w}^j := \frac{\frac{k_{\rm rw}(s^j)}{\mu_{\rm w}}}{\frac{k_{\rm rw}(s^j)}{\mu_{\rm w}} + \frac{k_{\rm ro}(s^j)}{\mu_{\rm o}}} \tag{2.12}$$

$$q_{\rm o}^j = \frac{\rho_{\rm o}(p^j)}{v^j}\,(1 - f_{\rm w}^j(s^j))\, q^j, \tag{2.13}$$

$$q_{\rm w}^j = \frac{\rho_{\rm w}(p^j)}{v^j}\, f_{\rm w}^j(s^j)\, q^j, \quad j \in \mathcal{N}_{\rm prod} \tag{2.14}$$

where f_w is the fractional flow rate of water, q^j is the rate of produced fluid in [m^3/s] and $\mathcal{N}_{\rm prod}$ is the set of indices in which a producer well is perforated.

Since the porosity ϕ is assumed to be independent of pressure, we have

$$\frac{\partial}{\partial t}\left(\phi \rho_i S\right) = \phi\left(S\frac{\partial \rho_i}{\partial t} + \rho_i \frac{\partial S}{\partial t}\right), \quad i \in \{\mathrm{o}, \mathrm{w}\}.$$

By defining the fluid compressibilities $c_{\rm w}$ and $c_{\rm o}$ as

$$c_i(p) := \frac{1}{\rho_i(p)}\frac{d\rho_i}{dp}(p), \quad i \in \{\mathrm{o}, \mathrm{w}\}, \tag{2.15}$$

the equations (2.5)-(2.14) for each of the N grid blocks can be replaced by a single equation of the form

$$\mathbf{E}(\mathbf{x}(t))\dot{\mathbf{x}}(t) = \tilde{\mathbf{A}}(\mathbf{x}(t))\mathbf{x}(t) + \tilde{\mathbf{B}}(\mathbf{x}(t))\mathbf{u}(t), \tag{2.16}$$

$$\mathbf{x}(0) = \bar{\mathbf{x}}_0. \tag{2.17}$$

where the control $\mathbf{u}$ is a vector containing the well rates q^j, $\bar{\mathbf{x}}_0$ is the initial condition and

$$\mathbf{E}(\mathbf{x}(t)) := \left[\begin{array}{c|c} \mathrm{diag}(\phi^j(1-s^j)\rho_{\rm o}(p^j)c_{\rm o}(p^j)) & \mathrm{diag}(-\phi^j\rho_{\rm o}(p^j)) \\ \hline \mathrm{diag}(\phi^j s^j \rho_{\rm w}(p^j)c_{\rm w}(p^j)) & \mathrm{diag}(\phi^j\rho_{\rm w}(p^j)) \end{array}\right].$$

If, in order to economize on notation, we assume that the reservoir is modeled by $N \times 1 \times 1$ grid blocks of fixed volume $v = \Delta x \times \Delta y \times \Delta z$ and there are only two wells (an injector in grid block 1 and a producer in grid block N),

$$\tilde{\mathbf{B}}(\mathbf{x}(t)) \quad := \quad \begin{bmatrix} 0 & 0 \\ 0 & 0 \\ \vdots & \vdots \\ 0 & 0 \\ 0 & \frac{\rho_{\mathrm{o}}(p^N)}{v}(1 - f_{\mathrm{w}}(s^N)) \\ \frac{\rho_{\mathrm{w}}(p^1)}{v} & 0 \\ 0 & 0 \\ \vdots & \vdots \\ 0 & 0 \\ 0 & \frac{\rho_{\mathrm{w}}(p^N)}{v} f_{\mathrm{w}}(s^N) \end{bmatrix}, \; \mathbf{u}(t) := \begin{bmatrix} q^1(t) \\ q^N(t) \end{bmatrix}.$$

At position $x = (j - 1/2)\Delta x$ in the reservoir (*i.e.* at the center of grid block j, denoted by a superscript j)

$$\begin{aligned} & \nabla \cdot \left(k \frac{k_{\mathrm{r}i}}{\mu_i} \rho_i \nabla p \right)^j \\ & \quad \approx \quad \frac{\left(k \frac{k_{\mathrm{r}i}}{\mu_i} \rho_i \nabla p \right)^{j,j+1} - \left(k \frac{k_{\mathrm{r}i}}{\mu_i} \rho_i \nabla p \right)^{j,j-1}}{\Delta x} \\ & \quad \approx \quad \frac{\rho_i(p^j)}{\mu_i} \frac{(k k_{\mathrm{r}i})^{j,j+1} \left(p^{j+1} - p^j \right) - (k k_{\mathrm{r}i})^{j,j-1} \left(p^j - p^{j-1} \right)}{\Delta x^2} \\ & \quad \approx \quad \frac{\rho_i(p^j)}{\mu_i} \frac{k^{j,j+1} k_{\mathrm{r}i}(s^j, s^{j+1}) \left(p^{j+1} - p^j \right) - k^{j,j-1} k_{\mathrm{r}i}(s^j, s^{j-1}) \left(p^j - p^{j-1} \right)}{\Delta x^2} \end{aligned}$$

for $i \in \{\mathrm{o}, \mathrm{w}\}$. The permeability k is evaluated at the grid block interfaces (*i.e.* at position $x = (j \pm 1/2)\Delta x$ in the reservoir, denoted by a superscript $j, j \pm 1$) using the harmonic average

$$k^{j,j\pm1} = \frac{2}{\frac{1}{k^j} + \frac{1}{k^{j\pm1}}}. \tag{2.18}$$

The relative permeability $k_{\mathrm{r}i}$ needs to be evaluated using the so-called upstream weighting in order to obtain correct convective behavior:

$$k_{\mathrm{r}i}^{j,j\pm1} \quad := \quad \begin{cases} k_{\mathrm{r}i}(s^j) & \text{if} \quad p^j \geq p^{j\pm1} \\ k_{\mathrm{r}i}(s^{j\pm1}) & \text{if} \quad p^j < p^{j\pm1} \end{cases}, \quad i \in \{\mathrm{o}, \mathrm{w}\}. \tag{2.19}$$

This leads to

$$
\begin{aligned}
\tilde{\mathbf{A}}(\mathbf{x}(t)) &:= \left[\begin{array}{c|c} \mathbf{A}_{\mathrm{o}}(\mathbf{x}(t)) & 0 \\ \hline \mathbf{A}_{\mathrm{w}}(\mathbf{x}(t)) & 0 \end{array}\right] \\
\mathbf{A}_i &:= \begin{bmatrix} -a_i^{1,2} & a_i^{1,2} & & & \\ a_i^{2,1} & -(a_i^{2,1}+a_i^{2,3}) & a_i^{2,3} & & \\ & \ddots & \ddots & \ddots & \\ & & & a_i^{N-1,N} & -a_i^{N-1,N} \end{bmatrix}, \\
a_i^{j,j\pm1} &:= \frac{\rho_i(p^j)}{\mu_i}\frac{k^{j,j\pm1}}{\Delta x^2}k_{\mathrm{r}i}^{j,j\pm1}(p^j,p^{j\pm1},s^j,s^{j\pm1}),\ \ i\in\{\mathrm{o},\mathrm{w}\}, \\
k^{j,j\pm1} &:= \frac{2}{\frac{1}{k^j}+\frac{1}{k^{j\pm1}}}, \\
k_{\mathrm{r}i}^{j,j\pm1} &:= \begin{cases} k_{\mathrm{r}i}(s^j) & \text{if} \quad p^j \geq p^{j\pm1} \\ k_{\mathrm{r}i}(s^{j\pm1}) & \text{if} \quad p^j < p^{j\pm1} \end{cases},\ \ i\in\{\mathrm{o},\mathrm{w}\}.
\end{aligned}
$$

$\mathbf{A}_i$ is tridiagonal because of the simplifying assumption that the reservoir is 1D (*i.e.* modeled by $N\times1\times1$ grid blocks). For 2D and 3D models, $\mathbf{A}_i$ becomes pentadiagonal and septadiagonal, respectively, as depicted in Figure 2.2. See Aziz and Settari (1979) for more details.

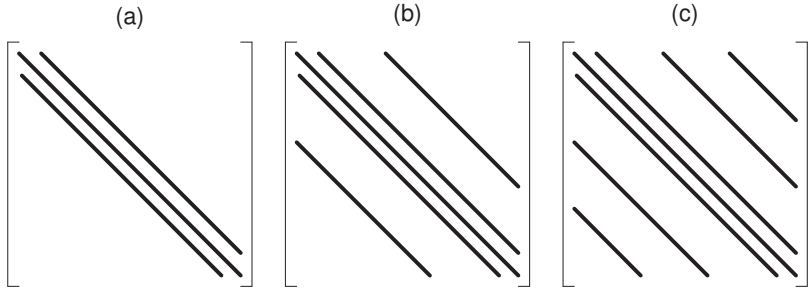

Figure 2.2: Structure of $\mathbf{A}_i$ for (a) 1D, (b) 2D and (c) 3D reservoir models.

We often only have indirect control over the flow rate q^j through a so-called well model

$$q^j = \alpha^j w^j(s^j)(p_{\mathrm{bh}}^j - p^j), \quad j\in\{\mathcal{N}_{\mathrm{inj}},\mathcal{N}_{\mathrm{prod}}\} \tag{2.20}$$

where p_{bh}^j is the well's bottom-hole pressure, and α^j a valve setting (simply a multiplication factor ranging from 0 to 1). The well index w^j contains the well's geometric flow factors and rock and fluid properties of the reservoir directly around the well, and throughout this thesis is computed using a so-called Peaceman model, after Peaceman (1978):

$$w^j(s^j) = \frac{2\pi k^j \Delta z}{\ln\left(0.14\sqrt{\Delta x^2+\Delta y^2}/r_{\mathrm{w}}\right)+S}\left(\frac{k_{\mathrm{ro}}(s^j)}{\mu_{\mathrm{o}}}+\frac{k_{\mathrm{rw}}(s^j)}{\mu_{\mathrm{w}}}\right). \tag{2.21}$$

Here, S is the skin factor which can be used to represent well impairment (*e.g.* due to sand clogging the well perforations). The wellbore radius r_{w} is used to represent logarithmic pressure-drop in the near wellbore-area, which is a sub grid-scale effect.

If we can directly control the valve setting α^j, the q^j term in $\mathbf{u}$ is replaced by α^j and the corresponding entries in $\tilde{\mathbf{B}}$ are modified to include the term $w^j(s^j)(p^j - p^j_{\mathrm{bh}})$. If a valve setting α^j is absent (or for some reason constant) but we can directly control the bottom-hole pressure p^j_{bh}, the q^j term in $\mathbf{u}$ is replaced by p^j_{bh} and the corresponding entries in $\tilde{\mathbf{B}}$ are modified to include the term $w^j(s^j)$. However, the (j,j) elements of $\mathbf{A}_{\mathrm{o}}$ and $\mathbf{A}_{\mathrm{w}}$ are also modified to include the term $w^j(s^j)$ because of the dependency on the grid block pressure p^j in (2.21).

Furthermore, we remark that including gravity effects and aquifers leads to extra terms on the right-hand side of (2.16) over which we have no control. Including capillary pressures affects $\tilde{\mathbf{A}}$ with terms in the columns multiplying the saturations.

Note that $\mathbf{E}$ is invertible as long as the fluids are compressible (meaning $c_{\mathrm{o}} \neq 0$ and $c_{\mathrm{w}} \neq 0$) and the porosity in all grid blocks is non-zero. Left-multiplying (2.16) by $\mathbf{E}^{-1}$ leads to an equation of the form

$$\dot{\mathbf{x}}(t) = \underbrace{\left[\begin{array}{c|c} \mathbf{A}_{11}(\mathbf{x}(t)) & 0 \\ \hline \mathbf{A}_{21}(\mathbf{x}(t)) & 0 \end{array}\right]}_{=\bar{\mathbf{A}}(\mathbf{x}(t))} \mathbf{x}(t) + \underbrace{\left[\begin{array}{c} \mathbf{B}_1(\mathbf{x}(t)) \\ \hline \mathbf{B}_2(\mathbf{x}(t)) \end{array}\right]}_{=\bar{\mathbf{B}}(\mathbf{x}(t))} \mathbf{u}(t), \tag{2.22}$$

$$\mathbf{x}(0) = \bar{\mathbf{x}}_0, \tag{2.23}$$

in which $\bar{\mathbf{B}} := \mathbf{E}^{-1}\tilde{\mathbf{B}}$ and $\bar{\mathbf{A}} := \mathbf{E}^{-1}\tilde{\mathbf{A}}$. An example of a heterogenous reservoir with 12 wells modeled by (2.22) considered throughout this thesis is depicted in Figure 2.3.

2.1.4 Single-phase flow reservoir models

The state-space formulation (2.22) is nonlinear due to the dependencies of $\mathbf{A}$ and $\mathbf{B}$ on $\mathbf{x}$. If there is one phase in the reservoir, the only states in the model are the pressures in the different grid blocks. If, in addition, the phase compressibility is constant the only remaining source of nonlinearity in (2.22) is the pressure-dependency of density. However, if the compressibility of the phase is small (as is common for fluids) and if the pressure differences throughout the reservoir are not very large, the density will remain nearly constant

$$\rho_i(p(t)) \approx \rho_i(p(0)), \quad i \in \{\mathrm{o}, \mathrm{w}\}. \tag{2.24}$$

Considering water as example, $\mathbf{s}(t) = \left[\begin{array}{ccc} 1 & \ldots & 1 \end{array}\right]^T$ for all t and we can write

$$\dot{\mathbf{p}}(t) = \mathbf{A}_{11}\mathbf{p}(t) + \mathbf{B}_1\mathbf{u}(t), \tag{2.25}$$

$$\mathbf{p}(0) = \bar{\mathbf{p}}_0. \tag{2.26}$$

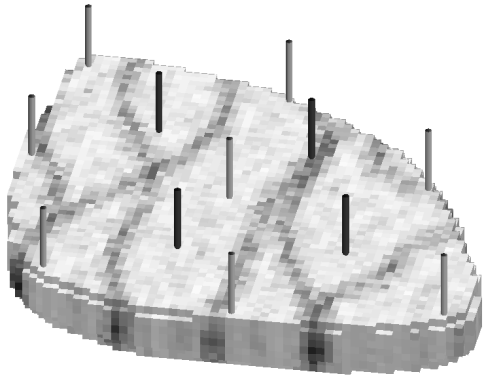

Figure 2.3: Reservoir considered throughout this thesis with 8 injectors (light), 4 producers (dark). The shading indicates permeability.

Note that the right-hand side of (2.25) is linear in terms of $\mathbf{p}$ and $\mathbf{u}$.

If the flow rates in all of the wells are directly controlled (*i.e.* $\mathbf{u}$ contains only q^j terms) $\mathbf{A}_{11}$ will contain an integrator, since the row and column sum of $\tilde{\mathbf{A}}$ are then zero. This is intuitively obvious: a step response on an injector then corresponds to injection without production, which due to the no-flow boundary conditions leads to ever increasing pressure. If the flow rate in at least one well is indirectly controlled through the bottom-hole pressure according to (2.20) (*i.e.* $\mathbf{u}$ contains at least one p^j_{bh} term), $\mathbf{A}_{11}$ will be Hurwitz. Single-phase flow models of the form (2.25) will be used in Chapters 6 - 7.

2.1.5 Time discretization

Whether considering an equation of the form (2.22) for multi-phase flow or (2.25) for single-phase flow, performing a reservoir simulation invariably requires discretization in time. The most common method is the first-order Euler scheme

$$\dot{\mathbf{x}}(t) \approx \frac{\mathbf{x}_{k+1} - \mathbf{x}_k}{\Delta t} \tag{2.27}$$

where Δt is the discretization time step and $\mathbf{x}_k := \mathbf{x}(k\Delta t)$. If the remaining terms in (2.22) or (2.25) are evaluated at time t the discretization is called explicit, as opposed to implicit if the terms are evaluated at time $t + \Delta t$. In Chapters 6 - 7 we will consider explicit time discretization of (2.25). With

$$\mathbf{A} := I + \mathbf{A}_{11}\Delta t \tag{2.28}$$

$$\mathbf{B} := \mathbf{B}_1\Delta t, \tag{2.29}$$

we can write

$$\mathbf{p}_{k+1} = \mathbf{A}\mathbf{p}_k + \mathbf{B}\mathbf{u}_k, \tag{2.30}$$

$$\mathbf{p}_0 = \mathbf{p}_{\text{init}} \tag{2.31}$$

as a difference equation approximating (2.25)-(2.26), where $\mathbf{u}_k := \mathbf{u}(k\Delta t)$. The discretization time step is set to

$$\Delta t = 0.5/\left|\lambda_{\min}\left(\mathbf{A}_{11}\right)\right| \tag{2.32}$$

where $\lambda_{\min}$ represents the most negative eigenvalue. This leads to quite small time-steps, and is referred to as the so-called Nyquist-Shannon sampling time needed to accurately capture all of the dynamics in (2.25) - see Astrom and Wittenmark (1990). In practice, the implicit time discretization scheme is usually preferred over the explicit one, in combination with much larger sampling times than in (2.32). Nevertheless, we use (2.32) to time discretize single-phase flow reservoir models because the analysis and results presented in Chapters 6-7 requires that all of the dynamics are accurately captured. Note that, as (2.25), the right-hand side of (2.30) is linear in terms of $\mathbf{p}_k$ and $\mathbf{u}_k$.

2.2 Constraints

In practice, there are many constraints which have to be met during the production process. Most of these can be translated into inequality constraints

$$\mathbf{g}(\mathbf{x}(t), \mathbf{u}(t)) \leq 0 \quad \forall \quad t \tag{2.33}$$

and equality constraints

$$\mathbf{h}(\mathbf{x}(t), \mathbf{u}(t)) = 0 \quad \forall \quad t \tag{2.34}$$

on both the states $\mathbf{x}$ and controls $\mathbf{u}$ in (2.22).

There are clearly always upper and lower bounds on the bottom-hole pressures, valve settings and flow rates in the individual wells, reflected by

$$\mathbf{u}_{\min} \leq \mathbf{u}(t) \leq \mathbf{u}_{\max} \quad \forall \quad t \tag{2.35}$$

for given $\mathbf{u}_{\min}, \mathbf{u}_{\max} \in \mathbb{R}^m$. This can be written as (2.33) with

$$\mathbf{g}(\mathbf{u}(t)) = \left[\begin{array}{cc} \mathbf{u}(t) - \mathbf{u}_{\min} & -\mathbf{u}(t) + \mathbf{u}_{\max} \end{array} \right]^T.$$

Note that a very common lower bound is $\mathbf{u}_{\min} = 0$, since an injector generally only injects fluids and a producer only produces them. This also holds for a producer that is converted into an injector (*e.g.* to maintain reservoir pressure), as it can then no longer produce fluids.

In order to avoid pressure decline in the reservoir, it is sometimes desirable to balance the total volumetric injection rate (*i.e.* sum of flow rates over all injector wells) with the total volumetric production rate (*i.e.* sum of flow rates over all producer wells). If we can directly control all of the well flow rates, this can be written as (2.34) with

$$\mathbf{h}(\mathbf{u}(t)) = \begin{bmatrix} 1 & \dots & 1 \end{bmatrix} \mathbf{u}(t).$$

In this thesis we do not model the dynamics of fluids flowing through the wells, nor do we model the surface facilities. We therefore implicitly assume that these omissions can be captured through constraints of the form (2.33) and (2.34).

2.3 Uncertainty in reservoir models

2.3.1 Sources of model uncertainty

As mentioned in Chapter 1, reservoir models of the form (2.22) are generally very uncertain. This section discusses some of the sources and effects of this uncertainty, and how it is commonly represented.

Model structure
Many simplifying assumptions have been made in deriving the model structure of (2.22). The black oil formulation and semi-empirical Darcy's Law, for example, are only approximations of the true physics dictating multi-phase flow, as is the spatial discretization of the reservoir (for a large reservoir the grid block dimensions can be $100\mathrm{m} \times 100\mathrm{m} \times 10\mathrm{m}$). Furthermore, the reservoir geometry (*e.g.* the no-flow boundary) is also not exactly known.

Parameters
Virtually all of the physical parameters entering (2.22) are uncertain. The fluid properties (*e.g.* relative permeability curves k_{rw} and k_{ro}) are determined by performing numerous tests on rock and fluid samples taken from wells. Even so, they are still only approximations as it is difficult to relate fluid properties on a micro-scale to properties on a grid-block size scale. The geological properties (*e.g.* the permeability k_j and porosity ϕ_j in grid blocks $j = 1, \dots, N$) are also very uncertain due to the limited number of wells from which core samples can be taken, and the limited capacity of seismic experiments to distinguish between the different layers of the subsurface.

Initial conditions
The initial conditions $\bar{\mathbf{x}}_0$ (*e.g.* the initial pressures and initial contact depths between the different phases, which are translated into grid block saturations) are uncertain, again because of the limited number of wells from which measurements can be taken and because of capillary pressure effects. Note the contact

depths are particular important, as these determine how much oil and gas is initially in place.

Disturbances
In some reservoirs there can be large disturbances affecting (2.22), such as the presence of an active aquifer, that are only known to a limited extent. While the effect of these disturbances is not always undesirable (*e.g.* an active aquifer will slow down undesired pressure decline), they can have a significant impact on predictions.

2.3.2 Representing model uncertainty by multiple models

For notational convenience, let us assume that the only source of uncertainty in a reservoir model of the form (2.22) is in the fluid and geological parameters. By stacking all of the uncertain parameters θ_i in a vector $\boldsymbol{\theta}$ as follows

$$\boldsymbol{\theta} := \begin{bmatrix} \theta_1 & \dots & \theta_M \end{bmatrix}^T, \tag{2.36}$$

we can write for a given configuration of wells

$$\dot{\mathbf{x}}(t) \quad = \quad \bar{\mathbf{A}}(\mathbf{x}(t), \boldsymbol{\theta})\mathbf{x}(t) + \bar{\mathbf{B}}(\mathbf{x}(t), \boldsymbol{\theta})\mathbf{u}(t). \tag{2.37}$$

Let us assume that a cumulative distribution function (cdf) for $\boldsymbol{\theta}$ has been determined, either through an identification / history matching procedure, or by engineering judgement. Such a cdf for $\boldsymbol{\theta}$ and a (deterministic) control $\mathbf{u}$ together now determine a cdf for the state trajectory $\mathbf{x}$ and thereby of future production of oil and gas. However, because (2.37) is nonlinear, this cdf cannot be evaluated analytically and must be approximated numerically. Unfortunately, the number of uncertain parameters M can be in the order of the number of grid blocks N (*i.e.* $10^4 - 10^6$). Even though these parameters are strongly correlated with each other, it is virtually impossible to approximate the cdf of $\mathbf{x}$ accurately due to the generally long computation time of a single reservoir simulation. The common approach to this numerical approximation is to decide upon a few sources of uncertainty that presumably have the largest impact on the predictions of future production as well as a few of their values. Let us denote these values by $\boldsymbol{\theta}_1, \dots, \boldsymbol{\theta}_L$, where $L \ll M$, and their probability by $w_1, \dots, w_L$, where $\sum_{i=1}^{L} w_i = 1$. These values and their probabilities are often determined using engineering judgement, sometimes in combination with a stochastic method (*e.g.* by sampling a Gaussian distribution around a specified mean).

The parameter vectors $\boldsymbol{\theta}_1, \dots, \boldsymbol{\theta}_L$, often called realizations when referring to permeability or porosity distributions, are then used to generate L reservoir models of the form (2.37). Figure 2.4 depicts six realizations of the permeability distribution of the reservoir depicted in Figure 2.3. For clarity, if permeability is the only source of uncertainty under consideration, the values of all six permeability distributions are stacked to form $\boldsymbol{\theta}_1, \dots, \boldsymbol{\theta}_6$, and subsequently lead to six different models of the form (2.37).

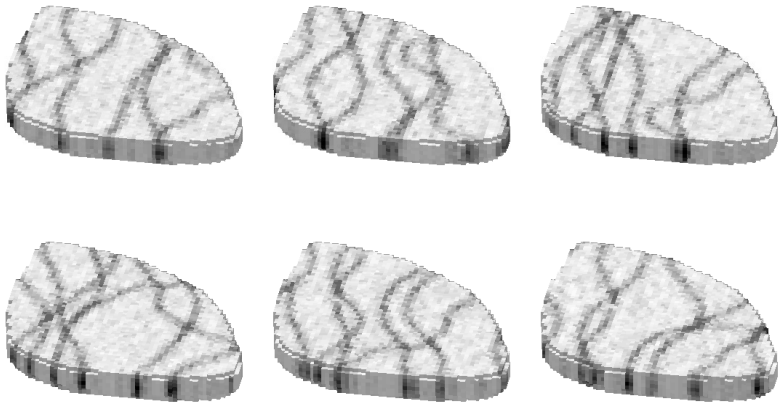

Figure 2.4: Six realizations of permeability for the reservoir in Figure 2.3, each depicting meandering channels of high permeability.

2.3.3 Limitations of reservoir models

Multiple models can be used to make predictions of future production, and the spread in these predictions together with their probabilities can be used to assess the impact of model uncertainty. Figure 2.5 depicts such a spread in predictions of future production. Unfortunately, this spread can be very large, and this forms a major limitation in using reservoir models to make field development decisions. Furthermore, a large spread will obviously worry oil companies, as it can imply significant financial risk in developing a particular field. This is discussed in more detail in Chapter 4.

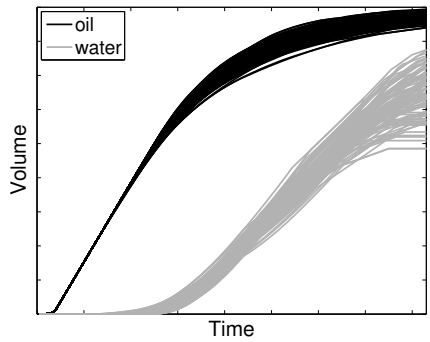

Figure 2.5: Predictions of future production by multiple reservoir models.

Despite their limited reliability, reservoir models are a widely used tool for field development planning. There are a number of reservoir simulators which essentially implement the equations of the form (2.37). Some of these simulators are commercially available (*e.g.* Schlumberger's Eclipse), and others proprietary (*e.g.* Shell's MoReS). The simulation results considered in this thesis have been obtained either by using MoReS, or by implementing (2.37) in MATLAB.

As mentioned in Chapter 1, another limitation of reservoir models is that, while they are widely used for field development planning, they are generally not used to determine the day-day decisions made in productions operations. In production operations, where the goal is often to maximize daily hydrocarbon production, decisions are often based on models accurately describing multi-phase flow through wells and related surface network. Coupling reservoir models with well and surface network models is an area of ongoing research - Coats et al. (2003), Kosmala et al. (2003).

2.4 Chapter conclusions

Reservoir models are often based on a black oil formulation, in which oil, water and gas are considered as phases. The equations governing the flow of these phases are a combination of a mass balance equation and Darcy's Law, which states that fluid flow rate is proportional to the pressure gradient. Because reservoirs are generally heterogeneous, these partial differential equations cannot be solved analytically, but must be evaluated numerically. The reservoir under consideration is therefore spatially discretized into a finite number of grid blocks, whose geological properties are assumed to be homogeneous. This leads to a large number of ordinary differential equations that can be written in state-space form, where the states are the fluid pressure and saturations in each grid block and the inputs are the production settings of the wells. Unfortunately, reservoir models contain a significant amount of uncertainty from various sources. It is common to represent this uncertainty by considering not one but several models to make predictions of future hydrocarbon production, and the spread in these predictions can be used to assess the impact of model uncertainty.

3 CHAPTER

Optimal Control of Production Settings

This chapter focuses on the optimal production settings of wells. First, necessary conditions for optimality are given. Then, based on these conditions, the structural properties of optimal production settings for a whole variety of optimal control problems is discussed. The main contribution of this chapter is to analyze why and under what conditions these problems can be expected to have bang-bang (on-off) optimal solutions, as well as the role of so-called singular arcs. Sufficient optimality conditions for bang-bang controls are given, as well as two gradient-based optimization procedures to actually find optimal settings. Finally, an application is presented to illustrate the results.

3.1 Problem formulation

Given a certain configuration of wells, finding the time-varying production settings over a time interval $[0, T]$ that maximize a reservoir's recovery factor can be posed as an optimal control problem. Since maximizing the recovery factor is equivalent to maximizing the volume of produced oil or minimizing the volume of remaining oil, the recovery factor can naturally be expressed as a performance measure in terms of the water saturations at the terminal time T, and we can write[1]

$$J_{\mathrm{rf}}(\mathbf{u}) = \sum_{j=1}^{N} S^j(T) \; . \tag{3.1}$$

However, since oil companies have an incentive to maximize the economic value as opposed to recovery factor of a reservoir, a very common performance measure is simple Net Present Value (NPV), defined as the total oil revenues minus

[1] See Chapter 2 for an explanation of the notation used throughout this chapter.

the total injection and production costs, in combination with a discount factor d representing the time value of money (*e.g.* interest rate). Letting r_{oil} denote oil revenue per unit volume, r_{inj} the injection cost per unit volume, and r_{prod} the water production cost per unit volume, we can write

$$J_{\text{npv}}(\mathbf{u}) = \int_0^T \{ \underbrace{\sum_{j\in\mathcal{N}_{\text{prod}}} r_{\text{oil}}(t)\left[1 - f_{\text{w}}^j(t)\right] q^j(t)}_{\text{oil revenue}} - \underbrace{\sum_{j\in\mathcal{N}_{\text{prod}}} r_{\text{prod}}(t) f_{\text{w}}^j(t) q^j(t)}_{\text{production cost}} + \underbrace{\sum_{j\in\mathcal{N}_{\text{inj}}} r_{\text{inj}}(t) q^j(t)}_{\text{injection cost}} \} \underbrace{\frac{1}{(1+d(t))^t}}_{\text{discount factor}} dt. \quad (3.2)$$

Both (3.2) and (3.1) are performance measures of the form

$$J(\mathbf{u}) = \psi(\mathbf{x}(T), T) + \int_0^T \left\{ l_1(\mathbf{x}(t), t) + \mathbf{l}_2^T(\mathbf{x}(t), t)\mathbf{u}(t) \right\} dt \quad (3.3)$$

where $\mathbf{u}(t)$ enters the integrand of (3.3) linearly. The additional time arguments in l_1 and $\mathbf{l}_2$ can be used to represent time-varying properties, such as volatile oil prices and interest rates.

From (2.22), for notational convenience let us define

$$\mathbf{f}_1(\mathbf{x}(t)) := \bar{\mathbf{A}}(\mathbf{x}(t))\mathbf{x}(t), \quad (3.4)$$
$$\mathbf{f}_2(\mathbf{x}(t)) := \bar{\mathbf{B}}(\mathbf{x}(t)). \quad (3.5)$$

Furthermore, let us for the moment assume that the only production constraints are upper and lower bounds on the control $\mathbf{u}(t)$. The reason for this assumption will be clarified later in this chapter. The optimal control problems we are considering are thereby of the following form.

Problem 1

$$\begin{aligned}
\text{maximize } J(\mathbf{u}) &= \psi(\mathbf{x}(T), T) + \int_0^T \left\{ l_1(\mathbf{x}(t), t) + \mathbf{l}_2^T(\mathbf{x}(t), t)\mathbf{u}(t) \right\} dt \\
\text{over } \mathbf{u} &\in \mathcal{L}_m^1[0, T] \\
\text{subject to } \dot{\mathbf{x}}(t) &= \mathbf{f}_1(\mathbf{x}(t)) + \mathbf{f}_2(\mathbf{x}(t))\mathbf{u}(t) \\
\mathbf{x}(0) &= \bar{\mathbf{x}}_0 \\
\mathbf{u}(t) &\in \mathcal{U} \; \forall \, t \in [0, T] \\
\mathcal{U} &= \{ \mathbf{w} \in \mathbb{R}^m : \; \mathbf{u}_{\min} \leq \mathbf{w} \leq \mathbf{u}_{\max} \}.
\end{aligned}$$

Here, $\mathcal{L}_m^1[0, T]$ denotes the space of m-valued absolute-integrable functions defined over the time period $t = 0$ to $t = T$. The norm of an element $\mathbf{u}^* \in \mathcal{L}_m^1[0, T]$ is given by

$$\|\mathbf{u}^*\| = \sum_{i=1}^m \int_{t=0}^T |u_i^*(t)| \, dt. \quad (3.6)$$

Note that we do not consider model uncertainty, and thereby implicitly assume that the reservoir model (2.22) is correct.

It is interesting to note that virtually all of the applications discussed in the literature overview in Section 1.4 involve problems that can be written as **Problem 1**, some with an additional equality constraint on the control. Of these, Sudaryanto and Yortsos (2000) and Sudaryanto and Yortsos (2001) are the only ones who state that the optimal solution is necessarily a bang-bang control - meaning that over the entire time interval, each component of $\mathbf{u}$ takes on either its minimum or maximum value. Consequently, they disregard the possibility of smooth optimal solutions and only consider bang-bang controls, parameterized in terms of switching times (times at which a component of the control switches from one extreme value to the other.) It turns out that the problems considered in Sudaryanto and Yortsos (2000) and Sudaryanto and Yortsos (2001) do not satisfy the conditions for which we can expect them to have bang-bang optimal solutions (Bellman (1956), Athans and Falb (1966) and Sussmann (1979)), the reasons for which are clarified later in this chapter.

In light of this work, the subsequent studies Brouwer (2004) and Brouwer and Jansen (2004), which consider optimizing individual rates and valve settings in water flooding, are particularly interesting. They find that the optimal rates are smooth, but that the optimal valve settings are sometimes bang-bang - even though they do not parameterize the control in terms of switching times. No explanation is given as to what causes this difference in type of solution.

Bang-bang controls have the obvious advantage over smooth controls in that they can be implemented using simple on-off valves, which are cheaper than valves with variable settings. The main contribution of this chapter is to analyze the conditions under which **Problem 1** can be expected to have bang-bang optimal solutions. To arrive at the previously mentioned conditions, we first inspect the necessary conditions for optimality.

3.2 Necessary conditions for optimality

The basic reasoning behind deriving necessary optimality conditions for **Problem 1** is that, given a candidate optimal control $\mathbf{u}^*$, the first order variation of the performance measure should be nonpositive for 'small' variations of $\mathbf{u}^*$. These derivations are given in virtually all textbooks on optimal control. See for example Athans and Falb (1966), Bryson and Ho (1975), Luenberger (1981) and Stengel (1986). For this derivation it is convenient to first consider a more general problem than **Problem 1** in which both $\dot{\mathbf{x}}(t)$ and the integrand of $J(\mathbf{u})$ do not depend linearly on $\mathbf{u}(t)$, as follows.

Problem 2

$$\begin{aligned} \text{maximize } J(\mathbf{u}) &= \psi(\mathbf{x}(T),T) + \int_0^T l(\mathbf{x}(t),\mathbf{u}(t),t)\,dt \\ \text{over } \mathbf{u} &\in \mathcal{L}_m^1[0,T] \\ \text{subject to } \dot{\mathbf{x}}(t) &= \mathbf{f}(\mathbf{x}(t),\mathbf{u}(t)) \\ \mathbf{x}(0) &= \bar{\mathbf{x}}_0 \\ \mathbf{u}(t) &\in \mathcal{U}\ \forall\, t \in [0,T] \\ \mathcal{U} &= \{\mathbf{w} \in \mathbb{R}^m :\ \mathbf{u}_{\min} \le \mathbf{w} \le \mathbf{u}_{\max}\}\,. \end{aligned}$$

We first derive necessary optimality conditions for **Problem 2**, and then analyze these solutions for **Problem 1**.

A common starting point is to define an auxiliary function, the so-called Hamiltonian, as follows

$$H(\mathbf{x}(t),\mathbf{u}(t),\boldsymbol{\lambda}(t),t) := l(\mathbf{x}(t),\mathbf{u}(t),t) + \boldsymbol{\lambda}^T(t)\mathbf{f}(\mathbf{x}(t),\mathbf{u}(t),t). \tag{3.7}$$

The vector $\boldsymbol{\lambda}(t) \in \mathbb{R}^{2N}$ is often referred to as the adjoint, co-state, Lagrange multiplier or tangent vector.

Consider a candidate optimal control $\mathbf{u}^*$ for **Problem 2** which is allowable (meaning $\mathbf{u}^*(t) \in \mathcal{U}\ \forall\, t \in [0,T]$) and an arbitrary allowable function $\mathbf{v}$ which is close to $\mathbf{u}^*$, in the sense that

$$\sum_{i=1}^{m} \int_{t=0}^{T} |u_i^*(t) - v_i(t)|\,dt < \varepsilon \tag{3.8}$$

for some small $\varepsilon > 0$. It can be shown that if $\boldsymbol{\lambda}$ satisfies the adjoint system equation

$$\dot{\boldsymbol{\lambda}}(t) = -\frac{\partial H}{\partial \mathbf{x}}^T (\mathbf{x}(t),\mathbf{u}^*(t),\boldsymbol{\lambda}(t),t) \tag{3.9}$$

with terminal-time condition

$$\boldsymbol{\lambda}(T) = \frac{\partial \psi}{\partial \mathbf{x}}^T (\mathbf{x}(T),T) \tag{3.10}$$

the effect on the performance measure is

$$J(\mathbf{v}) - J(\mathbf{u}^*) = \int_{t=0}^{T} \{H(\mathbf{x}(t),\mathbf{v}(t),\boldsymbol{\lambda}(t),t) - H(\mathbf{x}(t),\mathbf{u}^*(t),\boldsymbol{\lambda}(t),t)\}\,dt + o(\varepsilon) \tag{3.11}$$

in which $o(\varepsilon)$ denotes terms of smaller order than ε.

A first order necessary condition for $\mathbf{u}^*$ to be optimal for **Problem 2** is

$$H(\mathbf{x}(t),\bar{\mathbf{v}},\boldsymbol{\lambda}(t),t) \le H(\mathbf{x}(t),\mathbf{u}^*(t),\boldsymbol{\lambda}(t),t),\ \forall\, \bar{\mathbf{v}} \in \mathcal{U},\ \forall\, t \in [0,T]. \tag{3.12}$$

Note that $\bar{\mathbf{v}}$ is not a function but an element of $\mathcal{U}$, and that if (3.12) does not hold it is possible to construct an allowable $\mathbf{v}$ close to $\mathbf{u}^*$ for which $J(\mathbf{v}) > J(\mathbf{u}^*)$. This result is referred to as Pontryagin's Maximum Principle and it is one of the most important results in optimal control theory - see Pontryagin et al. (1962).

3.3 Bang-bang optimal solutions and singular arcs

An important observation is that, for the particular structure of **Problem 1**, these necessary conditions have a particular form. Let us define

$$\boldsymbol{\beta}^T(t) \quad := \quad \mathbf{l}_2^T(\mathbf{x}(t),t) + \boldsymbol{\lambda}^T(t)\mathbf{f}_2(\mathbf{x}(t),t). \tag{3.13}$$

According to (3.12), a first order necessary condition for $\mathbf{u}^*$ to be optimal for **Problem 1** is

$$\boldsymbol{\beta}^T(t)\bar{\mathbf{v}} \quad \leq \quad \boldsymbol{\beta}^T(t)\mathbf{u}^*(t) \; \forall \; \bar{\mathbf{v}} \in \mathcal{U}, \; \forall \, t \in [0,T]. \tag{3.14}$$

Note that the $\mathbf{f}_1$ and l_1 terms do not enter (3.14) because they appear identically on both sides of (3.12) and therefore cancel each other out. This necessarily leads to the following form of the components of $\mathbf{u}^*$

$$u_i^*(t) = \begin{cases} u_{\min,i}^* & \text{, if} \quad \beta_i(t) < 0 \\ u_{\max,i}^* & \text{, if} \quad \beta_i(t) > 0 \end{cases} \tag{3.15}$$

for $i = 1, ..., m$, where u_i^* denotes the i^{th} component of $\mathbf{u}^*$ and β_i denotes the i^{th} component of $\boldsymbol{\beta}$. The latter is often understandably referred to as the switching function and its zeros the switching times. Note that $\frac{\partial H}{\partial \mathbf{u}} = \boldsymbol{\beta}$ and that $\frac{\partial^k H}{\partial \mathbf{u}^k} = 0$ for $k \geq 2$. Loosely speaking, the component β_i at time t can therefore be viewed as the first order variation of J due to a small change in the component u_i^* at time t.

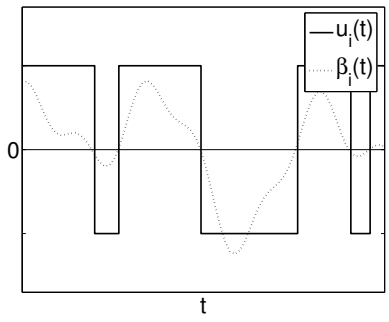

Figure 3.1: The i^{th} component β_i of the scaled switching function $\boldsymbol{\beta}$ and the corresponding bang-bang control component u_i.

For clarity, we emphasize that the control $\mathbf{u}$ determines the state $\mathbf{x}$ through (2.22), that the pair $(\mathbf{x}, \mathbf{u})$ determines the adjoint through (3.9) and (3.10), and that the

pair $(\mathbf{x}, \boldsymbol{\lambda})$ determines the switching function $\boldsymbol{\beta}$ through (3.13). The control $\mathbf{u}^*$ satisfies the first order necessary optimality conditions (3.12) if the zeros of the components of $\boldsymbol{\beta}$ coincide with the times that the components of $\mathbf{u}^*$ are discontinuous - as illustrated in Figure 3.1. How to actually compute such a control is discussed in Section 3.5.

If the switching function $\boldsymbol{\beta}$ contains only isolated zeros as in Figure 3.1, the problem is said to be regular. On the other hand, if any component of $\boldsymbol{\beta}$ is zero along an open time interval, the problem is said to be singular, and such an interval is called a singular arc. The difficulty lies in the fact that, along the singular arc, (3.12) no longer provides information on the optimality of $\mathbf{u}^*$ since the first order variation of J is then insensitive to variations in $\mathbf{u}^*$.

In short, any locally optimal solution to a reservoir flooding problem that can be written in the form of **Problem 1** is necessarily a bang-bang control, possibly in combination with singular arcs. This is not surprising, as it is in line with the intuitive notion that in a locally optimal solution of a static optimization problem, either the derivative vanishes or the to-be-optimized parameters are on the boundary of the feasible set. However, what is surprising is that pure bang-bang controls (without singular arcs) are widely encountered as optimal strategy for optimal control problems that can be written as **Problem 1**.

Some examples from other application fields where pure bang-bang controls are shown to be optimal include:

- minimum-time problems for linear systems - Bellman (1956),
- minimum-time problems for bilinear systems - Mohler (1973),
- optimal control of batch reactors - Blakemore and Aris (1962),
- optimal thermal control - Belghith et al. (1986),
- optimal drug administration in cancer chemotherapy - Ledzewicz and Schattler (2002).

According to the previously mentioned studies Sudaryanto and Yortsos (2000), Sudaryanto and Yortsos (2001), Brouwer (2004) and Brouwer and Jansen (2004), and the application treated in this chapter, it now seems that pure bang-bang controls are also sometimes (but not always) encountered as optimal strategy for reservoir flooding problems that can be written as **Problem 1**.

It is now clear why we only consider upper and lower bounds on the individual components of the control $\mathbf{u}$: the step from (3.14) to (3.15) in the derivation of bang-bang optimal control does not apply to problems involving more general (in)equality constraints on the control.

In fact, this is precisely the reason why the optimal rates in Brouwer (2004) and Brouwer and Jansen (2004) are smooth, while the optimal valve settings are sometimes bang-bang: there are additional equality constraints on the rates in order to balance total injection with total production, but not on the valve settings. Finally, we remark that the problems considered in Sudaryanto and Yortsos (2000) and Sudaryanto and Yortsos (2001) also have equality constraints on the rates, which is why there is no reason to expect them to have bang-bang optimal solutions.

In practice, more general (in)equality constraints on the control can be relevant (*e.g.* balancing the total injection and production rates), as can state constraints (*e.g.* keeping the pressure in the reservoir below a fracturing threshold, and above the bubble-point pressure). Unfortunately, optimal control problems with state constraints are, in general, difficult to solve. Some progress in handling state constraints in reservoir flooding problems has recently been achieved by Sarma et al. (2006a), de Montleau et al. (2006) and Kraaijevanger et al. (2007).

Remarks:

- **Local optimal vs. global optimal solutions**
  Since **Problem 1** is a nonconvex optimization problem due the nonlinear dynamics of (2.22), we cannot guarantee that a local optimal solution is also a global optimal solution. If an optimization scheme converges to the same solution for different initial conditions, we might have more confidence that that particular solution is indeed globally optimal - but we generally cannot prove it.

- **Smoothness**
  We assume that $\mathbf{f}_1$, $\mathbf{f}_2$, l_1, $\mathbf{l}_2$ and ψ are continuously differentiable with respect to $\mathbf{x}$ and t - see for example (3.9). In general, this is a reasonable assumption in reservoir flooding problems. For example, $\mathbf{f}_1$ and $\mathbf{f}_2$ are continuously differentiable as long as $(k_{\mathrm{rw}}, k_{\mathrm{ro}})$ depend smoothly on S, and $(\mu_{\mathrm{rw}}, \mu_{\mathrm{ro}}, \rho_{\mathrm{w}}, \rho_{\mathrm{o}})$ depend smoothly on p. It also is worthwhile to point out that the $\frac{\partial \mathbf{f}}{\partial \mathbf{x}}$ term in (3.9) is always available in a fully-implicit reservoir simulator - see Sarma et al. (2005).

- **Free terminal time problems**
  If the terminal time T is free, the so-called transversality condition

$$\frac{\partial \psi}{\partial T}\left(\mathbf{x}(T), T\right) + H(\mathbf{x}(T), \mathbf{u}(T), \boldsymbol{\lambda}(T), T) = 0 \tag{3.16}$$

  must be added to the set of necessary conditions for optimality - see Stengel (1986).

- **Continuous vs. discrete-time problems**
  The trajectory $\mathbf{x}$ can generally not be solved analytically for given $\mathbf{u}$ and $\bar{\mathbf{x}}_0$, and the same applies to $\boldsymbol{\lambda}$. Consequently, (2.16) and (3.9) are discretized in time and $\mathbf{u}$ is often taken to be piece-wise constant (*i.e.* step-like). The

optimality conditions, however, are largely similar to the continuous-time case; see Bryson and Ho (1975) for more details.

3.4 Sufficient conditions for optimality

To ensure that a control $\mathbf{u}^*$ satisfying the first order necessary conditions given in the previous subsection is indeed a local optimal solution to **Problem 1**, second order sufficient conditions must be verified. Many authors have been involved in deriving higher-order conditions, both necessary and sufficient, for optimality - see for example Krener (1973), Bressan (1985) and Kawski (2003). Recently, however, second order sufficient conditions specifically for pure bang-bang solutions have been derived in Agrachev et al. (2002), and their efficient numerical implementation have been discussed in Maurer et al. (2005).

In order to use the sufficient optimality conditions in Agrachev et al. (2002), we must make four assumptions:

(a) the terminal time T is fixed,

(b) the bang-bang control $\mathbf{u}^*$ satisfies the necessary optimality conditions and is regular (has no singular arcs), and

(c) only one component of $\mathbf{u}^*$ switches at any particular time.

Given n distinct switching times $t_k \in [0, T]$ with $t_1 < ... < t_n$, let us define the bang-bang vector $\boldsymbol{\tau}$ as

$$\boldsymbol{\tau} = \left[\begin{array}{ccc} t_1 & ... & t_n \end{array} \right]^T . \tag{3.17}$$

Furthermore, let $\boldsymbol{\tau}$ determine a bang-bang control $\mathbf{u}^*$. Due to assumptions (b) and (c), the components of $\boldsymbol{\tau}$ coincide with the zeros of the components of the switching function. That is, for each $k = 1, ..., n$ there is a unique index $i(k)$ such that only the component $u^*_{i(k)}$ is discontinuous at t_k, and only the component $\beta_{i(k)}$ is zero at t_k.

The fourth and final assumption is that

(d) the strict bang-bang property holds

$$\frac{d}{dt}\beta_{i(k)}\left(t_k\right)\left(u^{k+1}_{i(k)} - u^k_{i(k)}\right) > 0, \quad k = 1, ..., n \tag{3.18}$$

where $u^k_{i(k)}$ denotes the value of $u^*_{i(k)}(t)$ for $t_{k-1} < t < t_k$.

With this notation, $\left(u^{k+1}_{i(k)} - u^k_{i(k)}\right)$ represents the 'jump' of $u^*_{i(k)}(t)$ at the switching time t_k. Loosely speaking, (3.18) therefore requires that $u^*_{i(k)}(t)$ actually switches

from one value to another at $t = t_k$. Note that since $\mathbf{u}^*$ satisfies Pontryagin's Maximum Principle (3.12), the left hand side of (3.18) is always larger than or equal to zero - we simply require it to be strictly larger than zero.

The performance measure J is now a function of $\boldsymbol{\tau}$. If we have found a $\boldsymbol{\tau}$ such that $\mathbf{u}^*$ satisfies the first order necessary conditions for optimality, we can only conclude that $\mathbf{u}^*$ might be a local optimal solution to **Problem 1**. Surprisingly, if the Hessian $\frac{\partial^2 J}{\partial \boldsymbol{\tau}^2}(\boldsymbol{\tau}) \in \mathbb{R}^{n \times n}$ is negative definite

$$\frac{\partial^2 J}{\partial \boldsymbol{\tau}^2}(\boldsymbol{\tau}) \quad < \quad 0 \tag{3.19}$$

we can make the much stronger statement that $\mathbf{u}^*$ really is a local optimal solution. We stress that optimal here refers to variations of $\mathbf{u}^*$ satisfying (3.8) (*i.e.* optimal with respect to the $\mathcal{L}^1_m$-norm (3.6)).

If $\frac{\partial^2 J}{\partial \boldsymbol{\tau}^2}(\boldsymbol{\tau})$ is negative semi-definite, $\mathbf{u}^*$ again might be a local optimal solution, whereas if it is indefinite it certainly is not. Whatever the situation, (3.19) is clearly a simple condition to check. This is illustrated in the example of Section 3.6.

3.5 Optimization methods

3.5.1 Steepest descent method

As mentioned earlier, the equations (2.16) and (3.9) are usually discretized in time, with $\mathbf{u}$ taken to be piece-wise constant (*i.e.* step-like). Let $\mathbf{u}$ be divided into K equal intervals over $[0, T]$, let $\mathbf{u}_j^k \in \mathbb{R}^m$ denote the value of $\mathbf{u}(t)$ over the j-th time interval in the k-th iteration, and let

$$\mathbf{u}^k \quad := \quad \left[\begin{array}{ccc} \mathbf{u}_1^{k\,T} & \ldots & \mathbf{u}_K^{k\,T} \end{array} \right]^T. \tag{3.20}$$

An optimal solution to **Problem 1** can be found by iteratively improving upon an initial choice of $\mathbf{u}^k$ in a steepest descent[2] method

$$\tilde{\mathbf{u}}^{k+1} \quad = \quad \mathbf{u}^k + \delta^k \frac{dJ^T}{d\mathbf{u}^k}(\mathbf{u}^k), \tag{3.21}$$

$$u_j^{k+1} \quad = \quad \max\left(u_{\min,j} \, , \, \min\left(u_{\max,j} \, , \, \tilde{u}_j^{k+1} \right) \right), \quad j = 1, \ldots, mK. \tag{3.22}$$

Here, $\tilde{u}_j^k$ denotes the j^{th} component of $\tilde{\mathbf{u}}^k$, u_j^k the j^{th} component of $\mathbf{u}^k$ and δ_k the step size. Note that (3.22) is to ensure that $\mathbf{u}^{k+1}$ leads to an allowable control (*i.e.* within the required upper and lower bounds). $\frac{dJ}{d\mathbf{u}^k}$ is the (total) derivative of J, whose components are given by

$$\frac{\partial J}{\partial u_{j,i}^k}(\mathbf{u}^k) = \int_{t=(j-1)T/K}^{jT/K} \frac{\partial H}{\partial u_{j,i}}^T (\mathbf{x}(t), \mathbf{u}(t), \boldsymbol{\lambda}(t), t) \; dt. \tag{3.23}$$

[2]This is a slight abuse of terminology since, strictly speaking, it is only a 'steepest' descent method if there are no active constraints on $\mathbf{u}^k$.

for $j = 1, \ldots, K$ and $i = 1, \ldots, m$. Although it has the obvious advantage of being easy to implement, the steepest descent method is known for its slow convergence near an optimal solution. There are other methods that have better convergence properties, but these are not considered here.

3.5.2 Switching time methods

If we assume that the optimal solution to **Problem 1** is a bang-bang control, we can in principle very efficiently parameterize the control in terms of switching times. An optimal solution can then be found by iteratively improving upon an initial choice of the switching times, for example again using a steepest descent method. There are several methods to compute optimal bang-bang controls which focus on finding the optimal number and value of switching times, such as

- the Switching-Time-Variation Method (STVM) of Mohler (1973),
- the method of Glashoff and Sachs (1977),
- the Switching Time Optimization (STO) of Meier and Bryson (1990),
- the Switching Time Computation of Lucas and Kaya (2001).

A major challenge, however, is that the optimal number of switching times is not known beforehand. For regular optimal control problems involving linear n^{th}-order systems, it has been proven that the optimal solution has at most n switching times - see Bellman (1956) and Athans and Falb (1966). In Sussmann (1979), these results have been extended to problems involving nonlinear systems. Unfortunately, they are not of much practical use, since in our intended application n is in the order of $10^4 - 10^6$.

In all of the previously mentioned methods, the initial number of switching times is therefore set a priori. In light of this drawback we propose the following alternative descent method, which is a slight deviation from (3.21)-(3.22).

3.5.3 Alternative descent method

Choose an initial bang-bang control $\mathbf{u}^k$, and iteratively improve upon it in the following descent method

$$
\begin{aligned}
u_{j,i}^{k+1} &= u_{j,i}^k + h_{j,i}^k \,\text{sign}\left(\frac{\partial J}{\partial u_{j,i}^k}(\mathbf{u}^k)\right), \qquad (3.24)\\
h_{j,i}^k &= \begin{cases} u_{\max,i} - u_{\min,i} & \text{if } j,i \text{ is in } \Omega_1^k \\ 0 & \text{if } j,i \text{ is not in } \Omega_1^k \end{cases}\\
\Omega_1^k &= \text{set of indices of } \tilde{\delta}^k \text{ largest components of } \Omega_2\\
\Omega_2^k &= \text{set of } \left|\frac{\partial J}{\partial u_{j,i}^k}(\mathbf{u}^k)\right| \text{ for which } u_{j,i}^k \text{ is not aligned with } \frac{\partial J}{\partial u_{j,i}^k}(\mathbf{u}^k).
\end{aligned}
$$

Roughly speaking, this amounts to abruptly switching the $\tilde{\delta}^k$ most important components of $\mathbf{u}^k$ that are not yet aligned as in Figure 3.1 from one lower / upper bound to the other, until either the set Ω_2^k is empty (and the solution satisfies the necessary optimality conditions) or there is no more improvement (and the solution is suboptimal). $\tilde{\delta}^k$ can be viewed as the step size. The advantage of this method is that it does not work with switching times, while $\mathbf{u}^k$ (and thereby $\mathbf{u}$) is still a bang-bang control at each iteration and can therefore be implemented with simple on-off valves instead of variable-setting ones.

3.6 Application

Description

Consider a water flooding application of a 3-dimensional oil-water reservoir in a fluvial depositional environment. It is modeled with 18.553 grid blocks of dimension 20m×20m×20m, and there are 7 vertical layers. Figure 2.3 depicts the permeability field, together with the location of 12 vertical wells.

The modeling is as in Chapter 2, but with gravity effects. Geological and fluid properties are given in Table 3.1. The relative permeability curves are depicted in Figure 3.2.

Symbol	Value	Unit
ϕ	0.20	[-]
ρ_{o}(400 bar)	800 and 1000	[kg / m^3]
ρ_{w}(400 bar)	1000	[kg / m^3]
c_{o}	10^{-5}	[1 / bar]
c_{w}	10^{-5}	[1 / bar]
μ_{o}	10^{-3}	[Pa s]
μ_{w}	10^{-3}	[Pa s]
p_{bh}^j	390 - 415	[bar]
$\bar{\mathbf{p}}_0$	hydrostatic at 400m	[bar]
$\bar{\mathbf{S}}_0$	$0.10, \ldots, 0.10$	[-]

Table 3.1: Values of geological and fluid properties.

The well specifications are as follows:

- Each well is available as of time $t = 0$.
- Each well is vertical, and is perforated in all 7 layers of the reservoir.
- Each well operates at constant bottom-hole pressure. For the 8 injectors, the bottom-hole pressure is set to 415 bar at the lowest perforation. For the 4 producers, the bottom-hole pressure is set to 390 bar at the highest perforation.

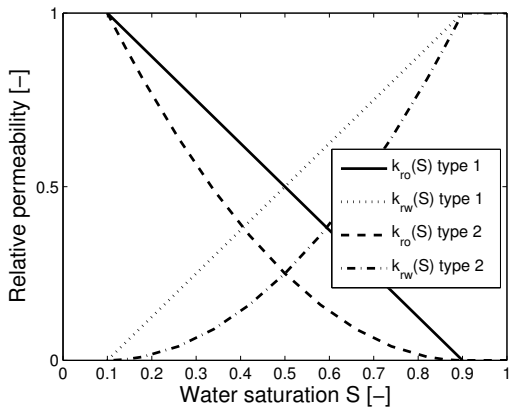

Figure 3.2: Relative permeabilities for cases in Table 3.3.

The pressures in the other perforations are computed assuming hydrostatic equilibrium in the wellbore.

- Each well is equipped with a single valve, whose setting can vary between 10^{-6} (a lower bound of 0 leads to numerical problems) and 1. In other words,

$$\mathcal{U} := \{\mathbf{w} \in \mathbb{R}^{12} : \ 10^{-6} \ \leq \ w_k \ \leq \ 1 \ , \ k = 1, \ldots, 12\}.$$

- The valve setting of a well applies to all 7 perforations.
- The well indices w^j are computed using a Peaceman model (2.21) with a wellbore radius $r_{\mathrm{w}} = 0.1$m and skin factor $S = 0$.

The initial pressure in the reservoir is computed assuming hydrostatic equilibrium, with the top of the reservoir at a depth of 4000m and at a pressure of 400 bar. Note that due to the constant bottom-hole pressures in the wells, the pressure in the reservoir always stays between 390 bar and 415 bar. The initial water saturation is 0.10 throughout the reservoir.

The performance measure is J_{npv} as defined in (3.2), using the values in Table 3.2. The goal is to maximize J_{npv} by varying the valve settings of the 8 injectors and 4 producers over the interval $[0, T]$. Three different terminal times are considered: 1.5, 3.0, and 4.5 years. These reservoir flooding problems can be written as **Problem 1**, and we aim to find optimal solutions for each of them using the conventional and steepest descent methods described in the previous sections.

The previously described model is implemented in the Shell proprietary reservoir simulator MoReS that also comprises the required adjoint model to compute gradients. The differential equations described in Section 3.2 are discretized using a fully-implicit scheme, with a maximum time-step size of $1/50$ year (≈ 1 week).

Symbol	Value	Unit
r_{oil}	20	[\$ / bbl]
r_{prod}	5	[\$ / bbl]
r_{inj}	0 and 1	[\$ / bbl]
d	0	[-]
T	1.5, 3.0 and 4.5	[years]

Table 3.2: Values for computing J_{npv}.

Results

The base case comparison is a conventional so-called reactive water flooding strategy. Here, all valve settings are initially one, but a producer valve setting is shut in (*i.e.* closed, and stays closed) when it is no longer profitable to produce from it. With $r_{\text{oil}} = 20$ \$/bbl and $r_{\text{prod}} = 5$ \$/bbl, this profitability threshold corresponds to a water cut of 80%.

In order to find optimal valve settings, the conventional steepest descent method (3.21)-(3.22) is used, with $\mathbf{u}$ also divided into intervals of $1/50$ year and initial guess $\mathbf{u}^k = 1$. At each iteration k, the step size δ^k is repeatedly reduced by a factor 2 until $J(\mathbf{u}^{k+1}) \geq J(\mathbf{u}^k)$, whereupon it is increased by a factor 1.6 for the beginning of the next iteration. Initially, δ^k is set to 10^{-5}.

The effects of terminal time, oil density, relative permeability, and water injection cost on the shape of the optimal solution are investigated by considering 6 numerical examples defined in Table 3.3, where results are also summarized.

Case	T [years]	Type of relperm	r_{inj} [\$ / bbl]	ρ_{o} [kg / m^3]	Type of control	Shape of control	J_{npv} [billion \$]	Increase [%]
1	1.5	2	0	800	reactive optimal	 bang-bang	1.350 1.365	 0.8
2	3.0	2	0	800	reactive optimal suboptimal	 singular bang-bang	1.871 1.934 1.933	 3.4 3.3
3	3.0	2	0	1000	reactive optimal suboptimal	 singular bang-bang	1.832 1.893 1.892	 3.3 3.3
4	3.0	2	1	800	reactive optimal suboptimal	 singular bang-bang	1.736 1.822 1.821	 5.0 4.9
5	3.0	1	0	800	reactive optimal suboptimal	 singular bang-bang	1.988 2.070 2.070	 4.1 4.1
6	4.5	1	1	1000	reactive optimal suboptimal	 singular bang-bang	1.900 2.140 2.119	 12.6 11.5

Table 3.3: J_{npv} and shape of reactive, optimal (*i.e.* using the steepest descent method) and suboptimal (*i.e.* using the alternative descent method) controls. The third column refers to the type of relative permeability used from Figure 3.2, T denotes the terminal time, r_{inj} the water injection cost and ρ_{o} the oil density.

For Case 1, the scheme indeed converges to a pure bang-bang control. We stress that this procedure could converge to a smooth solution, but does not because the optimal solution is apparently a pure bang-bang control. The optimal control for Case 1, denoted by $\mathbf{u}^*$, is depicted in Figure 3.3. The first order necessary optimality conditions are satisfied for $\mathbf{u}^*$, as can be seen by inspection of the sign of the corresponding switching function $\boldsymbol{\beta}^*$. At first sight, the resulting strategy for the producers seems to be a reactive one. In fact this is not true: the second producer valve is shut in at a water cut of 60% - far below the profitability threshold of 80%.

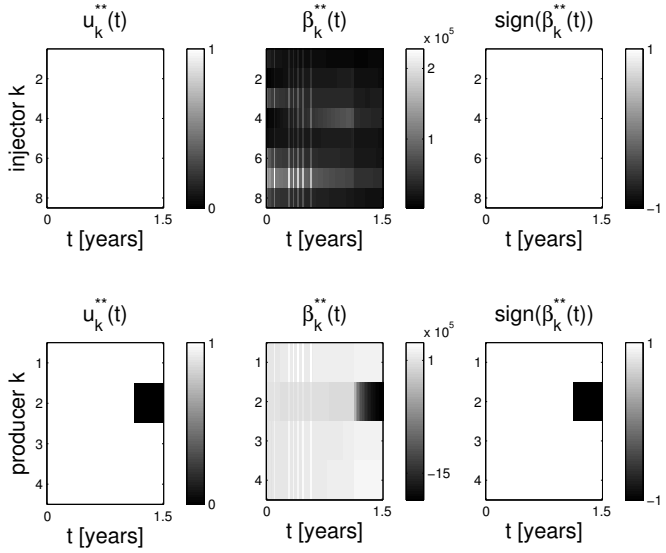

Figure 3.3: Optimal valve settings $\mathbf{u}^*$ and (sign of) the corresponding switching function $\boldsymbol{\beta}^*$ for Case 1.

From Figure 3.3, it can be seen that $\mathbf{u}^*$ satisfies the assumptions (a)-(d) in Section 3.4, and we can therefore check second order sufficient optimality conditions. Clearly, $\mathbf{u}^*$ has only one switching time at $\boldsymbol{\tau}^* = 1.12$ years for producer 2. Figure 3.4 shows that $\frac{\partial^2 J}{\partial \boldsymbol{\tau}^2}(\boldsymbol{\tau}^*) < 0$. In other words, $\mathbf{u}^*$ really is locally optimal.

For Cases 2-6, the scheme does not converge to a bang-bang control, but to one with short singular arcs for certain injectors. This situation is depicted for Case 2 in Figures 3.5 and 3.6.[3]

The improvement in J_{npv} of the optimal control compared to the reactive control is up to 12.6% - see Table 3.3. The cumulative oil and water production of both strategies for Case 6 are shown in Figure 3.7. Since there is no discount factor in-

[3] $\beta_1^{**}(t)$ is almost, but not identically, zero for $t \in [1.58, 2.52]$. This is why its sign is not gray in Figure 3.5.

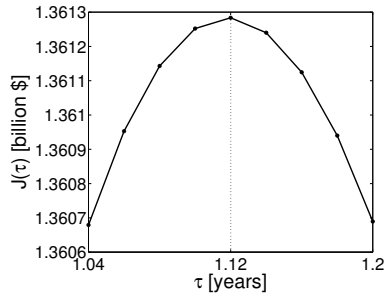

Figure 3.4: J_{npv} as a function of the switching time $\boldsymbol{\tau}$.

volved ($d = 0$), the increase in J_{npv} is solely due to a decrease in water production.

Improved valve settings can also be found using the alternative descent method (3.24), with $\mathbf{u}$ again divided into intervals of $1/50$ year and initial guess $\mathbf{u}^k = 1$. At each iteration k, the step size $\tilde{\delta}^k$ is repeatedly reduced by a factor 2 (and rounded off to the nearest integer) until $J(\mathbf{u}^{k+1}) \geq J(\mathbf{u}^k)$, whereupon it is increased by a factor 1.6 (and rounded off to the nearest integer) for the beginning of the next iteration. Initially, $\tilde{\delta}^k$ is set to 30.

For Case 1, the scheme converges to the same solution as that obtained with the steepest descent method. For the other situations, however, the scheme converges to a solution that is only slightly suboptimal (meaning with only a small loss in J_{npv}) - see Table 3.3. Obviously, this loss in NPV must be traded-off against the practical advantage of being able to implement the solution with simple on-off control valves.

Remarks:

- By comparing the optimal solution of Case 2 to Case 3, it does not seem that oil density has a significant effect on the shape of the optimal solution. However, we do expect singular arcs to play a significant role in coning problems, where it is common to operate wells below the highest allowable rate - Hoyland et al. (1989).

- By comparing the optimal solution of Case 2 to Case 4, it does not seem that water injection costs have a significant effect on the shape of the optimal solution.

- By comparing the optimal solution of Case 1 ($T = 1.5$ years) to Cases 2-5 ($T = 3.0$ years) to Case 6 ($T = 4.5$ years), we conclude that later terminal times generally lead to more and longer singular arcs. It would be interesting to see if this holds for problems with significant discounting in J_{npv}.

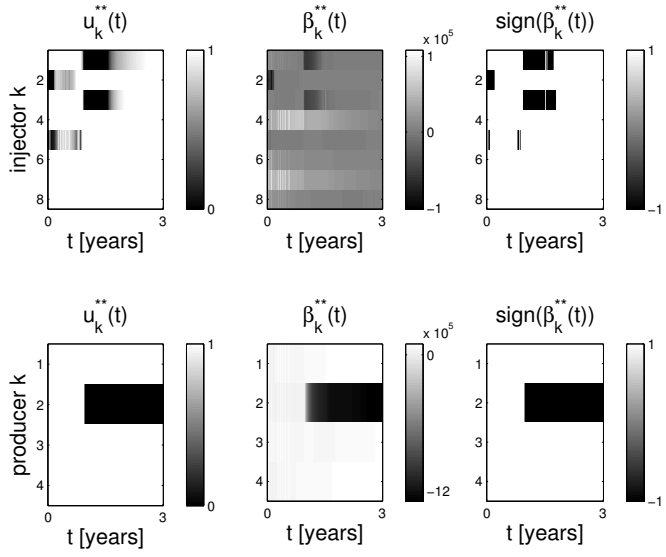

Figure 3.5: Optimal valve settings $\mathbf{u}^{**}$ and (sign) of the corresponding switching function $\boldsymbol{\beta}^{**}$ for Case 2.

- Problems with type 1 relative permeabilities (see Figure 3.2) generally have more and longer singular arcs than those with type 2 relative permeabilities.
- For Case 1, several (very similar) solutions were found that all satisfy the necessary conditions for optimality. The one shown in Figure 3.3 is the one with the highest J_{npv}.
- From the results in Table 3.3, we conclude that there is more scope for optimization in problems with later terminal times, type 1 relative permeabilities and, in particular, higher water injection costs.

3.7 Chapter conclusions

Many production setting optimization problems can be written as optimal control problems that are linear in the control. If the only constraints are upper and lower bounds on the control, due to their particular structure, these problems will sometimes have bang-bang optimal solutions. This is supported by a water flooding example, where for various situations the optimal solution is either bang-bang, or a bang-bang solution exists that is only slightly suboptimal. This has obvious practical implications, since bang-bang solutions can be implemented with simple on-off control valves.

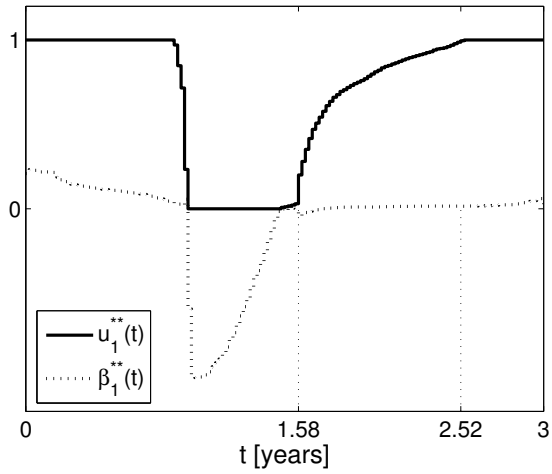

Figure 3.6: Valve settings u_1^{**} and (scaled) switching function β_1^{**} of injector 1 from Figure 3.5; there is a singular arc along the interval $[1.58, 2.52]$.

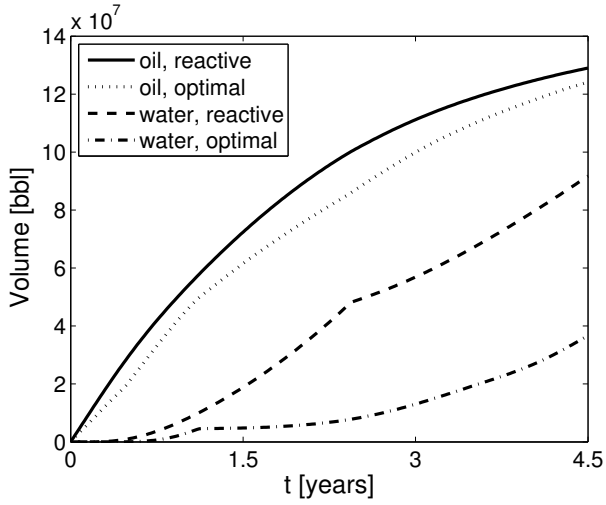

Figure 3.7: Cumulative oil and water production of the reactive and optimal control for Case 6.

4 CHAPTER

Robust Optimization of Production Settings

This chapter focuses on the application of robust optimization to find production settings that are robust against uncertainty in reservoir models. First, robust performance measures are discussed, followed by a gradient-based optimization procedure to find optimal solutions. The main contribution of this chapter is to demonstrate that the method can be used to find production settings that are robust against uncertainty as defined by an entire class of models within a geological structure, and not just its representation by a limited number of models. An application is given to illustrate these results.

4.1 Problem formulation

As discussed in Section 2.3, reservoir models generally contain a significant amount of uncertainty originating from many different sources and, as depicted in Figure 2.5, this can have a large influence on the predictions of future production. As a result, production settings based on a reservoir model that is 'far' from reality using the optimization procedure of Chapter 3 might be suboptimal when applied to the true reservoir. It therefore makes sense to define the performance of production settings not in terms of the performance of a single reservoir model, but in terms of the performance of an entire class of possible models.

Consider the model structure (2.37). For a given choice of the well production settings $\mathbf{u}$, a performance measure J of the form (3.3) now also depends on $\boldsymbol{\theta}$ through the state trajectory resulting from (2.37). In other words, we can write $J = J(\mathbf{u}, \boldsymbol{\theta})$. Figure 4.1(a) depicts such a (fictional) dependency for two uncertain parameters.

Let us assume that a cumulative density function (cdf) for $\boldsymbol{\theta}$ has been determined, either through an identification / history matching procedure, or by engineering judgement - see for example Figure 4.1(b). Such a cdf for $\boldsymbol{\theta}$ and a (deterministic) control $\mathbf{u}$ together now determine a cdf for the performance J. This is depicted in Figure 4.1(c), which is the result of combining the (again, fictional) cdf's of θ_1 and θ_2 in Figure 4.1(b) with Figure 4.1(a).

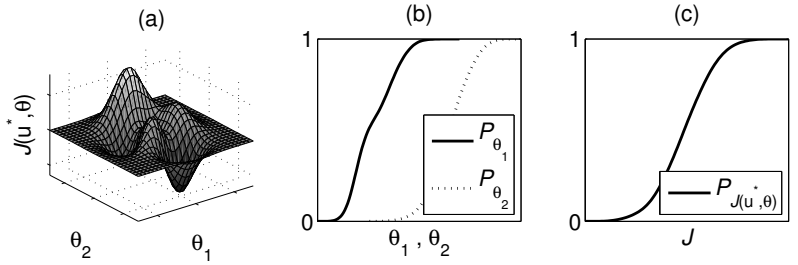

Figure 4.1: (a) Performance J as function of uncertain parameters θ_1 and θ_2, assumed to be uncorrelated, for given control $\mathbf{u}^*$, (b) cdf's of θ_1 and θ_2, and (c) resulting cdf of J.

In practice, an oil company will of course only develop a particular field if the cdf of the performance is favorable enough (*e.g.* if the expected value of J is above and the variance below certain thresholds.) Note that we can influence the cdf of J (*e.g.* Figure 4.1(c)) through both estimation (*e.g.* Figure 4.1(b)) and control (*e.g.* Figure 4.1(a)). In this chapter we only consider the latter possibility by applying so-called robust optimization: an approach often applied to batch processes in the chemical process industry - Terwiesch et al. (1994), Ruppen et al. (1995) Srinivasan et al. (2002a), Terwiesch et al. (1998).

The first step in robust optimization is to establish a so-called robust performance measure, denoted by $\tilde{J}$, which quantifies how good a certain control is for an entire class of models. There are many different types of robust performance measures - see Samsatli et al. (1998) for an overview. Two common ones are the expected value and the worst-case, denote by $\tilde{J}_{\mathrm{av}}$ and $\tilde{J}_{\mathrm{wc}}$, respectively, defined as

$$\tilde{J}_{\mathrm{av}}(\mathbf{u}) := E\left[J(\mathbf{u},\boldsymbol{\theta})\right], \tag{4.1}$$

$$\tilde{J}_{\mathrm{wc}}(\mathbf{u}) := \min_{\boldsymbol{\theta}} J(\mathbf{u},\boldsymbol{\theta}). \tag{4.2}$$

The main idea of robust optimization is to maximize $\tilde{J}$ over all allowable $\mathbf{u}$. However, as discussed in Section 2.3, it is virtually impossible to accurately determine the cdf of $\mathbf{x}$ (and thereby of J) which is why it is common to decide upon a few sources of uncertainty that presumably have the largest impact on the predictions of future production as well as a few of their values. As before, let us denote these values by $\boldsymbol{\theta}_1,\ldots,\boldsymbol{\theta}_L$ and their individual probabilities by $w_1,\ldots,w_L > 0$, where $\sum_{i=1}^{L} w_i = 1$. The set of values is denoted by $\Theta := \{\boldsymbol{\theta}_1,\ldots,\boldsymbol{\theta}_L\}$. The result of

this discretization is depicted in Figure 4.2(a), which shows several distinct pairs $(\boldsymbol{\theta}_i, J(\mathbf{u}^*, \boldsymbol{\theta}_i))$ based on Figure 4.1(a). These pairs can be combined with the probabilities w_i, depicted by cdf's in Figure 4.2(b) to form a cdf of J depicted in Figure 4.2(c). Hopefully, Figure 4.2(c) is a reasonable approximation of Figure 4.1(c).

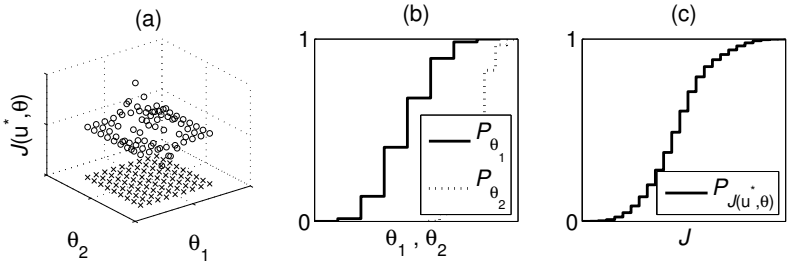

Figure 4.2: (a) Values of J ($\circ$) for specified values of θ_1 and θ_2 ($\times$) and given control $\mathbf{u}^*$, (b) cdf's of θ_1 and θ_2, and (c) resulting cdf of J.

We can now approximate $\tilde{J}_{\text{av}}$ and $\tilde{J}_{\text{wc}}$ by

$$\bar{J}_{\text{av}}(\mathbf{u}) := \sum_{i=1}^{L} w_i J(\mathbf{u}, \boldsymbol{\theta_i}) \tag{4.3}$$

$$\bar{J}_{\text{wc}}(\mathbf{u}) := \min_{\boldsymbol{\theta_i}} J(\mathbf{u}, \boldsymbol{\theta_i}), \quad \boldsymbol{\theta_i} \in \Theta, \tag{4.4}$$

or, more generally, we can approximate the robust performance $\tilde{J}$ by

$$\bar{J}(\mathbf{u}) := \varphi\left(J(\mathbf{u}, \boldsymbol{\theta}_1), \ldots, J(\mathbf{u}, \boldsymbol{\theta}_L)\right), \tag{4.5}$$

for some function φ. Instead of maximizing $\tilde{J}$, we can now solve the much easier problem

Problem 3

$$\begin{aligned}
\text{maximize} \quad \bar{J}(\mathbf{u}) &= \varphi\left(J(\mathbf{u}, \boldsymbol{\theta}_1), \ldots, J(\mathbf{u}, \boldsymbol{\theta}_L)\right) \\
\text{over} \quad \mathbf{u} &\in \mathcal{L}_m^1[0, T] \\
\text{subject to } J(\mathbf{u}, \boldsymbol{\theta}_i) &= \psi(\mathbf{x}_i(T), T) + \int_0^T \left\{ l_1(\mathbf{x}_i(t), t) + \mathbf{l}_2^T(\mathbf{x}_i(t), t)\mathbf{u}(t) \right\} dt, \\
\dot{\mathbf{x}}_i(t) &= \mathbf{f}_1(\mathbf{x}_i(t), \boldsymbol{\theta}_i) + \mathbf{f}_2(\mathbf{x}_i(t), \boldsymbol{\theta}_i)\mathbf{u}(t), \\
\mathbf{x}_i(0) &= \bar{\mathbf{x}}_0, \ i = 1, \ldots, L, \\
\mathbf{u}(t) &\in \mathcal{U} \ \forall\, t \in [0, T], \\
\mathcal{U} &= \left\{ \mathbf{w} \in \mathbb{R}^m : \ \mathbf{u}_{\min} \leq \mathbf{w} \leq \mathbf{u}_{\max} \right\}, \\
\sum_{j=1}^{m} u_j(t) &= 0 \ \forall\, t \in [0, T],
\end{aligned}$$

where, as in Chapter 3, we have defined

$$\mathbf{f}_1(\mathbf{x}_i(t), \boldsymbol{\theta}_i) := \bar{\mathbf{A}}(\mathbf{x}_i(t), \boldsymbol{\theta}_i)\mathbf{x}_i(t), \tag{4.6}$$
$$\mathbf{f}_2(\mathbf{x}_i(t), \boldsymbol{\theta}_i) := \bar{\mathbf{B}}(\mathbf{x}_i(t), \boldsymbol{\theta}_i). \tag{4.7}$$

Note that, when compared to **Problem 1**, **Problem 3** contains an additional equality constraint on the control $\mathbf{u}$. This is because in this chapter we consider injection and production flow rates as controls (*i.e.* the q^j terms), whereas valve settings (*i.e.* the α^j terms) are considered as controls in the previous chapter. The equality constraint states that at all times the total injection rate (over all wells) must equal the total production rate, which ensures that the average pressure in the reservoir stays more or less the same. The choice of flow rates over valve settings as control here is purely pragmatic: the adjoint model to compute gradients with respect to flow rates was available while conducting this particular research; the adjoint model to compute gradients with respect to valve settings was not.

There are several applications of robust optimization in the literature. Yeten et al. (2004) considered 5 realizations of the subsurface heterogeneity and risk of ICV failure as uncertainty, production settings as control, and decided on wether or not to deploy these ICV's using a decision-tree analysis. Guyaguler and Horne (2004) considered 23 realizations of the subsurface heterogeneity as uncertainty, well locations as control, and used a hybrid genetic algorithm to find optimal solutions. Aitokhuehi et al. (2004) considered 2 realizations of the subsurface heterogeneity as uncertainty, the well type, location and trajectory as controls, and used a genetic algorithm to find optimal solutions.

Interestingly, no-one has yet investigated robust optimization of production settings using a gradient-based procedure where the gradients are computed using an adjoint model (*i.e.* using (3.23) in Chapter 3). Furthermore, the robustness of the outcome in the previously mentioned applications is never validated against a different set of possible reservoir models (*i.e.* a different choice for Θ). In this sense it must still be demonstrated that robust optimization can reduce the effect of uncertainty as defined by an entire class of models, and not just its representation by a limited number of them. The main contribution of this chapter is to demonstrate that this can indeed be done.

4.2 Optimization method

An algorithm similar to the steepest descent method for solving **Problem 1** in Chapter 3 can be used to efficiently solve **Problem 3**. As before, let $\mathbf{u}$ be divided into K equal intervals over $[0, T]$, let $\mathbf{u}_j^k \in \mathbb{R}^m$ denote the value of $\mathbf{u}(t)$ over the j-th time interval in the k-th iteration, and let

$$\mathbf{u}^k := \left[\begin{array}{ccc} \mathbf{u}_1^{k\,T} & \ldots & \mathbf{u}_K^{k\,T} \end{array} \right]^T. \tag{4.8}$$

An optimal solution to **Problem 3** is then found by iteratively improving upon an initial choice of $\mathbf{u}^k$ using a gradient-based procedure. The gradient $\frac{\partial \bar{J}}{\partial \mathbf{u}^k}$ is given by

$$\begin{aligned}\frac{\partial \bar{J}}{\partial \mathbf{u}^k}(\mathbf{u}^k) &= \frac{\partial \varphi}{\partial \mathbf{u}^k}\left(J(\mathbf{u}^k,\boldsymbol{\theta}_1),\ldots,J(\mathbf{u}^k,\boldsymbol{\theta}_L)\right) \\ &= \begin{bmatrix} \frac{\partial J}{\partial \mathbf{u}^k}(\mathbf{u}^k,\boldsymbol{\theta}_1) & \ldots & \frac{\partial J}{\partial \mathbf{u}^k}(\mathbf{u}^k,\boldsymbol{\theta}_L) \end{bmatrix} \underbrace{\begin{bmatrix} \frac{\partial \varphi}{\partial J}(\mathbf{u}^k,\boldsymbol{\theta}_1) \\ \vdots \\ \frac{\partial \varphi}{\partial J}(\mathbf{u}^k,\boldsymbol{\theta}_L) \end{bmatrix}}_{=:\frac{\partial \varphi}{\partial J}(\mathbf{u}^k)}\end{aligned} \tag{4.9}$$

where $\frac{\partial J}{\partial \mathbf{u}^k}(\mathbf{u}^k,\boldsymbol{\theta}_i)$ can be computed with (3.23) using the state and adjoint trajectory pair $(\mathbf{x}_i,\boldsymbol{\lambda}_i)$ corresponding to $\boldsymbol{\theta}_i$ for $i=1,\ldots,L$. Note that for $\bar{J}_{\text{av}}$ we have $\frac{\partial \varphi}{\partial J}(\mathbf{u}^k) = \begin{bmatrix} w_1 & \ldots & w_L \end{bmatrix}^T$, whereas for $\bar{J}_{\text{wc}}$ we have $\frac{\partial J}{\partial \mathbf{u}^k}(\mathbf{u}^k,\boldsymbol{\theta}_i) = 1$ if $J(\mathbf{u}^k,\boldsymbol{\theta}_i) < J(\mathbf{u}^k,\boldsymbol{\theta}_j)\ \forall\, j \neq i,\ j \in \{1,\ldots,L\}$ and 0 otherwise.

However, $\frac{\partial \bar{J}}{\partial \mathbf{u}^{k^k}}$ might not be a feasible direction due to the constraints on the control. Recall that, for **Problem 1**, this was solved by 'clipping' the control as in (3.22). However, this will not work for **Problem 3** due to the additional equality constraint. We therefore use the so-called gradient projection method

$$\mathbf{u}^{k+1} = \mathbf{u}^k + s^k \mathbf{d}^k, \tag{4.10}$$

where $\mathbf{d}^k$ denotes the projection of the gradient $\frac{\partial \bar{J}}{\partial \mathbf{u}^k}$ onto the set of feasible directions and s_k is the step size. The projection is given by

$$\mathbf{d}^k = \left[I + \mathbf{U}^T\left(\mathbf{U}\mathbf{U}^T\right)^{-1}\mathbf{U}\right]\frac{\partial \bar{J}}{\partial \mathbf{u}^k}(\mathbf{u}^k). \tag{4.11}$$

where $\mathbf{U}$ is a matrix consisting of the rows of active constraints - see Luenberger (1973). For the equality constraint in **Problem 3** this means that $\mathbf{U}$ has one row consisting of ones. For the inequality constraints $\mathbf{U}$ has an additional row of zero's for each component of the control that is on the boundary of $\mathcal{U}$, with a $+1$ at the appropriate entry if $u^k_{j,i} = u_{\max,i}$, and a -1 if $u^k_{j,i} = u_{\min,i}$. The advantage of (4.10) - (4.11) is that $\mathbf{u}^{k+1}$ always satisfies the equality constraint, and also satisfies the inequality constraints for sufficiently small $s^k \geq 0$.

4.3 Generating subsurface realizations

Of the various sources of model uncertainty discussed in Section 2.3, the spatial distribution of permeability often has a significant impact on the fluid flow throughout a reservoir, and thereby on the production of oil, gas and water. A particular choice of the permeability (*e.g.* made by a geologist) is often referred to as a realization, and there are many methods to generate such realizations -

see de Marsily et al. (2005) for a historical overview. The applicability of a certain method obviously depends on the type of reservoir at hand, and the type of available measurements (*e.g.* seismics, well core samples, well logs). Besides these measurements, a geologist will often have an idea of the geological structure of a particular reservoir. This can be based on comparable reservoirs in the same region, on knowledge of the depositional environment, or on outcrops.

An example of such a geological structure is a

> *"fluvial depositional environment with meandering channels in the main flow direction North-South."*

This is of course a very loose description, which any number of realizations can satisfy - see for example the 6 realizations in Figure 2.4. These realizations were simply drawn by hand (*i.e.* are not based on a specific stochastic distribution) and all look very similar. We could create an infinite number of such realizations, and the challenge is to find production settings that perform well (in some sense) for all of them.

4.4 Application

Description

We consider a water flooding application of a 3-dimensional oil-water reservoir that is very similar to the one considered in Section 3.6. It has the same shape, the same configuration of wells, and is modeled by the same number of grid blocks. The main difference is that the grid block dimension is smaller: 8m×8m×4m as opposed to 20m×20m×20m previously. Geological and fluid properties are given in Table 3.1. Only one oil density is considered: $\rho_{\mathrm{o}} = 1000$ kg/m^3. The Type 1 curves from Figure 3.2 are used for the relative permeability.

The well specifications are as follows. Each well is available as of time $t = 0$, vertical, and is perforated in all 7 layers of the reservoir. The flow rate in each individual well can be directly controlled, between 0.1 bbl/day (a lower bound of 0 leads to numerical problems) and 400 bbl/day. In other words,

$$\mathcal{U} := \{\mathbf{w} \in \mathbb{R}^{12} : \ 0.1 \ \leq \ w_k \ \leq \ 400 \ , \ k = 1, \ldots, 12\}.$$

For the permeability distribution we drew 200 realizations by hand, all satisfying the previously mentioned geological structure and therefore very similar to the ones depicted in Figure 2.4, and labeled them $\boldsymbol{\theta}_1, \ldots, \boldsymbol{\theta}_{200}$. In other words, $\boldsymbol{\theta}_i$ is a vector containing all the permeability values of the i^{th} drawing. These realizations

are subsequently split into the so-called optimization set $\Theta_{\rm opt}$ and validation set $\Theta_{\rm val}$, respectively defined as

$$\Theta_{\rm opt} := \{\boldsymbol{\theta}_1, \ldots, \boldsymbol{\theta}_{100}\}, \tag{4.12}$$

$$\Theta_{\rm val} := \{\boldsymbol{\theta}_{101}, \ldots, \boldsymbol{\theta}_{200}\}. \tag{4.13}$$

Within each set the realizations are assumed to be equiprobable (*i.e.* $w_i = 0.01$ for $i = 1, \ldots, 200$).

The robust performance measure is average Net Present Value, $\bar{J}_{\rm av}(\mathbf{u})$ as defined in (4.3), with $J(\mathbf{u}, \boldsymbol{\theta}_i) = J_{\rm npv}(\mathbf{u}, \boldsymbol{\theta}_i)$ as defined in (3.2) using the values in Table 4.1, and $\boldsymbol{\theta}_i \in \Theta_{\rm opt}$. Note that the realizations in $\Theta_{\rm val}$ are not used at this point.

Symbol	Value	Unit
$r_{\rm oil}$	20	[\$ / bbl]
$r_{\rm prod}$	3	[\$ / bbl]
$r_{\rm inj}$	1	[\$ / bbl]
d	0	[-]
T	10	[years]

Table 4.1: Values for computing $J_{\rm npv}$.

These reservoir models are implemented in a proprietary reservoir simulator that also comprises the required adjoint model to compute gradients. The differential equations described in Section 3.2 are approximated using a fully-implicit scheme, with a maximum time-step size of 1/16 year.

Results

The 100 realizations in $\Theta_{\rm opt}$ are used to build 100 reservoir models of the form (2.37). In this section, the robustness of three production setting strategies is evaluated using these models: a 'reactive' strategy $\mathbf{u}_{\rm re}$, a 'nominal' strategy $\mathbf{u}_{\rm no}$ and a 'robust' strategy $\mathbf{u}_{\rm ro}$.

In the reactive strategy $\mathbf{u}_{\rm re}$ all valve settings are initially one, but a producer valve setting is shut in (and stays shut in) when it is no longer profitable to produce from it. With $r_{\rm oil} = 20$ \$/bbl and $r_{\rm prod} = 3$ \$/bbl, this profitability threshold corresponds to a water cut of 87%. The injection and production flow rates are fixed at 200 bbl/day and 400 bbl/day, respectively. Because there are 8 injection and 4 production wells, these flow rates satisfy the equality constraint in **Problem 3**. When a producer well is shut in, the injection rate of each injection well is proportionally scaled down in order to satisfy the equality constraint. Due to its reactive nature, this strategy does not require any knowledge of the geological structure of the reservoir. It does, however, require water cut measurements in the producer wells, and formally we would have to write $\mathbf{u}_{\rm re} = \mathbf{u}_{\rm re}(\boldsymbol{\theta}_i)$ since the water cut indirectly depends on the permeability. We stress, however, that these measurements

are not used by the other strategies, and in this sense the reactive strategy has an advantage over them.

The nominal strategy $\mathbf{u}_{\rm no}$ is based on a single arbitrary reservoir model out of the set of 100 possible ones - in this case the model resulting from $\boldsymbol{\theta}_1$. It is found by applying the gradient-based method (4.10) - (4.11) to **Problem 3** with $\bar{J}(\mathbf{u}) = J(\mathbf{u}, \boldsymbol{\theta}_1)$. We expect that, while $\mathbf{u}_{\rm no}$ maximizes $J(\mathbf{u}, \boldsymbol{\theta_1})$, it will not maximize $\bar{J}_{\rm av}(\mathbf{u})$ (*i.e.* we expect that there exists a $\mathbf{u}$ such that $\bar{J}_{\rm av}(\mathbf{u}) > \bar{J}_{\rm av}(\mathbf{u}_{\rm no})$). We stress, however, that any other reservoir model would probably lead to a different $\mathbf{u}_{\rm no}$, and thereby different results.

The robust strategy $\mathbf{u}_{\rm ro}$ is based on all 100 reservoir models. It is found by applying the gradient-based method (4.10) - (4.11) to **Problem 3** with $\bar{J}(\mathbf{u}) = \bar{J}(\mathbf{u})_{\rm av} = \sum_{i=1}^{100} w_i J(\mathbf{u}, \boldsymbol{\theta}_i)$, with $w_i = 0.01$ since the models are assumed to be equiprobable. We expect that, while $\mathbf{u}_{\rm ro}$ maximizes $J_{\rm av}(\mathbf{u})$, it will not maximize $J(\mathbf{u}, \boldsymbol{\theta_1})$ (*e.g.* we expect that $J(\mathbf{u}_{\rm no}, \boldsymbol{\theta_1}) > J(\mathbf{u}_{\rm ro}, \boldsymbol{\theta_1})$).

For both the nominal and robust strategy, the control is divided into intervals of 1/16 year, and the initial choice $\mathbf{u}^{k=1}$ for the injection and production flow rates is 150 bbl/day and 300 bbl/day, respectively. At each iteration k, the step size s^k is initially set to 1 and then repeatedly reduced by a factor 2 until $\bar{J}(\mathbf{u}^{k+1}) \geq \bar{J}(\mathbf{u}^k)$ and $\mathbf{u}^{k+1} \in \mathcal{U}$.

The three strategies $\mathbf{u}_{\rm re}$, $\mathbf{u}_{\rm no}$ and $\mathbf{u}_{\rm ro}$ each lead to 100 state trajectories (one corresponding to each $\boldsymbol{\theta}_i \in \Theta_{\rm opt}$). The corresponding trajectories for cumulative production are depicted in Figure 4.3, and the resulting values for $\bar{J}_{\rm av}$ are summarized in Table 4.2. The resulting cdf's of J are depicted in Figure 4.4.

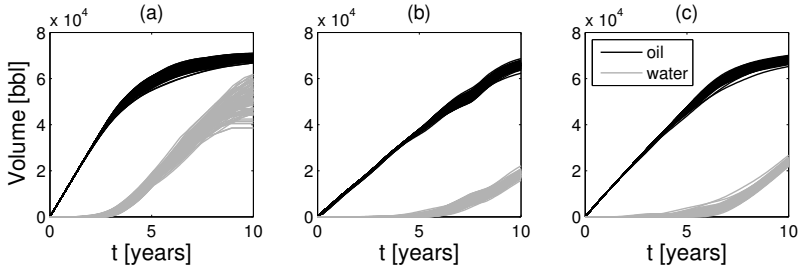

Figure 4.3: Cumulative production of all the reservoir models resulting from $\Theta_{\rm opt}$ with (a) reactive, (b) nominal, and (c) robust production settings.

The results are as expected. The nominal strategy is indeed the best in terms of the NPV of realization $\boldsymbol{\theta_1}$. The robust strategy, however, is the best in terms of the average NPV over the entire set $\Theta_{\rm opt}$. In other words, $\mathbf{u}_{\rm ro}$ is more robust (in an average sense) than $\mathbf{u}_{\rm re}$ and $\mathbf{u}_{\rm no}$ with respect to model uncertainty as defined

Production settings $\mathbf{u}$	$J(\mathbf{u}, \boldsymbol{\theta}_1)$ [million \$]	Increase [%]	$J_{\text{av}}(\mathbf{u})$ [million \$]	Increase [%]
Reactive $\mathbf{u}_{\text{re}}$	45.4		43.8	
Nominal $\mathbf{u}_{\text{no}}$	49.3	8.7	46.5	6.2
Robust $\mathbf{u}_{\text{ro}}$	48.4	6.6	47.8	9.1

Table 4.2: Performance of reactive, nominal, and robust strategies over Θ_{opt}.

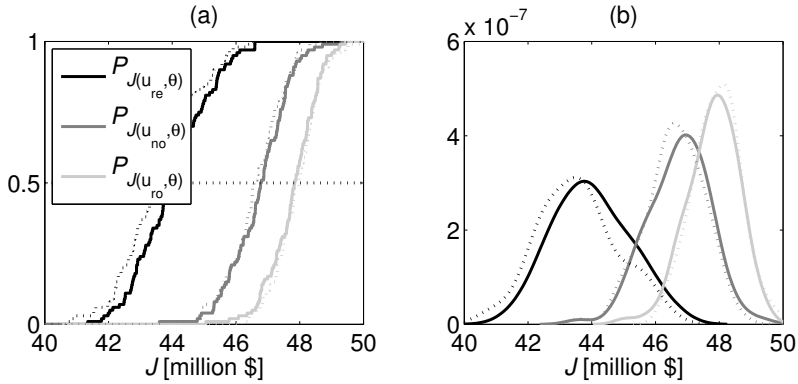

Figure 4.4: Cdf's (a) and approximated pdf's (b) of J based on Θ_{opt} (solid) and Θ_{val} (dotted) for reactive (black), nominal (dark gray) and robust (light gray) production settings.

by $\boldsymbol{\theta}_i \in \Theta_{\text{opt}}$. Yet we cannot claim that this will hold for a set of infinitely many realizations that satisfy the geological structure.

In order to make this claim more plausible, we apply the three strategies $\mathbf{u}_{\text{re}}$, $\mathbf{u}_{\text{no}}$ and $\mathbf{u}_{\text{ro}}$ to the 100 realizations in Θ_{val}. This again leads to three times 100 state trajectories (one corresponding to each $\boldsymbol{\theta}_i \in \Theta_{\text{val}}$), and the resulting cdf's of J are again depicted in Figure 4.4.

The cdf's of J are clearly very similar, indicating the following.

1. For this particular example, the true cdf of J (*i.e.* the one obtained with an infinite number of realizations) can be reasonably approximated with only 100 realizations. In other words, for this example, Figure 4.2(c) is indeed a reasonable approximation of Figure 4.1(c).

2. The production settings $\mathbf{u}_{\text{ro}}$ are indeed robust (in an average sense) with respect to uncertainty as defined by an entire class of models within a geological structure.

Similar results are obtained in van Essen et al. (2007), where the nominal strategies for all 100 realizations are computed and applied to both sets Θ_{opt} and Θ_{val}.

4.5 Chapter conclusions

The adjoint method to derive gradients of a cost function with respect to production settings as discussed in Chapter 3 can be combined with robust optimization to efficiently compute settings that are robust against uncertainty in reservoir models. A water flooding application demonstrates that production settings can be found that are robust against uncertainty as defined by an entire class of models within a geological structure, by optimizing over one set of 100 realizations of the permeability distribution, and validating over a second set of 100 realizations. However, in order to apply the approach presented in this chapter in practice, two important issues need to be addressed. First, as discussed in Chapter 2, there are many sources of uncertainty in reservoir models, while this chapter only considers the permeability distribution to be uncertain. It is clearly important to also investigate the effects of other sources of uncertainty. Second, in practice it will usually not be computationally tractable to perform a robust optimization over a set of 100 reservoir models. In this respect it is still unclear how to generate a *minimal* set of models that in some sense is representative of the entire uncertainty range.

5 CHAPTER

Optimal Well Placement

This chapter focuses on optimization of well locations. First, the effect of production settings on the well placement problem is analyzed. Then, as main contribution of this chapter, it is shown how the gradients used in production setting optimization - so efficiently derived using adjoint models - can also be used to find optimal well locations. Several applications are given to illustrate these results.

5.1 Problem formulation

Determining the number, type, location and trajectory of wells are among the most important decision factors in developing a reservoir, as they can cost up to several millions of dollars and to a large extent determine how much hydrocarbons will be produced. Their justification lies of course in the associated predictions of future hydrocarbon production, and these predictions are often based on models of the form (2.22) as discussed in Chapter 2.

Recall that these models consist of a finite number of grid blocks. For notational convenience, let us assume that such a reservoir model consists of $N = N_x N_y N_z$ grid blocks. Furthermore, let us assume that there are m vertical wells to be placed at time $t = 0$ and that their perforations are fixed (*e.g.* through all the N_z layers). As each well is vertical with predetermined perforations, the remaining degrees of freedom for each well are its production setting $u_i(t)$ from $t = 0$ to $t = T$, and its areal (*i.e.* horizontal, or xy) location. Let us number these locations by $1, \ldots N_x N_y$ and denote the set of all such locations by $\mathcal{N}_{xy}$,

$$\mathcal{N}_{xy} \quad := \quad \{1, \ldots, N_x N_y\}, \tag{5.1}$$

and the set of locations for m wells by $\mathcal{Z}$,

$$\mathcal{Z} \quad := \quad \{\underbrace{\mathcal{N}_{xy} \times \ldots \times \mathcal{N}_{xy}}_{m \text{ times}}\}. \tag{5.2}$$

Note that with this definition, several wells can be placed in one location. Let us denote the location of well i by $z_i \in \mathcal{N}_{xy}$ and a particular configuration of m wells by $\mathbf{z}$,

$$\mathbf{z} \;:=\; \begin{bmatrix} z_1 & \dots & z_m \end{bmatrix}^T \in \mathcal{Z}. \tag{5.3}$$

With this notation we can generalize (2.22) and write

$$\dot{\mathbf{x}}(t) = \bar{\mathbf{A}}(\mathbf{x}(t), \mathbf{z})\mathbf{x}(t) + \bar{\mathbf{B}}(\mathbf{x}(t), \mathbf{z})\mathbf{u}(t), \quad \mathbf{x}(0) = \bar{\mathbf{x}}_0. \tag{5.4}$$

A performance measure J of the form (3.3) now also depends on the well configuration $\mathbf{z}$ through the state trajectory resulting from (5.4). In other words, we can write $J = J(\mathbf{u}, \mathbf{z})$. We could try to maximize $J(\mathbf{u}, \mathbf{z})$ simultaneously over both $\mathbf{u}$ and $\mathbf{z}$. In the literature, such problems are often called mixed integer nonlinear programs (MINLP's), because they are nonlinear and involve a mixture of continuous decision variables $\mathbf{u}$ and discrete decision variables $\mathbf{z}$.

MINLP's frequently arise in the chemical process industry, and there are several methods to deal with them - see Kallrath (2000). Most of these methods, however, require far too many evaluations of the performance measure to be applicable to reservoir models. In practice, well locations are therefore invariably determined manually. There are, however, a few publications that consider maximizing $J(\mathbf{u}, \mathbf{z})$ using optimization methods. In addition to having predetermined number, type and perforations of the to-be-placed wells, a common assumption in these applications is that the production settings are fixed at, say, $\mathbf{u}^*$. Subsequently, $J(\mathbf{u}^*, \mathbf{z})$ is maximized over the well locations $\mathbf{z}$, thereby becoming an optimization problem involving discrete variables only. We will refer to this as the well placement problem, which can be written as follows

Problem 4

$$\begin{aligned}
\text{maximize } J(\mathbf{z}) &= \psi(\mathbf{x}(T), T) + \int_0^T \left\{ l_1(\mathbf{x}(t), t) + \mathbf{l}_2^T(\mathbf{x}(t), t)\mathbf{u}^*(t) \right\} dt \\
\text{over} \quad \mathbf{z} &\in \mathcal{Z} \\
\text{subject to } \dot{\mathbf{x}}(t) &= \mathbf{f}_1(\mathbf{x}(t), \mathbf{z}) + \mathbf{f}_2(\mathbf{x}(t), \mathbf{z})\mathbf{u}^*(t) \\
\mathbf{x}(0) &= \bar{\mathbf{x}}_0
\end{aligned}$$

where, as in Chapter 3, we have defined

$$\mathbf{f}_1(\mathbf{x}(t), \mathbf{z}) \;:=\; \bar{\mathbf{A}}(\mathbf{x}(t), \mathbf{z})\mathbf{x}(t), \tag{5.5}$$

$$\mathbf{f}_2(\mathbf{x}(t), \mathbf{z}) \;:=\; \bar{\mathbf{B}}(\mathbf{x}(t), \mathbf{z}). \tag{5.6}$$

We stress that **Problem 4** for $\mathbf{u}^*$ is different from the one for $\mathbf{u}^{**}$ if $\mathbf{u}^* \neq \mathbf{u}^{**}$.

The publications that consider the well placement problem can broadly be classified into local, or global optimization methods. Local optimization methods try

to iteratively improve upon an initial well configuration, much as in the previous optimization of production settings, until a local optimal solution[1] is reached. The main challenge in this application, again as in the optimization of production settings, is to effectively find improving directions[2] in which to alter the well configuration. Global methods, on the other hand, will sometimes tolerate lower performance measures in the hope of finding the global, as opposed to local, optimal solution.

Among the applications of global methods to the well placement problem are the following. Beckner and Song (1995) applied simulated annealing, Centilmen et al. (1999) neural networks, Bittencourt and Horne (1997), Montes et al. (2001) and Aitokhuehi et al. (2004) genetic algorithms, and Yeten (2003) a combination of the latter two. Although these applications have the virtue of simplicity (an optimization algorithm of choice is coupled with a reservoir simulator to evaluate the performance measure), they generally require many reservoir simulations to converge to an adequate solution.

Bangerth et al. (2006) compares two local methods for optimizing the location of vertical wells in a 2D reservoir model. The first one is the Finite Difference Gradient (FDG) method, which as the name suggests tries to find improving directions by perturbing each well location by one grid block in both the x and y direction. This has the obvious drawback of requiring $2m + 1$ reservoir simulations to compute an improving direction of m to-be-placed wells. The second method is the simultaneous perturbation stochastic approximation (SPSA) method of Spall (1992), which basically chooses a random direction in which to alter the wells and, if this does not yield an improvement in the performance measure, assumes that the opposite direction will. The obvious advantage is that an improving direction is almost always found in at most 2 reservoir simulations, with the disadvantage that this direction is generally far from the 'steepest' one.

In other words, an efficient method to find (almost) steepest improving directions using a very limited number of reservoir simulations is currently lacking. The main contribution of this chapter is to present such a method using the adjoint models derived in Chapter 3 for computing gradients in production setting optimization.

As mentioned earlier, all of the previously discussed applications in the literature solve **Problem 4** over the well locations $\mathbf{z}$ for fixed production settings $\mathbf{u}^*$. However, these production settings are often chosen to be constant - even after water has broken through in the production wells. In practice such a well is generally shut-in, yet this is often overlooked in the literature. This is surprising, as a well configuration $\mathbf{z}^*$ maximizing $J(\mathbf{u}, \mathbf{z})$ for $\mathbf{u} = \mathbf{u}^*$ may be far from optimal for a

[1] A well configuration is locally optimal if no improvement in the performance measure can be achieved by altering the location of a single well by a single grid block.

[2] The term 'improving directions' is used instead of 'gradient', because the latter is not defined for integer problems.

different choice of $\mathbf{u}$. Another contribution of this chapter is therefore to analyze the effect of production settings on the well placement problem.

5.2 Effect of production settings

We will investigate the effect of production settings through a water flooding example of a 2-dimensional oil-water reservoir, modeled by $21 \times 21 \times 1$ grid blocks of dimension 10m$\times$10m$\times$10m. Figure 5.1 depicts the permeability field. Geological and fluid properties are given in Table 5.1. The relative permeability curves are depicted in Figure 2.1. There are four producer wells whose location are fixed (one in each of the four corners), and one to-be-placed injector well.

Symbol	Value	Unit
ϕ	0.20	[-]
c_{o}, c_{w}	10^{-5}	[1 / bar]
μ_{o}, μ_{w}	10^{-3}	[Pa s]
ρ_{w}, ρ_{w}	1000	[kg / m^3]
$\bar{\mathbf{p}}_0$	$\begin{bmatrix} 400 & \dots & 400 \end{bmatrix}^T$	[bar]
$\bar{\mathbf{S}}_0$	$\begin{bmatrix} 0.10 & \dots & 0.10 \end{bmatrix}^T$	[-]

Table 5.1: Values of geological and fluid properties.

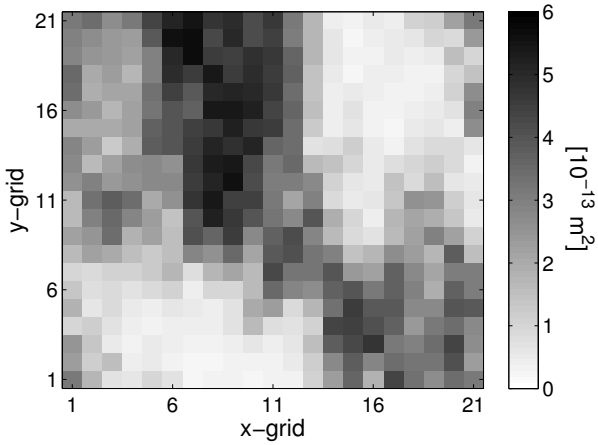

Figure 5.1: Permeability.

The performance measure is J_{npv} as defined in (3.2), using the values in Table 5.2. The goal is to maximize J_{npv} by varying the injector location $\mathbf{z} \in \mathcal{Z} = \{1, \dots, 441\}$. Three different terminal times are considered: 0.5, 2.5, and 10 years. The four producers operate at a constant bottom-hole pressure of 397 bar, and are each

Symbol	Value	Unit
r_{oil}	300	[\$ / m^3]
r_{prod}	15	[\$ / m^3]
r_{inj}	5	[\$ / m^3]
d	0	[-]
T	0.5, 2.5 and 10	[years]

Table 5.2: Values for computing J_{npv}.

equipped with a single valve. The well indices w^j are computed using a Peaceman model (2.21) with a wellbore radius $r_{\text{w}} = 0.1$m and skin factor $S = 0$. Three different production settings are considered.

- Constant production settings with the injector operating at a constant rate of 50 m^3/day, denoted by $\mathbf{u} = \mathbf{u}_{\text{con}}$.

- Reactive control, where the producers are shut-in at 95% water cut (*i.e.* the profitability threshold corresponding to $r_{\text{oil}} = 300$ \$/m^3 and r_{prod} = 15 \$/m^3), and with the injector operating at a constant rate of 50 m^3/day. This will be denoted by $\mathbf{u} = \mathbf{u}_{\text{re,rate}}$.

- Reactive control, where the producers are shut-in at 95% water cut, and with the injector operating at a constant bottom-hole pressure of 403 bar. This will be denoted by $\mathbf{u} = \mathbf{u}_{\text{re,bhp}}$

In short, we consider 9 well placement problems: 3 different terminal times T and 3 different production settings $\mathbf{u}$. There are 441 possible injector locations for each problem (*i.e.* $\mathcal{Z}$ contains 441 elements). For each problem, the value of $J_{\text{npv}}(\mathbf{u}, \mathbf{z})$ is computed for all $\mathbf{z} \in \mathcal{Z}$. These values can be plotted onto the 2D reservoir model grid to form maps of $J_{\text{npv}}(\mathbf{u}, \mathbf{z})$, from which it is easy to distinguish optimal from suboptimal areas for the water injector. We are of course particularly interested in how these areas depend on the particular choice of the production settings[3] $\mathbf{u}$.

The results are shown in Figure 5.2. The $J_{\text{npv}}(\mathbf{u}, \mathbf{z})$ maps for $\mathbf{u} = \mathbf{u}_{\text{con}}$ are quite intuitive: the best location for the injector is near the center of the reservoir. For $\mathbf{u} = \mathbf{u}_{\text{re,rate}}$, however, there is a clear shift in optimal locations and the difference in NPV for different injector locations is small compared to $\mathbf{u} = \mathbf{u}_{\text{con}}$. The optimal well locations for $T = 10$ years are in low permeability regions. However, for $\mathbf{u} = \mathbf{u}_{\text{re,bhp}}$ the results are quite different: the optimal well locations are in high permeability regions. This is clearly due to the injector well's BHP constraint: injecting 50 m^3/day of water into low permeable regions requires more pressure than the available 403 bar.

[3]To be thorough we should also consider optimal production settings as discussed in Chapter 3. However, this is computationally too demanding since finding optimal production settings for an arbitrary $\mathbf{z} \in \mathcal{Z}$ is an optimization problem in itself.

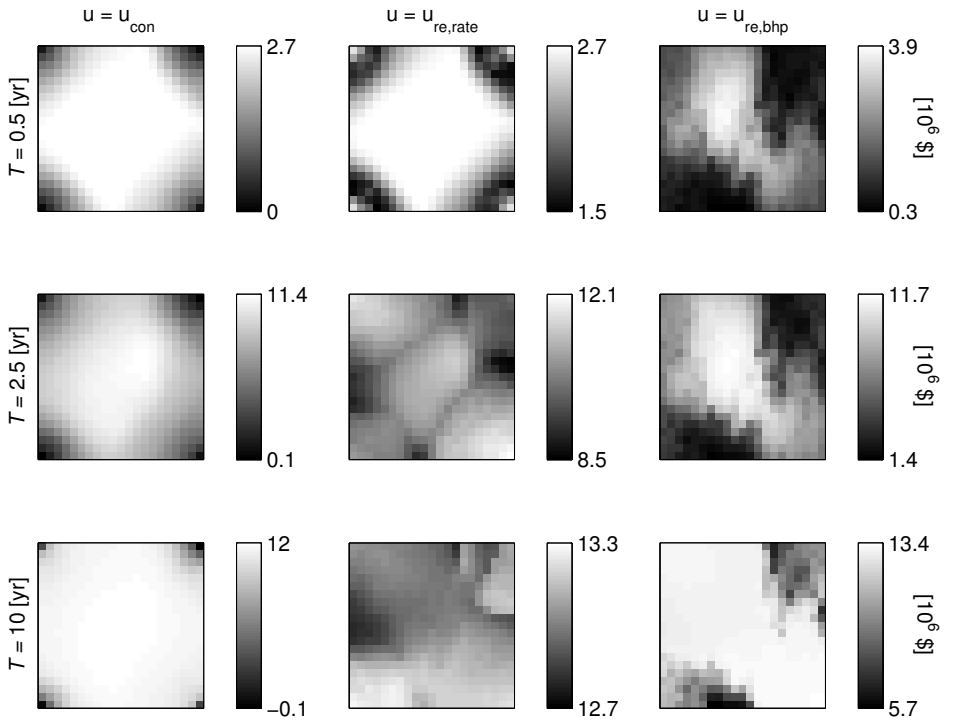

Figure 5.2: Performance $J_{\mathrm{npv}}(\mathbf{u}, \mathbf{z})$ for all possible injector locations $\mathbf{z} \in \mathcal{Z}$ for $T = 0.5$, 2.5 and 10 years of no control ($\mathbf{u} = \mathbf{u}_{\mathrm{con}}$), reactive control with a constant injection rate ($\mathbf{u} = \mathbf{u}_{\mathrm{re,rate}}$) and reactive control with a constant injection bottom-hole pressure ($\mathbf{u} = \mathbf{u}_{\mathrm{re,bhp}}$).

We conclude from these results that the type of production settings has significant impact on the well placement problem. Because in practice there is limited injection pressure and because wells are often operated using reactive production settings, from now on we only consider $\mathbf{u} = \mathbf{u}_{\mathrm{re,bhp}}$.

5.3 Optimal well placement using adjoint models

We will consider a local optimization method to find optimal well locations for **Problem 4**, which essentially tries to iteratively improve upon an initial well configuration until a local optimal solution is reached. Letting $\mathbf{z}_x^k$ and $\mathbf{z}_y^k$ denote the x and y co-ordinates of the well configuration $\mathbf{z}^k$ in iteration k, then this can be

written as follows.

$$\begin{bmatrix} \tilde{\mathbf{z}}_x^{k+1} \\ \tilde{\mathbf{z}}_y^{k+1} \end{bmatrix} = \begin{bmatrix} \mathbf{z}_x^k \\ \mathbf{z}_y^k \end{bmatrix} + s^k \underbrace{\begin{bmatrix} \mathbf{d}_x^k \\ \mathbf{d}_y^k \end{bmatrix}}_{=:\mathbf{d}^k}, \tag{5.7}$$

$$z_{x,j}^{k+1} = \max(1, \min(N_x, \tilde{z}_{x,j}^{k+1})), \quad j = 1, \ldots, m \tag{5.8}$$

$$z_{y,j}^{k+1} = \max(1, \min(N_y, \tilde{z}_{y,j}^{k+1})), \quad j = 1, \ldots, m \tag{5.9}$$

where $\mathbf{d}^k$ denotes an improving direction, $s^k \in \mathbb{N}$ the step size, $z_{x,j}^k$ the j^{th} component of $\mathbf{z}_x^k$ and $z_{y,j}^k$ the j^{th} component of $\mathbf{z}_y^k$. Note that s^k and the components of $\mathbf{d}^k$ are integers, and that (5.8)-(5.9) is to make sure that $\mathbf{z}^{k+1}$ is a well configuration within the $N_x \times N_y$ grid of the reservoir model. As mentioned earlier, the main challenge in this approach is to efficiently find improving directions. We consider $\mathbf{d}^k$ an improving direction if (5.7) - (5.9) using the smallest possible step size $s^k = 1$ leads to $J(\mathbf{u}, \mathbf{z}^{k+1}) \geq J(\mathbf{u}, \mathbf{z}^k)$.

Recall that adjoint models can be used to efficiently derive gradients of a performance measure J with respect to production settings $\mathbf{u}$. By surrounding each to-be-placed well by wells that operate at a very low constant flow rate (*i.e.* so-called pseudo wells) and computing their production setting gradients using (3.23), these gradients can be used to compute improving directions $\mathbf{d}^k$.

Let $n_{i,x}^k$ and $n_{i,y}^k$ denote the x and y co-ordinate, respectively, of well i in the k^{th} iteration. For simplicity, let us assume that this well is not located along the border of the reservoir model (*i.e.* $2 \leq n_{i,x}^k \leq N_x - 1$ and $2 \leq n_{i,y}^k \leq N_y - 1$), so that it can be surrounded by 8 pseudo wells. Let $q_1^i, \ldots, q_8^i$ denote the constant flow rates of these pseudo wells. We stress that these flow rates must be very small (*e.g.* less than 1% of the flow rate of the to-be-placed well) so as to have a negligible influence on the overall flow behaviour throughout the reservoir. The partial derivatives

$$\frac{\partial J}{\partial q_1^i}, \ldots, \frac{\partial J}{\partial q_8^i}$$

can be computed using (3.23) by summing over all K time intervals.

Let m^i denote the pseudo well with the largest partial derivative, or

$$m^i := \arg \max_{j=1,\ldots,8} \frac{\partial J}{\partial q_j^i}(\mathbf{u}), \tag{5.10}$$

and let m_x^i and m_y^i denote its x and y co-ordinate, respectively. If

$$\frac{\partial J}{\partial q_{m^i}^i}(\mathbf{u}) > 0$$

we conclude that, of the 8 flow rates $q_1^i, \ldots, q_8^i$, the performance measure will benefit the most from the slight increase in the flow rate $q_{m^i}^i$. A key observation is that

the flow rate $q^i_{m^i}$ will be significantly increased by making the pseudo well m^i the main well. This is the main reason why we expect the direction of the pseudo well m^i to be an improving direction for well i. In other words, we set

$$d^k_{i,x} = \begin{cases} -1 & \text{if} \quad m^i_x = n^k_{i,x} - 1 \\ 0 & \text{if} \quad m^i_x = n^k_{i,x} \\ 1 & \text{if} \quad m^i_x = n^k_{i,x} + 1 \end{cases} \tag{5.11}$$

$$d^k_{i,y} = \begin{cases} -1 & \text{if} \quad m^i_y = n^k_{i,y} - 1 \\ 0 & \text{if} \quad m^i_y = n^k_{i,y} \\ 1 & \text{if} \quad m^i_y = n^k_{i,y} + 1 \, . \end{cases} \tag{5.12}$$

The procedure (5.7) - (5.12) is visualized in Figure 5.3 for step size $s^k = 1$.

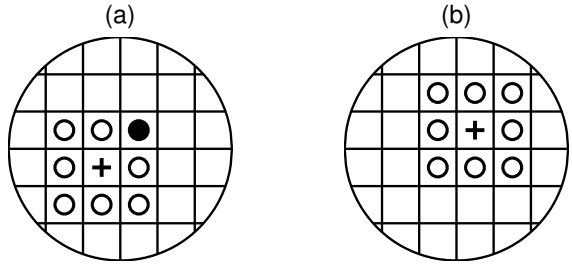

Figure 5.3: Top view of part of the grid of a 2D reservoir model with a main well (+) surrounded by 8 pseudo wells (o). The solid circle in (a) represents the pseudo well having the largest partial derivative in iteration k, and with step size $s^k = 1$ becomes the main well in iteration $k + 1$ as shown in (b).

The procedure's main benefit is that it computes a direction for all m wells in only one forward reservoir and one backward adjoint simulation. We stress, however, that there is no guarantee that this direction is improving, for the following reasons.

- The largest pseudo well partial derivative $\partial J / \partial q^i_{m^i}$ is not always positive, in which case $\mathbf{d}^k$ can be interpreted as the 'least harmfull' direction.
- For $s^k = 1$, the increase in flow rate of pseudo well m^i may be too large (*i.e.* the performance may decrease due to higher-order effects not captured by the first-order derivative).
- The decrease in flow rate of well i may have a negative effect on the performance, countering the positive effect expected by increasing the flow rate of pseudo well m^i.
- The location of all m wells is changed simultaneously, and the interaction between them may counter the positive effect expected by increasing the flow rates of each pseudo well individually.

The latter is also why the procedure (5.7) - (5.12) does not necessarily converge to a local optimal solution as discussed in Section 5.1. Although there may be no improving direction in which to change all m wells simultaneously, the performance might benefit from a change in the location of a single well. The procedure is therefore considered to have converged after k iterations if the well locations then alternate between two different locations (*i.e.* $\mathbf{z}^{k+2} = \mathbf{z}^k$).

In the following section the procedure (5.7) - (5.12) is applied to three different well placement problems, demonstrating that the computed directions are indeed often improving.

5.4 Applications

5.4.1 Application 1

Consider again the well placement problem from Section 5.2 with $\mathbf{u} = \mathbf{u}_{\mathrm{re,bhp}}$ and $T = 2.5$ years. Recall that the map of $J_{\mathrm{npv}}(\mathbf{u}_{\mathrm{re,bhp}}, \mathbf{z})$ for all possible injector locations $\mathbf{z} \in \mathcal{Z}$ is depicted in the middle right plot of Figure 5.2. To test whether (5.7) - (5.12) yields improving directions, each of the four corners of the reservoir is taken as the initial location of the to-be-placed water injector. The pseudo well rates are set to 0.01 m^3/day, which is less than 0.1% of the injection rate of the to-be-placed well. The results are shown in Figure 5.4. As expected, the injector moves towards the center from each of the four corners, demonstrating that - in this case - the directions are indeed improving. For each case, the injector alternates between two locations after around 10 iterations. Note that the final well location depends on the initial one, indicating that the method can lead to local maxima.

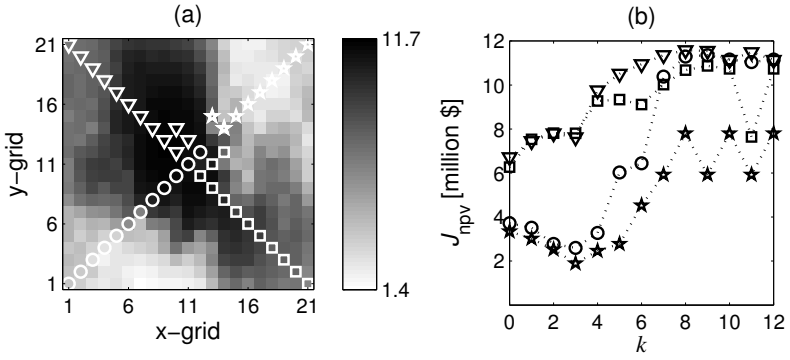

Figure 5.4: (a) Injector locations $\mathbf{z}^k$ for iterations $k = 0, \ldots, 12$ starting from 4 different initial locations projected onto map of performance $J_{\mathrm{npv}}(\mathbf{u}_{\mathrm{re,bhp}}, \mathbf{z})$ for all possible injector locations $\mathbf{z} \in \mathcal{Z}$ (*i.e.* middle right plot of Figure 5.2), and (b) corresponding values of $J_{\mathrm{npv}}(\mathbf{u}_{\mathrm{re,bhp}}, \mathbf{z}^k)$.

5.4.2 Application 2

Consider an application that only differs from the previous one in the size and permeability of the reservoir model, and the terminal time. The reservoir is modeled by 101×101 grid blocks of $10\text{m} \times 10\text{m} \times 10\text{m}$. The permeability is depicted in Figure 5.5. There are 9 to-be-placed producer wells, and 4 to-be-placed injector wells.

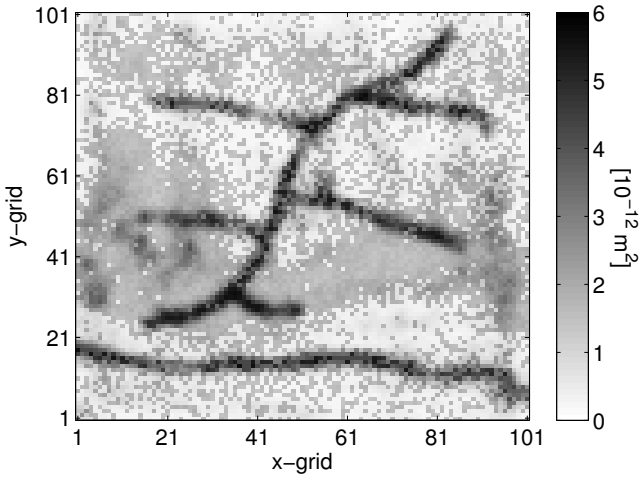

Figure 5.5: Permeability.

The performance measure is J_{npv} as defined in (3.2), using the values in Table 5.2. The goal is to maximize J_{npv} by varying the well locations. Note that with $N_x = 101$, $N_y = 101$ and $M = 13$ there are $(101 \times 101)^{13} \approx 10^{52}$ elements in $\mathcal{Z}$ (*i.e.* possible well configurations). The terminal time is 10 years. The producers are each equipped with a single valve, and are operated using the previously discussed reactive production settings $\mathbf{u} = \mathbf{u}_{\text{re,bhp}}$. The producers and injectors operate at a constant bottom-hole pressure of 397 bar and 403 bar, respectively. The pseudo well rates are set to 0.1 m^3/day, which is less than 1% of the flow rates of the to-be-placed wells.

This well placement problem can be written as **Problem 4**. The procedure (5.7) - (5.12) is applied starting from two different initial well configurations, referred to as the 'standard' and 'mini' one. The standard initial well configuration is a 13-spot pattern while the mini initial well configuration is a condensed version of the standard one - see Figure 5.7. As before, the step size is $s^k = 1$.

Figure 5.6 depicts J_{npv} per iteration and Figure 5.7 the well locations at iterations $k = 1, 20$ and 94 for two different initial well configurations. Figure 5.8 and Figure

5.9 illustrate the end-of-life water saturation for the initial and optimal well locations. Starting from the standard initial pattern the method leads to a 4% increase in $J_{\rm npv}$. Starting from the mini initial pattern, which will never be the preferred well configuration in a field development plan, $J_{\rm npv}$ increases to a value that is only slightly less than the optimized $J_{\rm npv}$ starting from the standard initial well pattern. This might seem surprising since the final well locations are completely different, but is because in both cases the reservoir is almost completely drained - see Figure 5.8(b) and Figure 5.9(b).

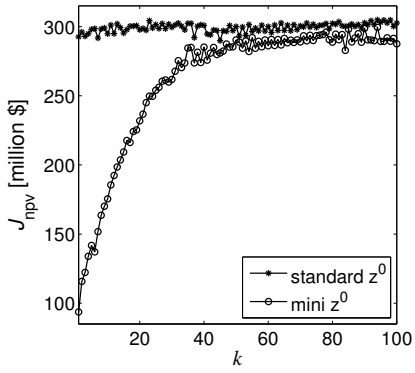

Figure 5.6: Performance $J_{\rm npv}(\mathbf{u}_{\rm re,bhp}, \mathbf{z}^k)$ per iteration k for standard and mini initial well configuration.

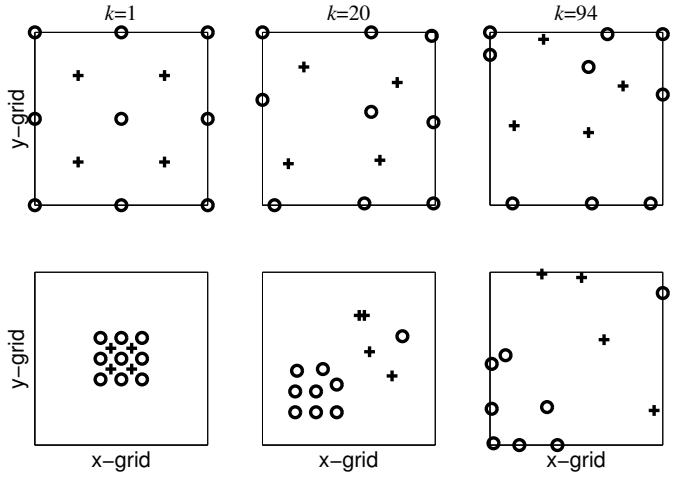

Figure 5.7: Well location path of 9 producers (o) and 4 injectors (+) for standard (top) and mini initial well configuration (bottom).

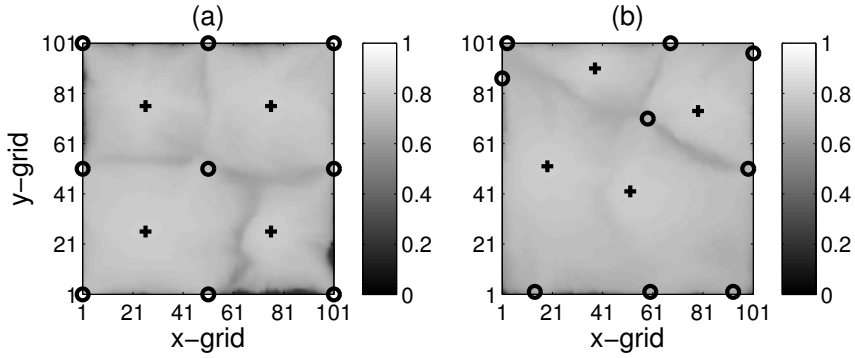

Figure 5.8: Water saturation at the terminal time for standard initial well configuration (a) and optimized well configuration (b). Crosses indicate injector wells, circles producer wells.

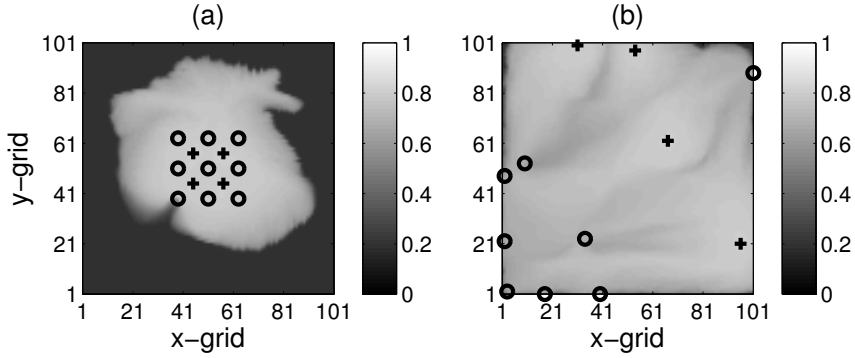

Figure 5.9: Water saturation at the terminal time for mini initial well configuration (a) and optimized well configuration (b). Crosses indicate injector wells, circles producer wells.

5.4.3 Application 3

Consider the reservoir treated in Section 3.6. There are 4 to-be-placed producer wells, and 8 to-be-placed injector wells. The performance measure is $J_{\rm npv}$ as defined in (3.2), using the values in Table 5.2. The goal is to maximize $J_{\rm npv}$ by varying the well locations. The terminal times is 10 years. The producers are each equipped with a single valve, and are operated using the previously discussed reactive production settings $\mathbf{u} = \mathbf{u}_{\rm re,bhp}$. For the 8 injectors, the bottom-hole pressure is set to 415 bar at the lowest perforation. For the 4 producers, the bottom-hole pressure is set to 390 bar at the highest perforation. The pressures in the other perforations are computed assuming hydrostatic equilibrium in the wellbore. The well indices are computed using a Peaceman model with a wellbore radius of 0.1m and zero skin factor. The pseudo well rates are set to 0.1 $\mathrm{m}^3/\mathrm{day}$, which is less than 0.1% of the flow rates of the to-be-placed wells.

This well placement problem can be written as **Problem 4**. The procedure (5.7) - (5.12) is applied starting from two different initial well configurations, again referred to as the 'standard' and 'mini' one - see Figure 5.11. As before, the step size is $s^k = 1$.

Figure 5.10 depicts $J_{\rm npv}$ per iteration and Figure 5.11 the well locations at iterations $k = 1, 10$ and 50 for two different initial well configurations. Starting from the standard initial pattern, the method leads to a 6% increase in $J_{\rm npv}$. As in Application 2, the optimized $J_{\rm npv}$ starting from the mini initial configuration is similar, while the final well locations are completely different. Again, this is because in both cases the reservoir is almost completely drained.

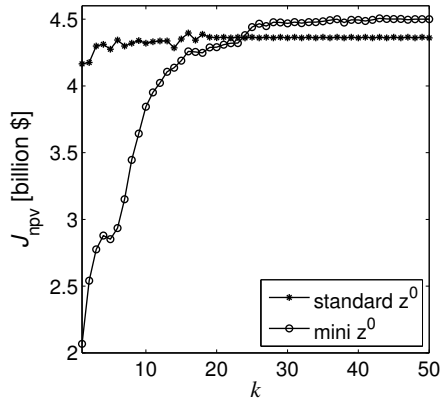

Figure 5.10: Performance $J_{\rm npv}(\mathbf{u}_{\rm re,bhp}, \mathbf{z}^k)$ per iteration k for standard and mini initial well configuration.

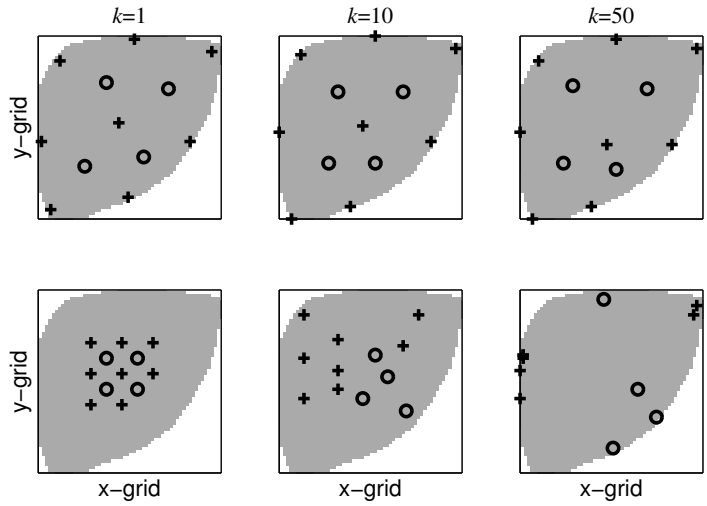

Figure 5.11: Well location path of 4 producers (o) and 8 injectors (+) for standard (top) and mini initial well configuration (bottom).

5.5 Discussion

The previous applications show that the directions computed using our adjoint-based method for well placement are often improving. The almost monotic increase in $J_{\rm npv}$ for Applications 2 and 3 starting from a mini initial well configuration, in particular, supports this claim.

A major advantage of our method is that it generates improving directions for all m wells in only one forward (reservoir) and one backward (adjoint) simulation. In comparison, the FDG method requires $2m + 1$ forward simulations to compute an improving direction, since each well location is sequentially perturbed by one grid block in both x-and y-direction. It turn out that the directions computed using both methods are similar, but not identical. In order to compare them, both methods were applied to Application 3 starting from the mini initial well configuration. The NPV values per iteration k, depicted in Figure 5.12 show similar increases, even though their well locations per iteration are different.

Finally, it is interesting to note that wells will occasionally merge - see Figure 5.7 and Figure 5.11. This is because once two injectors or producers share the same location they will never part, because the gradient data prodived by their respective pseudo wells is identical.

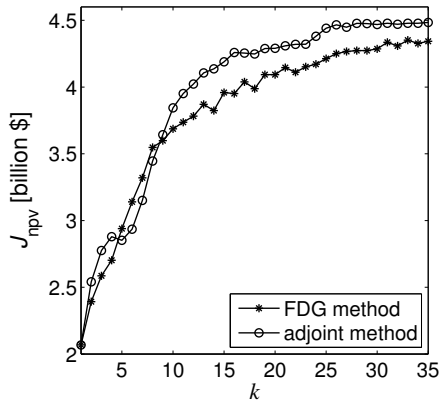

Figure 5.12: Performance $J_{\mathrm{npv}}(\mathbf{u}_{\mathrm{re,bhp}}, \mathbf{z}^k)$ per iteration k for FDG and adjoint-based method.

5.6 Chapter conclusions

The type of production settings (*e.g.* reactive versus constant) significantly effect the well placement problem, in that a well configuration that is optimal when the wells operated with one type of settings may be far from optimal when the wells are operated with another type of settings. Furthermore, the gradients used in production setting optimization can be used to efficiently compute directions in which to iteratively improve upon an initial well configuration by surrounding the to-be-placed wells by pseudo wells.

While this is a very promising step towards automatic well placement, there are several issues that need to be addressed before this method can be applied in practice. First of all, the concept of surrounding a well with pseudo-wells to efficiently compute improving directions is by no means restricted to a single 'ring'. Using two or more rings of pseudo wells for each well leads to more gradient information, and thereby possibly a better optimization procedure. Second, the water flooding application considered in this chapter demonstrates that the final well configuration is very dependent on the initial one. In practice, this is clearly undesirable. Third, the effect of model uncertainty needs to be addressed. It should be noted that it is conceptually straightforward to apply the robust optimization approach considered in Chapter 4 to well location optimization. It would be interesting to investigate under what conditions a well configuration that is robust against model uncertainty (*e.g.* geological uncertainty represented by a large set of realizations as in Chapter 4) resembles the commonly applied pattern-flood. Finally, the decisions concerning the number, scheduling and trajectory of wells need to be addressed. We remark that, as with well location optimization, well trajectory optimization might be tackled using the concept of pseudo-wells. Each grid block in which a to-be-optimized well is perforated should then be viewed as a separate well, and subsequently surrounded by pseudo-wells. The challenge is

then to improve upon an initial well trajectory while adhering to practical drilling constraints (*e.g.* curvature and length).

6 CHAPTER

Controllability and Observability of Reservoir Models

This chapter focuses on the controllability and observability properties of single-phase flow reservoir models, as well as the possibilities to obtain reduced order models through balancing and truncation. The main contribution of this chapter is to analyze and interpret the controllability and observability of single-phase flow reservoir models, and to investigate how these are affected by well locations, heterogeneity and fluid properties. The results are illustrated through two examples.

6.1 Problem formulation

Recall that this thesis considers three ways to increase the recovery factor: model-based optimization of production settings (Chapter 3) and well locations (Chapter 5), reducing the effect of model uncertainty by robust optimization (Chapter 4), and reducing model uncertainty itself by using measurements to estimate model states and parameters (Chapter 7). The degree to which the water flooding process can be optimized clearly depends on the ability to control the fluid flow in the reservoir at hand. Similarly, the degree to which uncertainty can be reduced clearly depends on the ability to estimate / identify the states / parameters of the reservoir at hand.

Despite the many reported applications of optimal control, estimation and identification in the reservoir engineering literature, the concepts of controllability and observability have not yet been analyzed in detail (although it should be mentioned that Fyrozjaee and Yortsos (2006) consider how to partition the flow rate in a well so that the displacement front can be steered according to pre-determined dynamics). This is surprising since these concepts essentially determine a reservoir's behavior and thereby the success of the chosen application.

The main contribution of this chapter is to analyze and interpret the controllability and observability properties of single-phase flow reservoir models, and how these are affected by well locations, heterogeneity and fluid properties. Since the concepts of controllability and observability are more complicated for nonlinear systems and since the nonlinearity of oil and gas reservoirs is mainly due to time-varying saturations in multi-phase flow, we only consider single-phase flow. The identification of reservoir parameters is discussed in Chapter 7.

6.2 Controllability and observability

Consider the discrete-time single phase flow model (2.30)-(2.31):

$$\begin{aligned} \mathbf{p}_{k+1} &= \mathbf{A}\mathbf{p}_k + \mathbf{B}\mathbf{u}_k, \\ \mathbf{p}_0 &= \bar{\mathbf{p}}_0. \end{aligned}$$

Recall that the flow rate q^j through a well in grid block j is related to its bottom-hole pressure $p^j_{\rm bh}$ through a well model (2.20)

$$q^j = \alpha^j w^j (p^j_{\rm bh} - p^j).$$

in which the well index w^j is computed using a Peaceman model (2.21). If we can measure the flow rate q^j in some of the production and injection wells and the pressure p^j in all of the observation (*i.e.* non-producing or injecting) wells, we can write

$$\mathbf{y}_k = \mathbf{C}\mathbf{p}_k + \mathbf{D}\mathbf{u}_k, \tag{6.1}$$

where $\mathbf{y}_k \in \mathbb{R}^{N_\mathbf{y}}$ is the so-called output vector containing the measurements at time $t = k\Delta t$. The (i, j) entry of $\mathbf{C} \in \mathbb{R}^{N_\mathbf{y} \times N}$ is:

- $-w^j$ if there is a production or injection well containing a flow meter in grid block j,
- 1 if there is an observation well containing a pressure gauge in grid block j,
- 0 otherwise.

The (i, i) entry of $\mathbf{D} \in \mathbb{R}^{N_\mathbf{y} \times N_\mathbf{y}}$ is w^j if the $i^{\rm th}$ measurement is a flow rate measurement and 0 otherwise.

For simplicity, from now on we only consider the discrete-time formulation (2.30), (6.1). The following section shows how the controllability and observability of the pressures throughout the reservoir model are determined by the matrix pairs $(\mathbf{A}, \mathbf{B})$ and $(\mathbf{A}, \mathbf{C})$, respectively. We stress, however, that both the theory and results that follow do not depend on implicit or explicit time discretization or on the particular value of the discretization time-step Δt, and also apply to the

continuous-time case.

The material treated in this section was pioneered by Kalman (1963), Moore (1981) and Glover (1984), and is usually included in any advanced course on systems and control. The reader is referred to these works or for example the textbooks Chen (1984) and Antoulas (2005) for details and proofs.

For a system (2.30), (6.1) with $N_{\mathbf{u}}$ control inputs (*i.e.* controlled flow rates or bottom-hole pressures) and $N_{\mathbf{y}}$ outputs (*i.e.* measured flow rates or bottom-hole pressures), the controllability matrix $\mathcal{C}_k$ and observability matrix $\mathcal{O}_k$ are defined as follows

$$\mathcal{C}_k(\mathbf{A},\mathbf{B}) := \begin{bmatrix} \mathbf{B} & \mathbf{AB} & \mathbf{A}^2\mathbf{B} & \dots & \mathbf{A}^{k-1}\mathbf{B} \end{bmatrix}, \tag{6.2}$$

$$\mathcal{O}_k(\mathbf{C},\mathbf{A}) := \begin{bmatrix} \mathbf{C} \\ \mathbf{CA} \\ \mathbf{CA}^2 \\ \vdots \\ \mathbf{CA}^{k-1} \end{bmatrix}. \tag{6.3}$$

By the so-called Cayley-Hamilton theorem, the rank of $\mathcal{C}_\infty$ and its image are determined by at most the first $N \times N_{\mathbf{u}}$ columns, where N is the state dimension. In other words, $\mathrm{im}(\mathcal{C}_\infty) = \mathrm{im}(\mathcal{C}_N) \subset \mathbb{R}^N$. Similarly, the rank of $\mathcal{O}_\infty$ and its kernel are determined by at most the first $N \times N_{\mathbf{y}}$ rows. In other words, $\ker(\mathcal{O}_\infty) = \ker(\mathcal{O}_N) \subset \mathbb{R}^N$.

From (2.30), (2.31) it follows that

$$\mathbf{p}_n = \mathbf{A}^n\bar{\mathbf{p}}_0 + \sum_{k=0}^{n-1} \mathbf{A}^{n-k-1}\mathbf{B}\mathbf{u}_k. \tag{6.4}$$

It is clear by inspection of (6.4) together with the previous remark on the image of $\mathcal{C}_N$ that $\mathbf{p}_k$ is a linear combination of the columns of $\mathcal{C}_N$ together with a $\mathbf{p}_0$-dependent term. Consequently, if $\mathcal{C}_N$ has full rank then $\mathrm{im}(\mathcal{C}_N) = \mathbb{R}^N$ and any $\mathbf{p}_N$ can be reached by suitable choice of $\{\mathbf{u}_0, \dots, \mathbf{u}_{N-1}\}$. This is why a linear system of the form (2.30), (6.1) is called controllable[1] if its controllability matrix $\mathcal{C}_N$ has full rank (*i.e.* rank N). If $\mathrm{rank}(\mathcal{C}_N) < N$, then

$$\mathbb{X}^{\mathrm{con}} := \mathrm{im}(\mathcal{C}_N(\mathbf{A},\mathbf{B})) \subset \mathbb{R}^N \tag{6.5}$$

is often referred to as the controllable subspace, and consists of the states that can be reached by suitable choice of the control.

[1] Under these conditions the system is actually called reachable in the systems and control literature, which is equivalent to controllable if $\mathbf{A}$ is nonsingular. Since $\mathbf{A}$ is nonsingular throughout this thesis, we stick to the term controllable.

It is clear by inspection of (6.4) and (6.1) that $\mathbf{y}_k$ equals $\mathbf{C}\mathbf{A}^k\bar{\mathbf{p}}_0$ plus a control-dependent term which we assume known. Consequently, if $\mathcal{O}_N$ has full rank then $\ker(\mathcal{O}_N) = \emptyset$ (empty) and any $\bar{\mathbf{p}}_0$ can be distinguished from zero through the measured output $\{\mathbf{y}_0, \ldots, \mathbf{y}_{N-1}\}$. This is why a linear system of the form (2.30), (6.1) is called observable if its observability matrix $\mathcal{O}_N$ has full rank. If $\text{rank}(\mathcal{O}_N) < N$, then

$$\mathbb{X}^{\text{unobs}} := \ker(\mathcal{O}_N(\mathbf{C}, \mathbf{A})) \subset \mathbb{R}^N \tag{6.6}$$

is often referred to as the unobservable subspace, and consists of the states that cannot be distinguished from zero through the measured output.

From (6.4) it appears that the pressures can become unbounded if $\mathbf{A}$ has an eigenvalue whose magnitude or absolute value is strictly larger than one. It turns out that if at least one well is controlled by its bottom-hole pressure, $\mathbf{A}$ has eigenvalues strictly smaller than one - see Chapter 2. This is quite intuitive, as increased reservoir pressure through injected water then automatically leads to increased production, which would not be the case if the flow rates of all the other wells are set to zero. Note that we have already assumed that some of the production and injection wells are controlled by their bottom-hole pressure.

Strictly speaking, all of the states in $\mathbb{X}^{\text{con}}$ can be reached provided that there are no bounds on the manipulated input (*i.e.* the bottom-hole pressures). Similarly, all of the states not in $\mathbb{X}^{\text{unobs}}$ can strictly speaking be distinguished from zero provided that there are no bounds on the accuracy of the measured output (*i.e.* the flow meters). In practice, neither is realistic. However, there are elements of $\mathbb{X}^{\text{con}}$ that require significantly more energy[2] in terms of

$$\sum_{k=0}^{\infty} \mathbf{u}_k^T \mathbf{u}_k$$

to be reached than others. Similarly, there are elements not in $\mathbb{X}^{\text{unobs}}$ that produce significantly more energy in terms of

$$\sum_{k=0}^{\infty} \mathbf{y}_k^T \mathbf{y}_k$$

when observed than others. To quantify this, the so-called controllability Gramian $\mathcal{P}$ and the observability Gramian $\mathcal{Q}$ are defined as follows

$$\mathcal{P} := \mathcal{C}_\infty(\mathbf{A}, \mathbf{B})\mathcal{C}_\infty^T(\mathbf{A}, \mathbf{B}) = \sum_{k=0}^{\infty} \mathbf{A}^k \mathbf{B}\mathbf{B}^T \left(\mathbf{A}^T\right)^k, \tag{6.7}$$

$$\mathcal{Q} := \mathcal{O}_\infty^T(\mathbf{C}, \mathbf{A})\mathcal{O}_\infty(\mathbf{C}, \mathbf{A}) = \sum_{k=0}^{\infty} \left(\mathbf{A}^T\right)^k \mathbf{C}^T \mathbf{C}\mathbf{A}^k, \tag{6.8}$$

[2]The term 'energy' is used loosely here, motivated by the fact that energy can often be written as a quadratic form (*e.g.* kinetic energy as a function of squared velocity). A more precise term is the squared l_2 norm of the input.

These can be computed by solving the so-called discrete-time Lyapunov (or Stein) equations

$$\mathbf{A}\mathcal{P}\mathbf{A}^T + \mathbf{B}\mathbf{B}^T = \mathcal{P}, \tag{6.9}$$

$$\mathbf{A}^T\mathcal{Q}\mathbf{A} + \mathbf{C}^T\mathbf{C} = \mathcal{Q}, \tag{6.10}$$

as can be seen by substituting (6.7)-(6.8) into (6.9)-(6.10) and using the fact that $\mathbf{A}^k \to 0$ for $k \to \infty$ since the eigenvalues of $\mathbf{A}$ are strictly smaller than one. Note that $\mathrm{im}(\mathcal{C}_N) = \mathrm{im}(\mathcal{P})$ and $\ker(\mathcal{O}_N) = \ker(\mathcal{Q})$.

Consider a reference state $\mathbf{p}_\mathrm{r} \in \mathbb{R}^N$. In Glover (1984) it is shown that the minimal energy J_con required to steer the state from 0 to $\mathbf{p}_\mathrm{r}$ is[3]

$$J_\mathrm{con}(\mathbf{p}_\mathrm{r}) = \mathbf{p}_\mathrm{r}^T\mathcal{P}^{-1}\mathbf{p}_\mathrm{r}, \tag{6.11}$$

and that the maximal energy J_obs produced by observing the output of the system whose initial state is given by $\mathbf{p}_\mathrm{r}$ is

$$J_\mathrm{obs}(\mathbf{p}_\mathrm{r}) = \mathbf{p}_\mathrm{r}^T\mathcal{Q}\mathbf{p}_\mathrm{r}. \tag{6.12}$$

This means that the elements in $\mathbb{X}^\mathrm{con}$ that require the most energy to reach have a significant component in the span of the eigenvectors of $\mathcal{P}$ corresponding to small (absolute) eigenvalues. Similarly, the elements not in $\mathbb{X}^\mathrm{unobs}$ that produce the least energy when observed have a significant component in the span of the eigenvectors of $\mathcal{Q}$ corresponding to small (absolute) eigenvalues.

The controllability and observability Gramians, however, are co-ordinate dependent, meaning that the energy required/produced to reach/observe reference states depends on the particular choice of co-ordinates (*e.g.* the grid block numbering). This can be seen by considering a linear combination of the original pressures

$$\hat{\mathbf{p}}_k = \mathbf{T}\mathbf{p}_k, \tag{6.13}$$

with $\mathbf{T} \in \mathbb{R}^{N\times N}$ nonsingular. The dynamics of $\hat{\mathbf{p}}_k$ are given by

$$\hat{\mathbf{p}}_{k+1} = \underbrace{\mathbf{T}\mathbf{A}\mathbf{T}^{-1}}_{=:\tilde{\mathbf{A}}}\hat{\mathbf{p}} + \underbrace{\mathbf{T}\mathbf{B}}_{=:\tilde{\mathbf{B}}}\mathbf{u}_k, \tag{6.14}$$

$$\mathbf{y}_k = \underbrace{\mathbf{C}\mathbf{T}^{-1}}_{=:\tilde{\mathbf{C}}}\hat{\mathbf{p}}_k + \mathbf{D}\mathbf{u}_k. \tag{6.15}$$

The associated Gramians $\tilde{\mathcal{P}}$ and $\tilde{\mathcal{Q}}$ satisfy

$$\tilde{\mathcal{P}} = \mathbf{T}\mathcal{P}\mathbf{T}^T,\ \tilde{\mathcal{Q}} = \mathbf{T}^{-T}\mathcal{Q}\mathbf{T}^{-1} \ \Rightarrow\ \tilde{\mathcal{P}}\tilde{\mathcal{Q}} = \mathbf{T}\mathcal{P}\mathcal{Q}\mathbf{T}^{-1}.$$

In other words, by choosing a transformation such that a particular reference state is easier to reach simultaneously makes it harder to observe, and vice-versa. Although the Gramians themselves are co-ordinate dependent, the eigenvalues of their product are not. The latter are called the Hankel singular values

$$\sigma_k := \sqrt{\lambda_k(\mathcal{P}\mathcal{Q})}, \quad k = 1, \ldots, N \tag{6.16}$$

and, being co-ordinate independent, are input-output system invariants.

[3] Assuming $\mathcal{P}^{-1}$ exist, which holds if the system is controllable.

6.3 Balancing and truncation

We can find a co-ordinate transformation such that the Gramians $\tilde{\mathcal{P}}$ and $\tilde{\mathcal{Q}}$ are equal, diagonal and nonnegative. By computing a Cholesky factorization of $\mathcal{P} = \mathbf{U}\mathbf{U}^T$ and $\mathcal{Q} = \mathbf{L}\mathbf{L}^T$ and a singular value decomposition of $\mathbf{U}^T\mathbf{L} = \mathbf{Z}\mathbf{\Sigma}\mathbf{Y}^T$, it can be shown that setting

$$\mathbf{T} = \underbrace{\mathbf{\Sigma}^{-1/2}\mathbf{Y}^T\mathbf{L}^T}_{=:\mathbf{T}_{\mathrm{bal}}} \quad \text{and} \quad \mathbf{T}^{-1} = \underbrace{\mathbf{U}\mathbf{Z}\mathbf{\Sigma}^{-1/2}}_{=:\mathbf{T}_{\mathrm{bal}}^{-1}} \tag{6.17}$$

leads to

$$\tilde{\mathcal{P}} = \tilde{\mathcal{Q}} = \mathbf{\Sigma} = \mathrm{diag}\left(\sigma_1, \ldots, \sigma_{\mathrm{N}}\right), \tag{6.18}$$

where $\sigma_1 \geq \sigma_2 \geq \ldots \geq \sigma_N$. $\mathbf{T}_{\mathrm{bal}}$ is called a balancing transformation matrix. Note that because in the balanced co-ordinates $\tilde{\mathcal{P}} = \tilde{\mathcal{Q}}$, states are equally difficult to reach as observe. In the original co-ordinates this means that, letting $\hat{\mathbf{t}}_j$ denote the j^{th} column of $\mathbf{T}_{\mathrm{bal}}^{-1}$, we have

$$J_{\mathrm{con}}(\hat{\mathbf{t}}_j) = 1/\sigma_j \quad \text{and} \quad J_{\mathrm{obs}}(\hat{\mathbf{t}}_j) = \sigma_j.$$

It is important to note that the k^{th} Hankel singular value σ_k can be interpreted as the energy contribution of the k^{th} component of the balanced state $\hat{p}_k$ to the input-output behavior of the system. If the Hankel singular values decrease rapidly, we can therefore conclude that most of the input-output behavior is determined by the first few balanced states.

The input-output behavior of a linear system is characterized by its so-called transfer function $\mathbf{G}$. Given a quadruple $\{\mathbf{A}, \mathbf{B}, \mathbf{C}, \mathbf{D}\}$ (or 'realization') describing the dynamics of a system through (2.30), (6.1), its transfer function is given by

$$\mathbf{G}(z) \quad := \quad \mathbf{C}\left(zI - \mathbf{A}\right)^{-1}\mathbf{B} + \mathbf{D}. \tag{6.19}$$

One of the reasons for considering the transfer function of a system is that, because of its linearity, a manipulated input sinusoid of frequency ω eventually leads to a measured output sinusoid of frequency ω. The magnitude and phase shift of this output can be determined by the complex number $\mathbf{G}(e^{j\omega})$, called the frequency response of $\mathbf{G}$. However, since for an arbitrary invertible $\mathbf{T}$

$$\mathbf{C}\mathbf{T}^{-1}\left(zI - \mathbf{T}\mathbf{A}\mathbf{T}^{-1}\right)^{-1}\mathbf{T}\mathbf{B} + \mathbf{D} = \mathbf{C}\left(zI - \mathbf{A}\right)^{-1}\mathbf{B} + \mathbf{D},$$

there are infinitely many realizations that can form the same transfer function $\mathbf{G}$, depending on the particular choice of coordinates (*e.g.* the grid block numbering). Any two such realizations can be transformed into one another through a suitable change of coordinates (6.14)-(6.15).

Because in balanced co-ordinates the states are equally difficult to control as observe, it is easy to distinguish between states that contribute to the input-output behavior and states that do not by considering the following partitioning

$$\mathbf{\Sigma} = \begin{bmatrix} \mathbf{\Sigma}_1 & 0 \\ 0 & \mathbf{\Sigma}_2 \end{bmatrix}, \tilde{\mathbf{A}} = \begin{bmatrix} \tilde{\mathbf{A}}_{11} & \tilde{\mathbf{A}}_{12} \\ \tilde{\mathbf{A}}_{21} & \tilde{\mathbf{A}}_{22} \end{bmatrix}, \tilde{\mathbf{B}} = \begin{bmatrix} \tilde{\mathbf{B}}_1 \\ \tilde{\mathbf{B}}_2 \end{bmatrix}, \tilde{\mathbf{C}} = \begin{bmatrix} \tilde{\mathbf{C}}_1 & \tilde{\mathbf{C}}_2 \end{bmatrix},$$

where $\mathbf{\Sigma}_1 := \mathrm{diag}(\sigma_1, \ldots, \sigma_k)$, $\mathbf{\Sigma}_2 := \mathrm{diag}(\sigma_{k+1}, \ldots, \sigma_N)$ and

$$\sigma_1 \geq \sigma_2 \geq \ldots \geq \sigma_N.$$

The following transfer function

$$\hat{\mathbf{G}}(z) \quad := \quad \tilde{\mathbf{C}}_1 \left(zI - \tilde{\mathbf{A}}_{11} \right)^{-1} \tilde{\mathbf{B}}_1 + \mathbf{D} \tag{6.20}$$

is a reduced k^{th} order approximation $\hat{\mathbf{G}}$ of the full N^{th} order transfer function $\mathbf{G}$. The former is called reduced because it has $N - k$ less states than the latter, and has been obtained by simply truncating the $N - k$ balanced states that contribute the least to its input-output behavior.

Because a linear time-invariant system is characterized by its transfer function or, equivalently, its frequency response, two systems are considered close to each other if their frequency responses are similar. To quantify this, let us define the so-called H_∞ norm

$$\|\mathbf{G}\|_{H_\infty} := \sup_{z \in \bar{\mathcal{D}}} \sigma_{\max} \left(\mathbf{G}(z) \right) \tag{6.21}$$

as a measure of the size of $\mathbf{G}$, where $\bar{\mathcal{D}} \subset \mathbb{C}$ denotes the complement of the closed unit disc and $\sigma_{\max}$ the largest singular value. The H_∞ norm can be interpreted as the worst case energy norm, meaning that the energy of the measured output is at most the H_∞ norm times the energy of the manipulated input. It is shown in Hinrichsen and Pritchard (1990) that the error of the approximation $\hat{\mathbf{G}}$ of $\mathbf{G}$ satisfies the following bound

$$\left\| \mathbf{G} - \hat{\mathbf{G}} \right\|_{H_\infty} \leq 2 \left(\sigma_{k+1} + \ldots \sigma_N \right), \tag{6.22}$$

or twice the sum of the deleted $N - k$ Hankel singular values.

In the following sections this type of model reduction is not actually applied to reservoir models (as done in Markovinovic et al. (2002), Heijn et al. (2004) and Gildin et al. (2006). We merely point out that we can analyze when a high-order model in fact behaves like a low-order one. Moreover, we can distinguish between those linear combinations of the pressures that contribute to the input-output behavior, and those that do not. In the following sections the controllability and observability properties of single-phase flow reservoir models are analyzed and interpreted, and it is shown how these are affected by well locations, heterogeneity and fluid properties.

6.4 Examples

6.4.1 Example 1: homogeneous permeability

Consider a 2D homogeneous reservoir containing one phase and modeled as in the previous section. The model has $21 \times 21 \times 1$ grid blocks of $10\text{m} \times 10\text{m} \times 10\text{m}$. The absolute permeability is 10 mDarcy. The remaining geological and fluid properties are given in Table 6.1. There are five wells configured in a standard 5-spot pattern depicted in see Figure 6.1. Wells 1, 3, 5 and 4 are production or injection wells. In wells 1, 3 and 5 we can control the bottom-hole pressure; in well 4 the flow rate. Wells 1, 3, 5 and 2 have pressure gauges or flow meters. In wells 1, 3 and 5 we can measure the flow rate; in well 2 (a non-producing or injecting well) the bottom-hole pressure. The well indices w^j are computed using a Peaceman model (2.21) with a wellbore radius $r_{\text{w}} = 0.1\text{m}$ and skin factor $S = 0$.

Symbol	Value	Unit
N_x, N_y, N_z	21,21,1	[-]
N	441	[-]
$\Delta x, \Delta y, \Delta z$	10,10,10	[m]
$\phi^1, \ldots, \phi^{441}$	$0.20, \ldots, 0.20$	[-]
c	10^{-10}	[1 / Pa]
μ	10^{-3}	[Pa s]

Table 6.1: Geological and fluid properties.

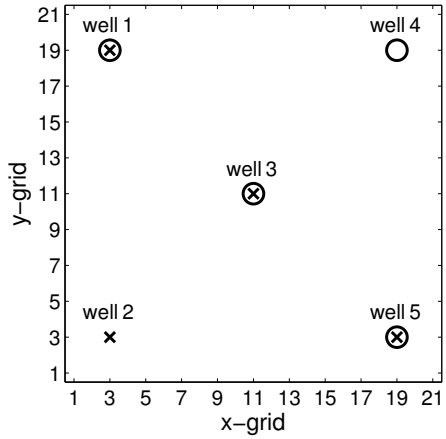

Figure 6.1: Well locations: wells 1, 3 and 5 are bottom-hole pressure controlled production or injection wells containing a flow meter (⊗), well 4 is a flow rate controlled production or injection well without a pressure gauge (◯), and well 2 is an observation well containing a pressure gauge (×).

The matrices $\mathbf{A}$ and $\mathbf{B}$ are computed as in Chapter 2 with a discretization time step given by (2.32), which in this example leads to $\Delta t = 1.2$ seconds. The matrices $\mathbf{C}$ and $\mathbf{D}$ are computed as in Section 6.2. In this particular example, the nonzero entries in $\mathbf{C}$ corresponding to the flow rate measurements (*i.e.* the well indices w^j of wells 1, 3 and 5) are in the order of 10^{-8}: much smaller than the nonzero entry in $\mathbf{C}$ corresponding to the pressure measurement in well 2, which is equal to 1. This is problematic, because the previously discussed energy produced by observing pressures in well 2 (in $[\text{Pa}]^2$) will then generally be much larger than the energy produced by observing flow rates in wells 1, 3 and 5 (in $[\text{m}^3/\text{s}]^2$). In the following examples, the nonzero entry in $\mathbf{C}$ corresponding to the pressure measurement is therefore scaled to the well index w^j of well 2. Similarly, the nonzero entries in $\mathbf{B}$ corresponding to the bottom-hole pressure controlled wells (*i.e.* wells 1, 3 and 5) are much smaller than the nonzero entry in $\mathbf{B}$ corresponding to the flow rate controlled well (*i.e.* well 4). In the following examples, the nonzero entry in $\mathbf{B}$ corresponding to the flow rate controlled well is therefore scaled to the well index w^j of well 4. Subsequently, All of the matrices discussed in the previous section (*e.g.* Gramians, Hankel singular values, balancing transformation) are computed using the MATLAB functions `gram` and `balreal`.

The Hankel singular values, depicted on a logarithmic scale in Figure 6.2, decrease very rapidly. This is in line with earlier results from Markovinovic et al. (2002), Heijn et al. (2004) and Gildin et al. (2006), and means that the 441^{th} order reservoir model behaves like a model of much lower order.

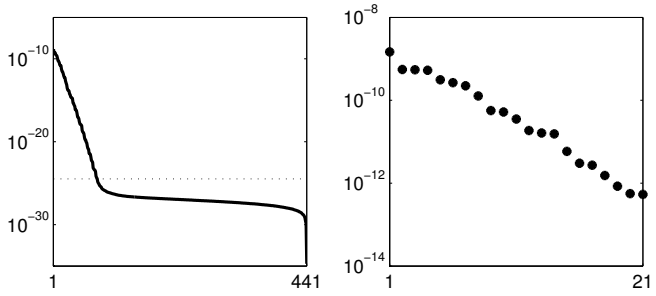

Figure 6.2: All 441 Hankel singular values $\sigma_1, \ldots, \sigma_{441}$ (left) and 21 largest ones $\sigma_1, \ldots, \sigma_{21}$ (right) for homogeneous example. The dashed line represents machine precision.

The eigenvectors corresponding to the three largest absolute eigenvalues of the Gramians $\mathcal{P}$ and $\mathcal{Q}$ as well as the first three columns of the inverse balancing matrix $\mathbf{T}_{\text{bal}}^{-1}$ are depicted in Figure 6.3. In each of the plots, the vector under consideration is projected onto the model grid. Since each component of the state relates to the pressure in a specific grid block, and thereby a specific physical location, this projection allows us to interpret how the reservoir model's controllability and observability properties vary over space. Note that the scales of these plots differ

and that the nonzero areas are of particular interest, as these represent areas where reference pressures are controllable and / or observable.

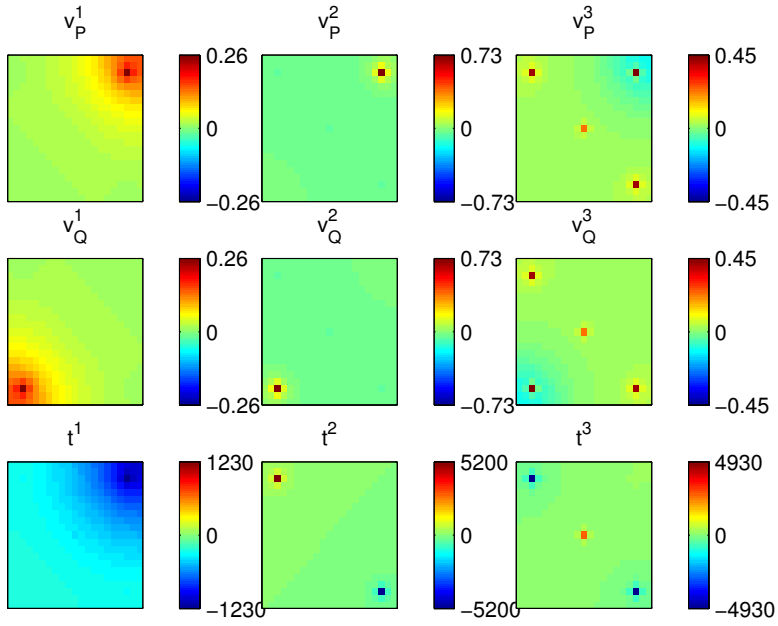

Figure 6.3: Eigenvectors corresponding to 3 largest absolute eigenvalues of controllability Gramian $\mathcal{P}$ (top row), observability Gramian $\mathcal{Q}$ (middle row), and first 3 columns of inverse transformation matrix $\mathbf{T}_{\text{bal}}^{-1}$ (bottom row) projected onto model grid for homogeneous example.

Since the observation well (well 2 in Figure 6.1) is the only well that does not appear as a nonzero area in the plots of the controllability Gramian, we conclude that reference pressures in areas near production or injection wells require the least energy to reach. Similarly, since the production well without any measurement (well 4 in Figure 6.1) is the only well that does not appear as a nonzero area in the plots of the observability Gramian, we conclude that reference pressures in areas near wells with flow meters or pressure gauges produce the most energy when observed. In short, pressures near wells in which we can control the flow rate or bottom-hole pressure are controllable, whereas pressures near wells in which we can measure the flow rate or bottom-hole pressure are observable. Since a column $\hat{\mathbf{t}}_j$ of the inverse balancing matrix $\mathbf{T}_{\text{bal}}^{-1}$ represents a state (*i.e.* a vector of pressures) that is equally difficult to reach as observe, it makes sense that particularly the wells in which we can control *and* observe (wells 1, 3 and 5 in Figure 6.1) appear as nonzero areas in the plots of $\mathbf{T}_{\text{bal}}^{-1}$.

6.4.2 Example 2: heterogeneous permeability

Consider the same reservoir model as in the previous example, but with a high permeability zone of 1000 mDarcy in the North-West corner, a low permeability zone of 10 mDarcy in the South-East corner, and a permeability of 100 mDarcy throughout the rest of the reservoir - see Figure 6.4. The discretization time step Δt is still given by (2.32) and its value is therefore different than before, namely $\Delta t = 0.013$ seconds.

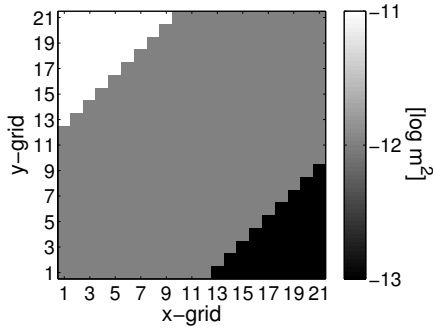

Figure 6.4: Heterogeneous permeability.

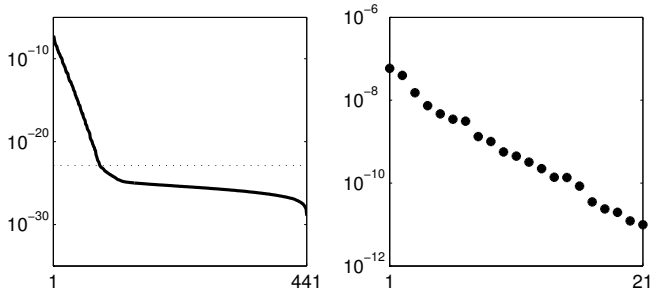

Figure 6.5: All 441 Hankel singular values $\sigma_1, \ldots, \sigma_{441}$ (left) and 21 largest ones $\sigma_1, \ldots, \sigma_{21}$ (right) for heterogeneous example. The dashed line represents machine precision.

The results are similar to the homogeneous example. The Hankel singular values, depicted in Figure 6.5, decrease very rapidly. As before, this indicates that the 441^{th} order reservoir model behaves like a model of much lower order.

The eigenvectors corresponding to the three largest absolute eigenvalues of the Gramians $\mathcal{P}$ and $\mathcal{Q}$ as well as the first three columns of $\mathbf{T}_{\text{bal}}^{-1}$ are depicted in Figure 6.6. Contrary to Figure 6.3, only the production well in the high permeable zone (well 1 in Figure 6.1) appears as a nonzero area in the plots of the controllability

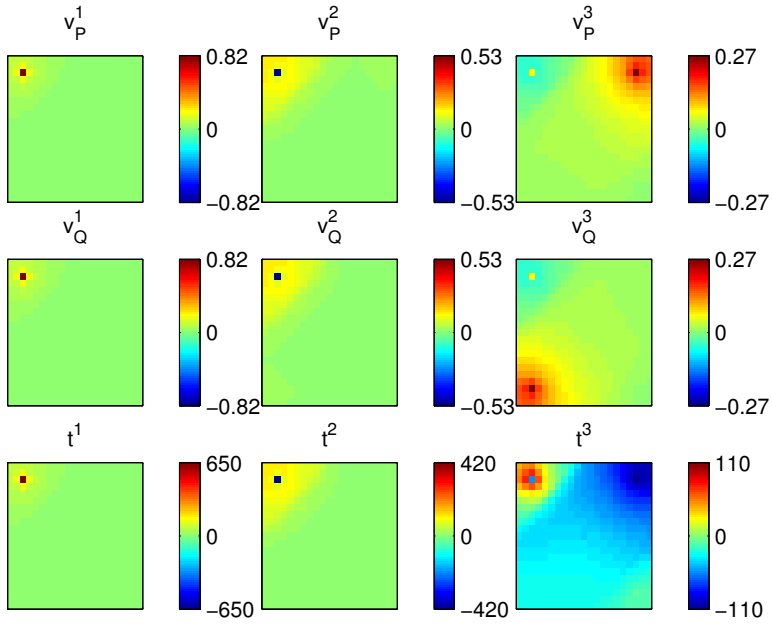

Figure 6.6: Eigenvectors corresponding to 3 largest absolute eigenvalues of controllability Gramian $\mathcal{P}$ (top row), observability Gramian $\mathcal{Q}$ (middle row), and first 3 columns of inverse transformation matrix $\mathbf{T}_{\text{bal}}^{-1}$ (bottom row) projected onto model grid for heterogeneous example.

Gramian. From this we conclude that reference pressures in areas near production wells in high permeable zones require the least energy to reach. Contrary to Figure 6.3, only the well with a measurement in the high permeable zone (well 1 Figure 6.1) appears as a nonzero area in the plots of the observability Gramian. From this we conclude that reference pressures in areas near observation wells in high permeable zones produce the most energy when observed.

The following section shows how these results depend on the physical reservoir parameters, the time discretization and the spatial discretization.

6.5 Effect of physical reservoir parameters

Recall that the matrices $\mathbf{A}$ and $\mathbf{B}$ in (2.30) are given by (2.28)-(2.29):

$$\begin{aligned} \mathbf{A} &= I + \mathbf{A}_{11}\Delta t, \\ \mathbf{B} &= \mathbf{B}_1 \Delta t. \end{aligned}$$

From (2.16) in Chapter 2, it can be seen that scaling the value of

- compressibility c to $(1/\epsilon)c$, or
- the entire porosity field $\begin{bmatrix} \phi_1 & \dots & \phi_N \end{bmatrix}$ to $(1/\epsilon)\begin{bmatrix} \phi_1 & \dots & \phi_N \end{bmatrix}$ or
- viscosity μ to $(1/\epsilon)\mu$, or
- the entire permeability field $\begin{bmatrix} k_1 & \dots & k_N \end{bmatrix}$ to $\epsilon \begin{bmatrix} k_1 & \dots & k_N \end{bmatrix}$,

for some $\epsilon > 0$ leads to

$$\begin{aligned} \mathbf{A} &= I + \epsilon \mathbf{A}_{11}\Delta t, & (6.23) \\ \mathbf{B} &= \epsilon \mathbf{B}_1 \Delta t. & (6.24) \end{aligned}$$

In other words, scaling the above mentioned physical parameters by ϵ has the same effect on $\mathbf{A}$ and $\mathbf{B}$ as scaling the discretization time step Δt by ϵ. Furthermore, from Section 6.2 it can be seen that for the viscosity or the entire permeability this also leads to a scaling of the values of $\mathbf{C}$ and $\mathbf{D}$ in (6.1) to $\epsilon\mathbf{C}$ and $\epsilon\mathbf{D}$, respectively.

It is important to note that the dynamics of the discrete-time reservoir model (2.30), (6.1) are unaffected by scaling Δt, provided that $\epsilon\Delta t$ is still smaller than the value given by (2.32)[4]. In fact, the results obtained in this chapter (in terms of Hankel singular values and spatial variation of controllability and observability properties) using the original continuous-time matrices $(\mathbf{A}_{11}, \mathbf{B}_1)$ are virtually the same. Given (6.23)-(6.24), this therefore also holds for the compressibility and porosity scalings mentioned above. The viscosity and permeability scalings on the other hand also influence $\mathbf{C}$, leading to a scaling of the Hankel singular values $\begin{bmatrix} \sigma_1 & \dots & \sigma_N \end{bmatrix}$ in (6.16) to $\epsilon \begin{bmatrix} \sigma_1 & \dots & \sigma_N \end{bmatrix}$.

The spatial discretization also does not have a significant influence on the results: the spatial patterns depicted in Figure 6.3 and Figure 6.6 clearly resemble the ones obtained by modelling the reservoir with, say, $11 \times 11 \times 1$ or $31 \times 31 \times 1$ grid blocks. This is important, as it points out that controllability and observability are reservoir properties, and not just reservoir model properties. Furthermore, the overall decrease in Hankel singular values is very similar - see Figure 6.7. This is important, as it points out that the number of grid blocks, often chosen as high as computationally possible, does not have a significant influence on the relevant order of the pressure dynamics throughout the reservoir.

[4]Recall that a discrete-time model (2.30) obtained with a time-step larger than (2.32) does not capture all of the dynamics of the original continuous-time model (2.25).

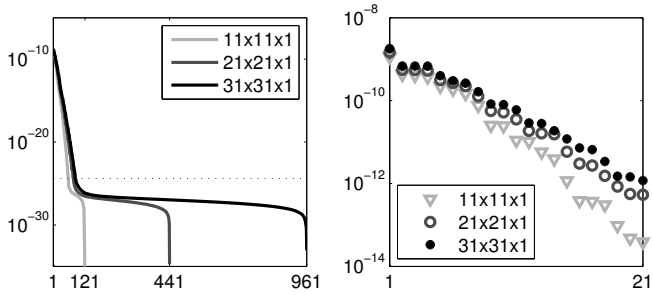

Figure 6.7: All Hankel singular values (left) and 21 largest ones (right) of three reservoir models based on the reservoir treated in homogenous example, where each model is spatially discretized by a different number of grid blocks.

6.6 Chapter conclusions

The most controllable and observable pressures in single-phase flow reservoir models can be computed by performing an eigenvalue decomposition of the controllability and observability Gramians. By projecting the eigenvectors corresponding to the largest absolute eigenvalues of the Gramians onto the model grid, we can interpret how the reservoir model's controllability and observability properties vary over space. It turns out that pressures near wells in which we can control the flow rate or bottom-hole pressure are controllable, whereas pressures near wells in which we can measure the flow rate or bottom-hole pressure are observable. Furthermore, the controllability and observability properties are determined by the well configuration (*i.e.* the number and location of wells) and to a lesser extent the heterogeneity of the reservoir at hand. The Hankel singular values of single-phase flow reservoir models decrease rapidly, indicating that they behave as models of much lower order.

Despite these results, there is much work still to be done in this area. Since a reservoir's recovery factor can be defined in terms of the saturations at the end of its lifecycle, a reservoir's saturations dynamics are at least as relevant for field development planning as its pressure dynamics. However, a reservoir's saturation dynamics are described by nonlinear equations, and it is therefore important to investigate how the controllability and observability of saturations change with time. This could be done by linearizing the nonlinear dynamics along a certain trajectory.

7 CHAPTER

Identification of Reservoir Parameters

Th is chapter focuses on the identification of physical parameters of single-phase flow reservoir models through history matching of production data. The main contributions are to show how to compute an upper bound on the number of identifiable parameters, and to present a new method to regularize the history matching problem using the controllability and observability analysis of the previous chapter. The benefits of this method are illustrated through an application.

7.1 Problem formulation

As discussed in Section 2.3, reservoir models generally contain a significant amount of uncertainty originating from many different sources and, as depicted in Figure 2.5, this can have a large influence on the predictions of future production. In order to reduce the uncertainty associated with physical reservoir parameters, it is common to define a cost function (typically the weighted squared difference between predicted and measured data), and minimize it over all possible parameter values. In reservoir engineering this procedure is referred to as history matching, and in this chapter we consider history matching production data to identify physical parameters in single-phase flow reservoirs.

As in (2.36), let us stack all of the uncertain parameters in a vector $\boldsymbol{\theta}$. Furthermore, let us assume that measurements $\bar{\mathbf{y}}_1, \ldots, \bar{\mathbf{y}}_n$ are available, and that these have been generated by the system

$$\begin{aligned} \mathbf{p}_{k+1} &= \mathbf{A}(\boldsymbol{\theta})\mathbf{p}_k + \mathbf{B}(\boldsymbol{\theta})\mathbf{u}_k, && (7.1)\\ \mathbf{p}_0 &= \bar{\mathbf{p}}_0 && (7.2)\\ \mathbf{y}_k &= \mathbf{C}(\boldsymbol{\theta})\mathbf{p}_k + \mathbf{D}(\boldsymbol{\theta})\mathbf{u}_k && (7.3) \end{aligned}$$

for some unknown $\boldsymbol{\theta} = \bar{\boldsymbol{\theta}}$ (*i.e.* the true physical reservoir parameters), known manipulated input $\mathbf{u}_0, \ldots, \mathbf{u}_{n-1}$ and known initial state $\bar{\mathbf{p}}_0$, where (7.1) and (7.3) are

the generalizations of (2.30) and (6.1), respectively. If water and oil have similar properties, this assumption can be justified by the previously discussed difference in dynamics. For example if the measurements have been gathered over a period of one month, the saturation front - which typically moves less than 1 meter per day - can be assumed to have stayed nearly constant, and thereby so can $\mathbf{A}_{11}$, $\mathbf{A}_{21}$, $\mathbf{B}_1$ and $\mathbf{B}_2$. We also assume that the input contains enough frequencies to obtain informative measurements, also called persistently exciting - Ljung (1999). A common history matching approach is then to consider the following nonlinear least-squares problem

Problem 5

$$\begin{aligned} \text{minimize } \mathrm{V}(\boldsymbol{\theta}) &:= \sum_{k=1}^{n} \left[\bar{\mathbf{y}}_k - \mathbf{y}_k(\boldsymbol{\theta})\right]^T \left[\bar{\mathbf{y}}_k - \mathbf{y}_k(\boldsymbol{\theta})\right] \\ \text{over } \boldsymbol{\theta} &\in \mathbb{R}^M \\ \text{subject to } \mathbf{p}_{k+1} &= \mathbf{A}(\boldsymbol{\theta})\mathbf{p}_k + \mathbf{B}(\boldsymbol{\theta})\mathbf{u}_k, \\ \mathbf{p}_0 &= \bar{\mathbf{p}}_0, \\ \mathbf{y}_k &= \mathbf{C}(\boldsymbol{\theta})\mathbf{p}_k + \mathbf{D}(\boldsymbol{\theta})\mathbf{u}_k. \end{aligned}$$

Because we assume that all modeling errors are captured in $\boldsymbol{\theta}$ and that the measurements are noisefree, **Problem 5** is a least-squares problem with

$$V(\bar{\boldsymbol{\theta}}) = 0, \quad \frac{\partial V}{\partial \boldsymbol{\theta}}(\bar{\boldsymbol{\theta}}) = 0 \quad \text{and} \quad \frac{\partial^2 V}{\partial \boldsymbol{\theta}^2}(\bar{\boldsymbol{\theta}}) \geq 0.$$

If **Problem 5** has a unique local minimum at $\boldsymbol{\theta} = \bar{\boldsymbol{\theta}}$ (*e.g.* $\partial^2 V/\partial \boldsymbol{\theta}^2(\bar{\boldsymbol{\theta}}) > 0$), the model structure (7.1)-(7.3) is said to be locally identifiable. If this minimum is global, the structure is said to be globally identifiable - see Bellman and Astrom (1970), Glover and Willems (1974) and Ljung (1999) for a more detailed discussion.

It is well-known in the petroleum engineering community that if the vector of to-be-estimated physical parameters $\boldsymbol{\theta}$ contains the geological properties (*e.g.* permeability values) in all grid blocks, virtually all reservoir models of the form (7.1)-(7.3) are not identifiable. Often called ill-posed, this lack of identifiability in **Problem 5** is mentioned in almost all publications on history matching, and is problematic because a wrongly updated estimate $\boldsymbol{\theta}_{\mathrm{up}}$ of $\bar{\boldsymbol{\theta}}$ can lead to a perfect history match (*i.e.* $V(\boldsymbol{\theta}_{\mathrm{up}}) = 0$) but incorrect long-term predictions (*e.g.* when the saturation front has significantly advanced) - see Tavassoli et al. (2004).

Since permeability cannot be uniquely estimated from production data, it is common to regularize the problem (*i.e.* render it 'less' ill-posed). The most common method is to add the difference between $\boldsymbol{\theta}$ and the initial estimate $\boldsymbol{\theta}_{\mathrm{init}}$ to the original cost function V

$$V_{\mathrm{reg}}(\boldsymbol{\theta}) := \sum_{k=1}^{n} \left[\bar{\mathbf{y}}_k - \mathbf{y}_k(\boldsymbol{\theta})\right]^T \mathbf{P}_{\mathbf{y}} \left[\bar{\mathbf{y}}_k - \mathbf{y}_k(\boldsymbol{\theta})\right] + \left[\boldsymbol{\theta} - \boldsymbol{\theta}_{\mathrm{init}})\right]^T \mathbf{P}_{\boldsymbol{\theta}} \left[\boldsymbol{\theta} - \boldsymbol{\theta}_{\mathrm{init}})\right],$$

where $\mathbf{P_y} \in \mathbb{R}^{N_y}$ and $\mathbf{P}_{\boldsymbol{\theta}} \in \mathbb{R}^{N}$ are weighting matrices. By weighting the data and prior mismatch terms, the resulting problem can, under certain conditions, be interpreted as finding the maximum a posteriori estimate. This is often referred to as the Bayesian estimation approach to history matching - see Gavalas et al. (1976) and Tarantola (2005).

Whatever the history-match cost function V that is considered, it is often minimized using a gradient-based optimization procedure. The gradients $\partial V/\partial \boldsymbol{\theta}$ can be efficiently computed using the so-called adjoint method from optimal control theory - see Jacquard and Jain (1965), Carter et al. (1974) and Chavent (1975). The Gauss-Newton and Levenberg-Marquardt methods have been applied, among others, in Reynolds et al. (1996) and Li et al. (2003). A disadvantage of these methods is that they require the sensitivities or partial derivatives of the measurements $\{\mathbf{y}_1, \ldots, \mathbf{y}_n\}$ with respect to the to-be estimated parameters $\boldsymbol{\theta}$. Despite the use of the adjoint method, this becomes computationally demanding when the number of measurements and the number of parameters is large.

Reducing the computational burden in history matching has been one of the main motivations for re-parameterizing $\boldsymbol{\theta}$ by a small number of basis functions (the other being the desire to generate estimates that are geologically realistic). Some of the re-parameterization techniques applied in history matching to achieve this include

- zonation - Jacquard and Jain (1965), Jahns (1966), and adapted versions thereof - Grimstad et al. (2003), Berre et al. (2007),
- grad zones - Bissell (1994), Bissell et al. (1994), Brun et al. (2004),
- spectral decomposition and subspace methods - Shah et al. (1978), Reynolds et al. (1996), Abacioglu et al. (2001),
- kernel principle component analysis - (Sarma et al. (2007)),
- discrete cosine transform - (Jafarpour and McLaughlin (2007a), Jafarpour and McLaughlin (2007b)).

Despite all of these applications, it is not clear how many parameters can be uniquely identified for any particular reservoir model.

7.2 Number of identifiable parameters

For any k^{th} order linear system of the form (7.1)-(7.3) with $N_{\mathbf{u}}$ manipulated inputs and $N_{\mathbf{y}}$ measured outputs, there exists a transformation $\mathbf{T}_{\text{can}}$ such that, in the transformed co-ordinates, the state-space matrices that result from (6.14)-(6.15) are in a so-called canonical form, which we will denote by

$$\hat{\mathbf{A}}(\boldsymbol{\theta}) := \mathbf{T}_{\text{can}}\mathbf{A}(\boldsymbol{\theta})\mathbf{T}_{\text{can}}^{-1}, \quad \hat{\mathbf{B}}(\boldsymbol{\theta}) := \mathbf{T}_{\text{can}}\mathbf{B}(\boldsymbol{\theta}), \quad \hat{\mathbf{C}} := \mathbf{C}(\boldsymbol{\theta})\mathbf{T}_{\text{can}}^{-1}, \quad \mathbf{D}(\boldsymbol{\theta}).$$

There are several canonical forms for linear multivariable systems. We consider the one discussed in Luenberger (1967), Denham (1974) and Ljung (1999), which has the following form.

- $\hat{\mathbf{A}}$ is initially filled with zeros and ones along the superdiagonal. The $N_{\mathbf{y}}$ rows $r_1, r_2, r_{N_{\mathbf{y}}}$, where $r_0 = 0$ and $r_{N_{\mathbf{y}}} = k$, are filled with parameters.
- $\hat{\mathbf{B}}$ is filled with parameters.
- $\hat{\mathbf{C}}$ is filled with zeros, but each row i has a one in column $r_{i-1} + 1$.

The parameterization is uniquely characterized by the $N_{\mathbf{y}}$ numbers r_i that are to be chosen by the user. Note that only $N_{\mathbf{y}}$ rows in $\hat{\mathbf{A}}$ have elements not equal to zero or one, $\hat{\mathbf{B}}$ is a full matrix and $\hat{\mathbf{C}}$ only contains zeros and ones.

As an example, for the specific situation that $k = 9$, $N_{\mathbf{u}} = 2$, $N_{\mathbf{y}} = 3$, $r_1 = 3$, $r_2 = 5$, and $r_3 = 9$ this canonical form is as follows

$$\hat{\mathbf{A}}(\boldsymbol{\theta}) = \begin{bmatrix} 0 & 1 & 0 & 0 & 0 & 0 & 0 & 0 & 0 \\ 0 & 0 & 1 & 0 & 0 & 0 & 0 & 0 & 0 \\ \times & \times & \times & \times & \times & \times & \times & \times & \times \\ 0 & 0 & 0 & 0 & 1 & 0 & 0 & 0 & 0 \\ \times & \times & \times & \times & \times & \times & \times & \times & \times \\ 0 & 0 & 0 & 0 & 0 & 0 & 1 & 0 & 0 \\ 0 & 0 & 0 & 0 & 0 & 0 & 0 & 1 & 0 \\ 0 & 0 & 0 & 0 & 0 & 0 & 0 & 0 & 1 \\ \times & \times & \times & \times & \times & \times & \times & \times & \times \end{bmatrix}, \quad \hat{\mathbf{B}}(\boldsymbol{\theta}) = \begin{bmatrix} \times & \times \\ \times & \times \\ \times & \times \\ \times & \times \\ \times & \times \\ \times & \times \\ \times & \times \\ \times & \times \\ \times & \times \end{bmatrix},$$

$$\hat{\mathbf{C}} = \begin{bmatrix} 1 & 0 & 0 & 0 & 0 & 0 & 0 & 0 & 0 \\ 0 & 0 & 0 & 1 & 0 & 0 & 0 & 0 & 0 \\ 0 & 0 & 0 & 0 & 0 & 1 & 0 & 0 & 0 \end{bmatrix}, \qquad \mathbf{D}(\boldsymbol{\theta}) = \begin{bmatrix} \times & \times \\ \times & \times \\ \times & \times \end{bmatrix}$$

and as such is completely described by the nonzero elements of $\hat{\mathbf{A}}$, $\hat{\mathbf{B}}$ and $\mathbf{D}$. In other words, any k^{th} order linear system of the form (7.1)-(7.3) with $N_{\mathbf{u}}$ manipulated inputs and $N_{\mathbf{y}}$ can be completely described by at most

$$N_{\max} = (N_{\mathbf{u}} + N_{\mathbf{y}}) \times k + N_{\mathbf{u}}N_{\mathbf{y}} \tag{7.4}$$

parameters - Ljung (1999). In the example above, $N_{\max} = 51$.

However, as shown in Chapter 6, the relevant order k of single-phase flow reservoir models is much smaller than their original order N (determined by the number of grid blocks, often chosen as high as possible). Furthermore, while the physical reservoir parameters (*e.g.* the grid block permeabilities) do influence the input-output behavior, they do not significantly influence the relevant *order* of the input-output behavior (*e.g.* Figure 6.2 and Figure 6.5 show the same rapid decline in Hankel singular values). This means that unless there are many wells $N_{\mathbf{u}}$ in which we can control the flow rate or bottom-hole pressure and many wells $N_{\mathbf{y}}$ in which we can observe the flow rate or bottom-hole pressure, the number of identifiable parameters will be much smaller than the number of grid blocks N. Consequently, if the grid block permeabilities are to be estimated, the resulting reservoir model structure is not identifiable. We stress that this lack of identifiability is not the result of applying a particular transformation to the original state-space matrices $\{\mathbf{A}(\boldsymbol{\theta}), \mathbf{B}(\boldsymbol{\theta}), \mathbf{C}(\boldsymbol{\theta}), \mathbf{D}(\boldsymbol{\theta})\}$ describing single-phase flow, but that there are fundamental reasons for it.

For example, consider again the homogeneous single-phase flow reservoir model of Section 6.4.1. Recall that the reservoir is modeled by $21 \times 21 \times 1$ grid blocks, and the order of the model is therefore $N = 441$. However, the Hankel singular values depicted in Figure 6.2 decline very rapidly. In fact, we have

$$2(\sigma_{16} + \ldots + \sigma_{441}) = 8.0 \times 10^{-3}.$$

According to (6.22), the H_∞ norm of the error between the full order model and a 15^{th} order approximation is therefore less than 10^{-2}. In other words, the relevant order of the model is $k = 15$ and the relevant input-output behavior is described by at most

$$N_{\max} = (N_{\mathbf{u}} + N_{\mathbf{y}}) \times k + N_{\mathbf{u}} N_{\mathbf{y}} = (4 + 4) \times 15 + 4 \times 4 = 136$$

parameters. If $\boldsymbol{\theta}$ contains the permeability in all 441 grid blocks, then the model structure (7.1)-(7.3) is clearly not identifiable. This gap between the maximum number of identifiable parameters $N_{\max}$ and the number of to-be-identified parameters (*e.g.* N in the case of grid block permeabilities) is much larger for realistic reservoir models with $N = 10^4 - 10^6$ grid blocks.

7.3 Relevant spatial patterns of permeability

In Chapter 6 it was demonstrated that (7.1)-(7.3) can be decomposed into a part that is both controllable and observable (*i.e.* belongs to the k largest Hankel singular values) and a part that is poorly controllable and / or poorly observable (*i.e.* belongs to the $N - k$ smallest Hankel singular values). The choice of k of course depends on what is considered to be relevant for the input-output behavior. For example, if the H_∞ norm of the approximation error should be less than 10^{-3}, k will generally be larger than for 10^{-2}. Let us assume that a particular choice for k has been made, and let $\mathbf{T}_{\text{bal}}$ denote the balancing matrix as introduced in

Section 6.3 corresponding to (7.1)-(7.3). As mentioned earlier, the controllable and observable part of (7.1)-(7.3) is represented by the triple

$$\{\tilde{\mathbf{A}}_{11}(\boldsymbol{\theta}), \tilde{\mathbf{B}}_1(\boldsymbol{\theta}), \tilde{\mathbf{C}}_1(\boldsymbol{\theta}), \mathbf{D}(\boldsymbol{\theta})\}$$

resulting from

$$\left[\begin{array}{cc|c} \mathbf{T}_{\mathrm{bal},1} & & 0 \\ \mathbf{T}_{\mathrm{bal},2} & & 0 \\ \hline 0 & & I \end{array}\right] \left[\begin{array}{c|c} \mathbf{A}(\boldsymbol{\theta}) & \mathbf{B}(\boldsymbol{\theta}) \\ \hline \mathbf{C}(\boldsymbol{\theta}) & \mathbf{D}(\boldsymbol{\theta}) \end{array}\right] \left[\begin{array}{cc|c} \hat{\mathbf{T}}_{\mathrm{bal},1} & \hat{\mathbf{T}}_{\mathrm{bal},2} & 0 \\ \hline 0 & 0 & I \end{array}\right] = \left[\begin{array}{cc|c} \tilde{\mathbf{A}}_{11}(\boldsymbol{\theta}) & \tilde{\mathbf{A}}_{12}(\boldsymbol{\theta}) & \tilde{\mathbf{B}}_1(\boldsymbol{\theta}) \\ \tilde{\mathbf{A}}_{21}(\boldsymbol{\theta}) & \tilde{\mathbf{A}}_{22}(\boldsymbol{\theta}) & \tilde{\mathbf{B}}_2(\boldsymbol{\theta}) \\ \hline \tilde{\mathbf{C}}_1(\boldsymbol{\theta}) & \tilde{\mathbf{C}}_2(\boldsymbol{\theta}) & \mathbf{D}(\boldsymbol{\theta}) \end{array}\right],$$

where $\mathbf{T}_{\mathrm{bal}}$ and $\mathbf{T}_{\mathrm{bal}}^{-1}$ have been partitioned according to the first k rows and columns, respectively:

$$\mathbf{T}_{\mathrm{bal}} = \left[\begin{array}{c} \mathbf{T}_{\mathrm{bal},1} \\ \mathbf{T}_{\mathrm{bal},2} \end{array}\right] \quad , \quad \mathbf{T}_{\mathrm{bal}}^{-1} = \left[\begin{array}{cc} \hat{\mathbf{T}}_{\mathrm{bal},1} & \hat{\mathbf{T}}_{\mathrm{bal},2} \end{array}\right].$$

This decomposition is depicted in Figure 7.1.

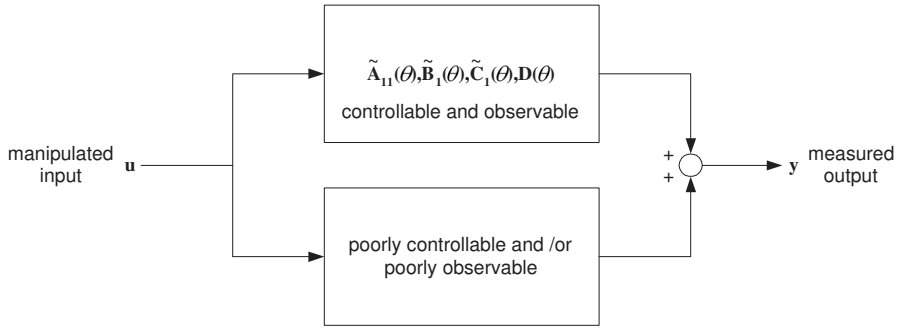

Figure 7.1: Decomposition of a reservoir model into a controllable and observable part, and a poorly controllable and / or poorly observable part.

From a history-matching perspective, it clearly only makes sense to change an initial permeability estimate in a direction that affects the cost function V as defined in **Problem 5**. Similarly, from a controllability and observability perspective, it clearly only makes sense to change an initial permeability estimate in a direction that affects the controllable and observable part of the reservoir model (*i.e.* the quadruple $\{\tilde{\mathbf{A}}_{11}(\boldsymbol{\theta}), \tilde{\mathbf{B}}_1(\boldsymbol{\theta}), \tilde{\mathbf{C}}_1(\boldsymbol{\theta}), \mathbf{D}(\boldsymbol{\theta})\}$ in Figure 7.1). If the inputs are persistently exciting, this boils down to the same thing.

Consider the special situation that $\boldsymbol{\theta}$ contains the permeability values in all N grid blocks, or

$$\boldsymbol{\theta} = \left[\begin{array}{ccc} k_1 & \ldots & k_N \end{array}\right]^T. \tag{7.5}$$

Let us focus on the effect of a variation $\Delta\boldsymbol{\theta}$ on $\{\tilde{\mathbf{A}}_{11}(\boldsymbol{\theta}), \tilde{\mathbf{B}}_1(\boldsymbol{\theta}), \tilde{\mathbf{C}}_1(\boldsymbol{\theta}), \mathbf{D}(\boldsymbol{\theta})\}$ in the coordinates corresponding to a fixed $\mathbf{T}_{\mathrm{bal}}$. Recall from Chapter 2 that the

permeability value k_j only enters $\mathbf{B}$ if grid block j contains a well. A variation $\Delta\theta_j$ will therefore only have an effect on $\tilde{\mathbf{B}}_1$ if grid block j contains a well. The same reasoning applies to $\tilde{\mathbf{C}}_1$ and $\mathbf{D}$. On the other hand, the effect of a variation $\Delta\boldsymbol{\theta}$ on $\tilde{\mathbf{A}}_{11}$ is

$$\mathbf{T}_{\mathrm{bal},1}\mathbf{A}(\boldsymbol{\theta}+\Delta\boldsymbol{\theta})\hat{\mathbf{T}}_{\mathrm{bal},1} - \underbrace{\mathbf{T}_{\mathrm{bal},1}\mathbf{A}(\boldsymbol{\theta})\hat{\mathbf{T}}_{\mathrm{bal},1}}_{=\tilde{\mathbf{A}}_{11}(\boldsymbol{\theta})} = \sum_{j=1}^{N} \mathbf{T}_{\mathrm{bal},1}\frac{\partial \mathbf{A}}{\partial \theta_j}(\boldsymbol{\theta})\hat{\mathbf{T}}_{\mathrm{bal},1}\Delta\theta_j + o(\Delta\boldsymbol{\theta}). \quad (7.6)$$

By defining $\Pi(\boldsymbol{\theta}) \in \mathbb{R}^{k^2 \times N}$ as

$$\Pi(\boldsymbol{\theta}) := \left[\mathrm{vec}\left\{\mathbf{T}_{\mathrm{bal},1}\tfrac{\partial \mathbf{A}}{\partial \theta_1}(\boldsymbol{\theta})\hat{\mathbf{T}}_{\mathrm{bal},1}\right\} \quad \dots \quad \mathrm{vec}\left\{\mathbf{T}_{\mathrm{bal},1}\tfrac{\partial \mathbf{A}}{\partial \theta_N}(\boldsymbol{\theta})\hat{\mathbf{T}}_{\mathrm{bal},1}\right\} \right] \quad (7.7)$$

we can rewrite (7.6) as

$$\mathrm{vec}\left\{ \mathbf{T}_{\mathrm{bal},1}\mathbf{A}(\boldsymbol{\theta}+\Delta\boldsymbol{\theta})\hat{\mathbf{T}}_{\mathrm{bal},1} - \underbrace{\mathbf{T}_{\mathrm{bal},1}\mathbf{A}(\boldsymbol{\theta})\hat{\mathbf{T}}_{\mathrm{bal},1}}_{=\tilde{\mathbf{A}}_{11}(\boldsymbol{\theta})} \right\} = \Pi(\boldsymbol{\theta})\Delta\boldsymbol{\theta} + o(\Delta\boldsymbol{\theta}). \quad (7.8)$$

Consider again the homogeneous example of Section 6.4.1. In Section 7.2 we computed that the relevant order of the model is $k = 15$. The matrix Π can now be computed using (7.7). The right singular vectors corresponding to the three largest singular values of Π are depicted in Figure 7.2. In each of the plots, the vector under consideration is projected onto the model grid. Since each component of $\boldsymbol{\theta}$ relates to the permeability k_j in a specific grid block j and thereby a specific physical location, this projection allows us to interpret how the reservoir model's relevant input-output behavior (as captured by $\tilde{\mathbf{A}}_{11}$) varies over space. Note that the scales of these plots differ and that the nonzero areas are of particular interest, as these represent areas where changes in permeability effect the input-output behavior.

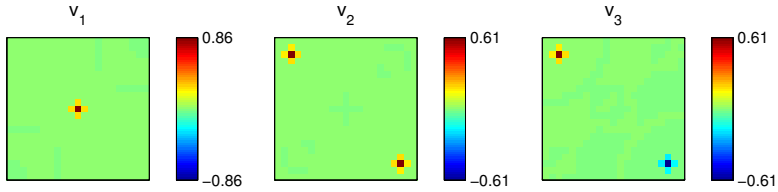

Figure 7.2: Right singular vectors corresponding to three largest singular values of Π projected onto model grid for homogeneous example.

Since wells 2 and 4 from Figure 6.1 do not appear as nonzero areas in the plots of Figure 7.2, we conclude that permeability variations in grid blocks near wells in which we can both control and observe affect the input-output behavior more

than permeability variations in grid blocks far from these wells. This is in line with results presented in Van Doren et al. (2008), and is also very similar to the results from Chapter 6 on how a reservoir model's controllability and observability properties vary over space. In fact, the nonzero areas in the plots of Figure 7.2 strongly resemble those in the bottom row of Figure 6.3. In other words, the relevant spatial patterns of pressure strongly resemble the relevant spatial patterns of permeability. This can be explained as follows.

Recall from Chapter 2 that the matrices $\mathbf{A}_{\mathrm{o}}$ and $\mathbf{A}_{\mathrm{w}}$, which are used to construct $\mathbf{A}$, have a very sparse structure - see Figure 2.2. Consequently, $\mathbf{A}$ also has a very sparse structure, as does $\partial\mathbf{A}/\partial\boldsymbol{\theta}_j$. In fact, due to the sparsity in $\mathbf{A}$, $\partial\mathbf{A}/\partial\boldsymbol{\theta}_j$ has at most 13 nonzero elements for a 2D reservoir model - see Figure 7.3. Moreover, the nonzero components of $\partial\mathbf{A}/\partial\boldsymbol{\theta}_j$ only appear in the rows and columns corresponding to grid block j and its neighbors.

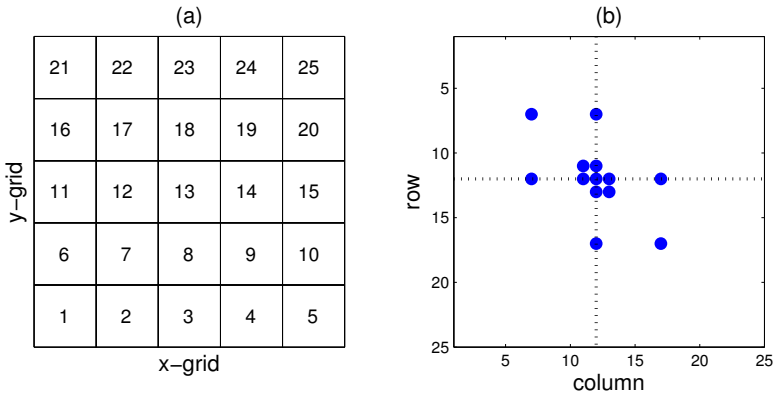

Figure 7.3: Grid block numbering for a 2D model of 5×5 grid blocks (a) and corresponding nonzero elements of $\partial\mathbf{A}/\partial\theta_{12}$ (b). Note that these only appear in the rows and columns of grid block 12 and its neighbors 7, 11, 13 and 17.

Similarly, Figure 6.3 and Figure 6.6 show that the nonzero components of $\hat{\mathbf{T}}_{\mathrm{bal},1}$ spatially correspond to grid blocks near wells in which we can both control and observe. Although not depicted in any of the figures, this also holds for the rows of $\mathbf{T}_{\mathrm{bal},1}$. Consequently, the

$$\mathbf{T}_{\mathrm{bal},1}\frac{\partial\mathbf{A}}{\partial\theta_j}(\boldsymbol{\theta})\hat{\mathbf{T}}_{\mathrm{bal},1}$$

term in (7.6) and thereby the j^{th} column of Π only contains nonzero elements if j corresponds to a grid block near a production or injection well with a flow meter or a pressure gauge.

To summarize: the relevant spatial patterns of permeability strongly resemble the relevant spatial patterns of pressure. This is quite intuitive, as it implies that permeability in an area where we can control and observe has a greater effect on the input-output behavior than in an area where we cannot.

7.4 Controllability and observability-based re- parameterization

In Section 7.2 it was shown that the model structure the (7.1)-(7.3) is not identifiable if $\boldsymbol{\theta}$ contains the grid block permeability values as in (7.5). We therefore propose to regularize **Problem 5** by re-parameterizing $\boldsymbol{\theta}$ as

$$\boldsymbol{\theta} \quad = \quad \boldsymbol{\Phi}\boldsymbol{\alpha} \tag{7.9}$$

where $\boldsymbol{\Phi} \in \mathbb{R}^{N \times L}$ is called the re-parameterization matrix and $L \ll N$ is the number of to-be-estimated (non-physical) parameters (*i.e.* the number of elements in $\boldsymbol{\alpha}$). The columns of $\boldsymbol{\Phi}$ are referred to as basis functions, and linear combinations of these can represent relevant spatial patterns of permeability.

Since the relevant spatial patterns of permeability strongly resemble the relevant spatial patterns of pressure, we propose to choose the first $L-1$ columns of the inverse balancing matrix $\hat{\mathbf{T}}_{\mathrm{bal},1}$, with an additional vector of ones to account for an overall increase or decrease in permeability. By solving the regularized problem

Problem 6

$$\begin{aligned}
\text{minimize } \mathrm{V}(\boldsymbol{\Phi}\boldsymbol{\alpha}) &= \sum_{k=1}^{n} \left[\bar{\mathbf{y}}_k - \mathbf{y}_k(\boldsymbol{\Phi}\boldsymbol{\alpha})\right]^T \left[\bar{\mathbf{y}}_k - \mathbf{y}_k(\boldsymbol{\Phi}\boldsymbol{\alpha})\right] \\
\text{over} \quad \boldsymbol{\alpha} &\in \mathbb{R}^L \\
\text{subject to} \quad \mathbf{p}_{\mathrm{k+1}} &= \mathbf{A}(\boldsymbol{\Phi}\boldsymbol{\alpha})\mathbf{p}_k + \mathbf{B}(\boldsymbol{\Phi}\boldsymbol{\alpha})\mathbf{u}_k, \\
\mathbf{p}_0 &= \bar{\mathbf{p}}_0, \\
\mathbf{y}_k &= \mathbf{C}(\boldsymbol{\Phi}\boldsymbol{\alpha})\mathbf{p}_k + \mathbf{D}(\boldsymbol{\Phi}\boldsymbol{\alpha})\mathbf{u}_k.
\end{aligned}$$

using a gradient-based optimization procedure starting from an initial estimate $\boldsymbol{\theta}_{\mathrm{init}} = \boldsymbol{\Phi}\boldsymbol{\alpha}_{\mathrm{init}}$, we only update the permeability in directions that affect the controllable and observable part of the reservoir model and thereby V. Note that L should be smaller or equal to $N_{\max}$ as given by (7.4) if **Problem 6** is to have a unique solution.

However, $\hat{\mathbf{T}}_{\mathrm{bal},1}$ varies with $\boldsymbol{\theta}$ - see for example the lower plots in Figure 6.3 which closely resemble but are not identical to those in Figure 6.6. Therefore our approach might lead to a local minimum for **Problem 6** that is not equal to zero (*i.e.* not a perfect history match). An alternative method is therefore depicted in Figure 7.4. Here, $\hat{\mathbf{T}}_{\mathrm{bal},1}$ is re-evaluated if there is no more decrease in V and a local minimum for **Problem 6** is found. This re-evaluation leads to a new set of basis functions, which might possibly succeed in further decreasing V. This controllability and observability-based regularization is applied in the following example.

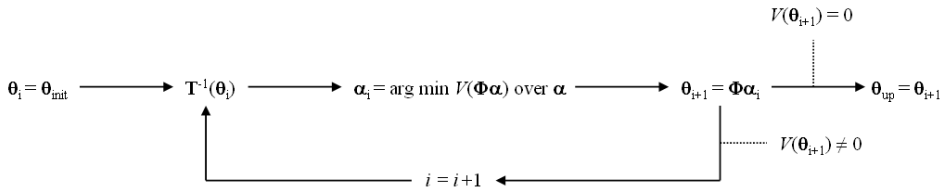

Figure 7.4: Iterative procedure for controllability and observability-based reparameterization of grid block permeabilities.

7.5 Application

Consider again the heterogeneous reservoir treated in Chapter 6, and the problem of identifying the logarithm[1] of its permeability distribution as depicted in Figure 6.4. This permeability, whose logarithm is denoted by $\bar{\boldsymbol{\theta}}$, is assumed to be the only source of uncertainty. There are 200 perfect pressure measurements $\bar{\mathbf{y}}_1, \ldots, \bar{\mathbf{y}}_{200}$ (from wells 1, 2, 3 and 5) available every $\Delta t = 0.013$ seconds, which have been generated by (7.1)-(7.3) using $\boldsymbol{\theta} = \bar{\boldsymbol{\theta}}$, an initial state of $\mathbf{p}_0 = 100$ bar, and a manipulated input $\mathbf{u}_0, \ldots, \mathbf{u}_{199}$ depicted in Figure 7.5. This input contains enough frequencies to obtain informative measurements (*i.e.* it is persistently exciting).

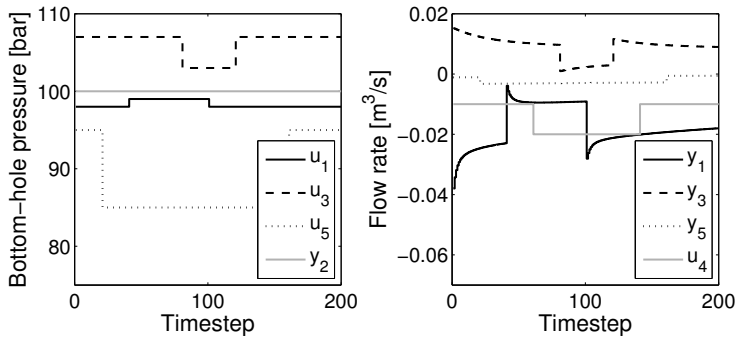

Figure 7.5: Bottom-hole pressures (left) and flow rates (right).

The initial estimate $\boldsymbol{\theta}_{\text{init}}$ of $\bar{\boldsymbol{\theta}}$ is a homogeneous permeability of 5 mDarcy. Based on this estimate, the Hankel singular values and the balancing matrix $\mathbf{T}_{\text{bal}}(\boldsymbol{\theta}_{\text{init}})$ are computed as in Chapter 6 using $\Delta t = 0.013$ seconds. We stress that this balancing matrix corresponds to the initially estimated model, and not the true one. The squared difference of the measured outputs of this model with the true measured outputs as defined in (7.10) is $V(\boldsymbol{\theta}_{\text{init}}) = 8.7 \times 10^{-2}$. The goal is to update this estimate by solving **Problem 6** using a gradient-based optimization procedure (*e.g.*

[1]The logarithm of permeability is used in order to avoid negative permeability estimates and to improve the numerical conditioning of the problem.

the MATLAB function `lsqnonlin`).

The re-parameterization matrix $\mathbf{\Phi}$ is chosen as

$$\mathbf{\Phi} = \left[\begin{array}{cccc} I_{N\times 1} & \hat{\mathbf{t}}_1 & \dots & \hat{\mathbf{t}}_L \end{array} \right], \tag{7.10}$$

$$\boldsymbol{\alpha}_{\text{init}} = \left[\begin{array}{cccc} -13.3 & 0 & \dots & 0 \end{array} \right]. \tag{7.11}$$

where $\hat{\mathbf{t}}_j$ denotes the j^{th} column of $\mathbf{T}_{\text{bal}}^{-1}$. The number of columns L of the re-parameterization matrix $\mathbf{\Phi}$ should be smaller or equal to the maximum number of identifiable parameters, which in this case is $N_{\max} = 120$. However, very good history matches are achieved with far fewer basis functions. This is shown in Figure 7.6, which depicts the minimum value of **Problem 6** that is achieved with $L = 1, \dots, 10$. Note that V decreases by 5 orders of magnitude using only 6 basis functions. The corresponding updated permeability estimate, depicted in Figure 7.7, only shows a resemblance with the true permeability, depicted in Figure 6.4, in the vicinity of the wells in which we can control and observe.

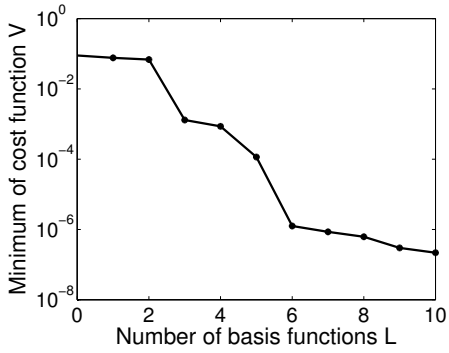

Figure 7.6: Minimum value of history match cost function V for different number of basis functions L.

It is interesting to note that we can construct permeability estimates that appear different, but lead to virtually the same input-output behavior and thereby history match cost function V using the columns of $\hat{\mathbf{T}}_{\text{bal},2}$. Three such estimates are depicted in Figure 7.8: these are constructed by adding linear combinations of columns of $\hat{\mathbf{T}}_{\text{bal},1}$ to the estimate depicted in Figure 7.8. The value of the history match cost function V, originally 1.3×10^{-6}, hardly changes.

Finally, it should be noted that this particular application involves history matching 200 measurements taken every $\Delta t = 0.013$ seconds, which is clearly not very realistic - see the signals depicted in Figure 7.5. This is due to the reservoir's relatively small size and high permeability, as well as the low compressibility of the fluid. However, for larger reservoirs with lower permeability and higher compressibility the sampling time Δt can be much larger.

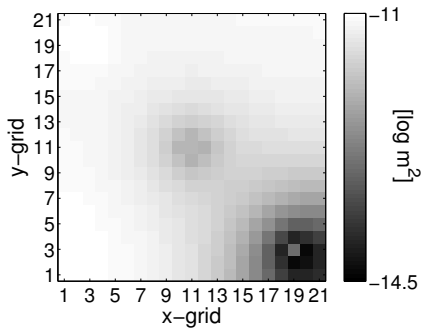

Figure 7.7: Updated estimate of heterogeneous permeability using 4 basis functions.

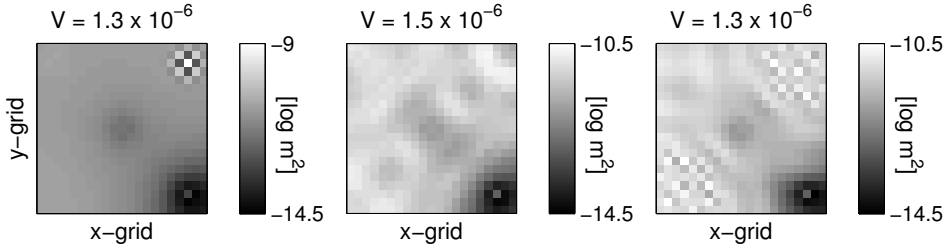

Figure 7.8: Alternative estimates of heterogeneous permeability constructed by adding right columns of $\mathbf{T}_{\mathrm{bal}}^{-1}$ to the estimate depicted in Figure 7.7, and corresponding values of history match cost function V.

7.6 Chapter conclusions

Reservoir models are generally of very high order because the number of grid blocks is often set as high as computationally possible. However, the Hankel singular values of single-phase flow reservoir models decrease very rapidly, indicating that they behave as models of much lower order. This severely limits the number of identifiable parameters. An upper bound $N_{\max}$ for the maximum number of identifiable parameters is given. It is shown that if the vector of to-be-estimated parameters contains the N grid block permeabilities, then $N_{\max} \ll N$ and the model structure is not identifiable. Furthermore, by inspecting how the controllable and observable part of a reservoir model depends on permeability, it is shown that the relevant spatial patterns of permeability strongly resemble the relevant spatial patterns of pressure. Consequently, a new method of regularization is to re-parameterize permeability through a linear combination of the most relevant spatial patterns of pressure. A history matching example shows that this controllability and observability-based regularization leads to good results. Nonetheless, this method needs to be tested on more realistic problems (*e.g.* 3D, multi-phase flow reservoir models with noisy measurements) before it can be

applied in practice. Even more importantly, it must still be demonstrated that the resulting permeability estimate leads to better predictions of saturations, and not only pressures.

8 CHAPTER

Conclusions and Recommendations

This thesis aims at developing efficient tools for dynamic optimization of wells and their production settings to maximize the recovery factor of petroleum reservoirs based on uncertain reservoir models. This chapter presents the conclusions and recommendations for future research.

8.1 Conclusions

In Chapter 1 it was argued that, despite the many applications of optimization and estimation techniques in the petroleum engineering literature, there are still many open problems in reservoir management and production operations processes. Consequently, there is significant scope to increase the recovery factor of oil and gas fields by tailoring tools from the systems and control community to *efficiently* perform dynamic optimization of wells and their production settings based on uncertain reservoir models, in the sense that they lead to good decisions while requiring limited time from the user. Four solution directions were outlined to actually develop these tools, and in the following section the conclusions are categorized along these four directions.

Optimal control of production settings

Many production setting optimization problems can be written as optimal control problems that are linear in the control. If the only constraints are upper and lower bounds on the control, these problems can be expected to have pure bang-bang optimal solutions. In situations where the optimal solutions are not purely bang-bang but also smooth (*i.e.* containing so-called singular arcs), it is shown for the example considered that pure bang-bang solutions exist which are only slightly suboptimal. This has obvious practical implications, since bang-bang solutions can be implemented with simple on-off control valves.

Robust control of production settings

The adjoint method to derive gradients of a cost function with respect to production settings can be combined with robust optimization to efficiently compute settings that are robust against uncertainty in reservoir models. A water flooding application demonstrates that production settings can be found that are robust against uncertainty as defined by an entire class of models within a geological structure, by optimizing over one set of 100 realizations of the permeability distribution, and validating over a second set of 100 realizations.

Optimal well placement

The type of production settings (*e.g.* reactive versus constant) significantly effect the well placement problem, in that a well configuration that is optimal when the wells are operated with one type of settings may be far from optimal when the wells are operated with another type of settings. Furthermore, the gradients used in production setting optimization can be used to efficiently compute directions in which to iteratively improve upon an initial well configuration by surrounding the to-be-placed wells by pseudo wells (*i.e.* wells that operate at a negligible rate).

Controllability, observability and identifiability of reservoir models

The most controllable and observable pressures in single-phase flow reservoir models can be computed by performing an eigenvalue decomposition of the controllability and observability Gramians. By projecting the eigenvectors corresponding to the largest absolute eigenvalues of the Gramians onto the model grid, we can interpret how the reservoir model's controllability and observability properties vary over space. It turns out that pressures near wells in which we can control the flow rate or bottom-hole pressure are controllable, whereas pressures near wells in which we can measure the flow rate or bottom-hole pressure are observable. Furthermore, the controllability and observability properties are determined by the well configuration (*i.e.* the number and location of wells) and to a lesser extent by the heterogeneity of the reservoir at hand. The Hankel singular values of single-phase flow reservoir models decrease rapidly, indicating that they behave as models of much lower order. This severely limits the number of identifiable parameters. From the systems and control literature an upper bound $N_{\max}$ for the maximum number of identifiable parameters is given. It is shown that if the vector of to-be-estimated parameters contains the N grid block permeabilities, then $N_{\max} \ll N$ and the model structure is not identifiable. Furthermore, by inspecting how the controllable and observable part of a reservoir model depends on permeability, it is shown that the relevant spatial patterns of permeability strongly resemble the relevant spatial patterns of pressure. Consequently, a new method of regularization is to re-parameterize permeability through a linear combination of the most relevant spatial patterns of pressure. A history matching example shows that this controllability and observability-based regularization leads to good results.

Discussion

Each of these results make closed-loop reservoir management and production operations more efficient.

- By examining the type of constraints on wells it is possible to determine in advance whether or not simple on-off control valves are likely to be as effective as variable-setting ones. Although this inspection will not give a conclusive answer, it points to situations when it can be beneficial, in terms of control valve costs, to put extra effort into searching for pure bang-bang (sub)optimal production settings.
- The negative effect of geological uncertainty on the recovery factor can be reduced by applying robust optimization over a large number of subsurface realizations.
- Given a reservoir model, optimal well locations can be determined much more efficiently by applying the automatic well placement algorithm presented in this thesis than by manual well placement. The time that this saves during field development planning can be used to focus on other aspects of a development plan.
- The upper bound on the number of identifiable parameters as well as the controllability and observability-based method of regularization can potentially be used to improve history matching reservoir permeability.

8.2 Recommendations

Although these results solve some of the current problems in closed-loop reservoir management, the research in this area is far from finished. The following recommendations for future research are given.

- There is still a large gap between reservoir management and production operations in terms of goals and models used to achieve them. The resulting inconsistencies in decision-making need to be addressed. A first step in this direction could be to investigate how the terminal time, oil price and discount factor affect the scope for improvement and the shape of optimal production settings. In the applications in this thesis, the improvement in NPV is solely due to reduced water production. However, the frequently associated delayed oil production has no effect on NPV because the discount factor in these applications is zero. For significant discount factors (*e.g.* around 15%) this clearly no longer holds, and in many applications it may then be difficult to improve upon the reactive control strategy commonly employed in production operations.
- The number, scheduling and trajectory of wells are very important decision factors when developing a reservoir, but have not been considered in this

thesis. Scheduling might be easier when only considering pure bang-bang production settings with a single switching time for each well, since the decision factors are then simply when to drill and abandon wells. As with well location optimization, well trajectory optimization might be tackled using the concept of pseudo-wells. However, each grid block in which a to-be-optimized well is perforated should then be viewed as a separate well, and subsequently surrounded by pseudo-wells. The challenge is then to improve upon an initial well trajectory while adhering to practical drilling constraints (*e.g.* curvature and length).

- The concept of surrounding a well with pseudo-wells to efficiently compute an improving direction in well location optimization is by no means restricted to a single 'ring'. Using two or more rings of pseudo wells for each well leads to more gradient information, and thereby possibly a better optimization procedure.

- Conceptually, it is straightforward to apply the robust optimization approach considered in this thesis to well location optimization. It would be interesting to investigate under what conditions a well configuration that is robust against model uncertainty (*e.g.* geological uncertainty represented by a large set of realizations as in Chapter 4) resembles the commonly applied pattern-flood.

- While there are many sources of uncertainty in reservoir models, this thesis only considers the permeability distribution to be uncertain. It is clearly important to also investigate the effects of other sources of uncertainty and to extend the system boundary (*e.g.* by considering multi-phase flow in wells and the interaction with surface facilities). Also, it is still unclear how to generate a minimal set of models that is representative of the entire uncertainty range, which is important to reduce the computational burden of applying robust optimization.

- Since a reservoir's recovery factor can be defined in terms of the saturations at the end of its lifecycle, a reservoir's saturations dynamics are at least as relevant for field development planning as its pressure dynamics. However, a reservoir's saturation dynamics are described by nonlinear equations, and it is therefore important to investigate how the controllability and observability of saturations change with time. This could be done by linearizing the nonlinear dynamics along a certain trajectory and might lead to explanations as to why, as observed in optimization studies, the control action of optimal production settings at early times is often at the injection wells, and at later times at the production wells.

- It is unclear which estimation technique is the most reliable for history matching reservoir models. While there have been many successful applications, a rigorous comparison of the (dis)advantages of these techniques would be very beneficial to making automatic history matching standard practice in reservoir management.

- Reducing the computational load of a reservoir simulation would be very beneficial to making near-continuous closed-loop reservoir management feasible in practice. Further research into model reduction and numerical solvers is therefore highly recommended.

Bibliography

Abacioglu, Y., D. Oliver and A. Reynolds (2001). Efficient reservoir history matching using subspace vectors. *Computational Geosciences* **5**, 151–172.

Agrachev, A.A., G. Stefani and P.L. Zezza (2002). Strong optimality for a bang-bang trajectory. *SIAM Journal on Control and Optimization* **41**(4), 991–1014.

Aitokhuehi, I., L. J. Durlofsky, V. Artus, B. Yeten and K. Aziz (2004). Optimization of advanced well type and performance. In *9th European Conference on the Mathematics of Oil Recovery*, Cannes.

Anderson, B. D. O. and J. B. Moore (1979). *Optimal Filtering*. Prentice Hall.

Antoulas, A. C. (2005). *Approximation of Large-Scale Dynamical Systems*. SIAM.

Asheim, H. (1987). Optimal control of water drive. *SPE Journal (SPE 15978)*.

Asheim, H. (1988). Maximization of water sweep efficiency by controlling production and injection rates. In *SPE European Petroleum Conference (SPE 18365)*, London.

Astrom, K. J. and B. Wittenmark (1990). *Computer Controlled Systems (2nd Edition)*. Prentice Hall.

Athans, M. (1971). The role and use of the stochastic linear-quadratic-gaussian problem in stochastic control. *IEEE Transactions on Automatic Control* **16**(6), 529–552.

Athans, M. and P. L. Falb (1966). *Optimal Control - An Introdution to the Theory and Its Applications*. McGraw-Hill.

Aziz, K. and A. Settari (1979). *Petroleum Reservoir Simulation*. Applied Science Publishers.

Bangerth, B. L., W. H. Klie, M. F. Wheeler, P. L. Stoffa and M. K. Sen (2006). On optimization algorithms for the reservoir oil well placement problem. *Computational Geosciences* **10**, 303–319.

Beckner, B. L. and X. Song (1995). Field development planning using simulated annealing - optimal economic well scheduling and placement. In *SPE Annual Technical Conference and Exhibition (SPE 30650)*, Dallas.

Belghith, S. F., F. Lamnabhi-Lagarrigue and M. M. Rosset (1986). Bang-bang solutions for a class of problems arising in thermal control. In *Algebraic and Geometric Methods in Nonlinear Control Theory*, pp. 623–632. D. Reichel.

Bellman, R. (1956). On the "bang-bang" control problem. *Quarterly of Applied Mathematics* **14**, 11–18.

Bellman, R. and K.J. Astrom (1970). On structural identifiability. *Mathematical Biosciences* **7**, 329–339.

Bennett, A. F. (2002). *Inverse modeling of the ocean and atmosphere*. Cambridge University Press.

Berre, I., M. Lien and T. Mannseth (2007). A level-set corrector to an adaptive multiscale permeability prediction. *Computational Geosciences* (11), 27–42.

Bissell, R. C. (1994). Calculating optimal parameters for history matching. In *4th European Conference on the Mathematics of Oil Recovery*, Roros.

Bissell, R. C., Y. Sharma and J. E. Killough (1994). History matching using the method of gradients: Two case studies. In *SPE Annual Conference and Exhibition (SPE 28590-MS)*, New Orleans.

Bittencourt, A. C. and R. N. Horne (1997). Reservoir development and design optimization. In *SPE Annual Technical Conference and Exhibtion (SPE 38895)*, San Antonio.

Blakemore, N. and R. Aris (1962). Studies in optimization - v. the bang-bang control of a batch reactor. *Chemical Engineering Science* **17**, 591–598.

Bos, R. (2006). *Monitoring of Industrial Processes using Large Scale First Principles Models*. Ph. D. thesis, Delft University of Technology.

Bressan, A. (1985). A high-order test for the optimality of bang-bang controls. *SIAM Journal on Control and Optimization* **23**, 38–48.

Brouwer, D. R. (2004). *Dynamic Water Flood Optimization With Smart Wells Using Optimal Control Theory*. Ph. D. thesis, Delft University of Technology.

Brouwer, D. R. and J. D. Jansen (2004). Dynamic optimization of waterflooding with smart wells using optimal control theory. *SPE Journal (SPE 78278)* **9**(4), 391–402.

Brouwer, D. R., G. Naevdal, J. D. Jansen, E. H. Vefring and C. P. J. W. van Kruijsdijk (2004). Improved reservoir management through optimal control and continuous model updating. In *SPE Annual Technical Conference and Exhibition (SPE 90149)*, Houston.

Brun, B., O. Gosselin and J. W. Barker (2004). Use of prior information in gradient-based history matching. *SPE Journal (SPE 87680-PA)* **9**(1), 67–78.

Bryson, A. E. and Y. C. Ho (1975). *Applied optimal control: optimization, estimation and control*. Hemisphere-Wiley.

Carter, R. D., L. F. Kemp, A. C. Pierce and D. L. Williams (1974). Performance matching with constraints. *SPE Journal (SPE 4260)* (April), 187–196.

Centilmen, A., T. Ertekin and A. S. Grader (1999). Applications of neural networks in multiwell field development. In *SPE Annual Technical Conference and Exhibition (SPE 56433)*, Houston.

Chavent, G. (1975). History matching by use of optimal theory. *SPE Journal (SPE 4627)* (February), 74–86.

Chen, C. T. (1984). *Linear System Theory and Design (2nd Edition)*. Holt, Rinehart and Winston.

Chierici, G. L. (1992). Economically improving oil recovery by advanced reservoir management. *Journal of Petroleum Science and Engineering* **8**, 205–219.

Coats, B. K., G. C. Fleming, J. W. Watts, M. Rame and G. S. Shiralkar (2003). A generalized wellbore and surface facility model, fully coupled to a reservoir simulator. In *SPE Reservoir SImulation Symposium (SPE 79703)*, Houston.

de Marsily, G., F. Delay, J. Goncalves and P. Renard (2005). Dealing with spatial heterogeneity. *Hydrogeology Journal* **13**, 161–183.

de Montleau, P., A. Cominelli, K. Neylon, D. Rowan, I. Pallister, O. Tesaker and I. Nygard (2006). Production optimization under constraints using adjoint gradients. In *10th European Conference on the Mathematics of Oil Recovery*, Amsterdam.

Deffeyes, K. S (2001). *Hubbert's Peak: The Impending World Oil Shortage*. Princeton University Press.

Denham, M. J. (1974). Canonical forms for the identification of multiviarable linear systems. *IEEE Transactions on Automatic Control* **19**(6), 646–656.

EIA (2006). International energy outlook 2006. Technical report, Energy Information Administration.

Evensen, G. (2007). *Data Assimilation*. Springer.

Ewing, R. E. (1983). *The Mathematics of Reservoir Simulation*. SIAM.

Fel'dbaum, A. A. (1965). *Optimal Control Systems*. Academic Press.

Fyrozjaee, M. H. and Y. C. Yortsos (2006). Control of a displacement front in potential flow using flow rate partition. In *SPE Intelligent Energy Conference and Exhibition (SPE 99524)*, Amsterdam.

Gao, G. and A. C. Reynolds (2006). An improved implementation of the lbfgs algorithm for automatic history matching. *SPE Journal (SPE 90058-PA)* **11**(1), 5–17.

Garcia, C. E., D. M. Prett and M. Morari (1989). Model predictive control: Theory and practice - a survey. *Automatica* **23**(3), 335–348.

Gavalas, G. R., P. C. Shah and J. H. Seinfeld (1976). Reservoir history matching by bayesian estimation. *SPE Journal (SPE 5740-PA)* **16**(6), 337–350.

Gildin, E., H. Klie, A. Rodriguez and M. F. Wheeler (2006). Development of low-order controllers for high-order reservoir models and smart wells. In *SPE Annual Techical Conference and Exhibition (SPE 102214-MS)*, San Antonio.

Glashoff, K. and E. Sachs (1977). On theoretical aspects of the bang-bang principle. *Numerische Mathematik* **29**, 93–113.

Glover, K. (1984). All optimal hankel-norm approximations of linear multivariable systems and their $\mathcal{L}^\infty$-error bounds. *International Journal of Control* **39**(6), 1115–1193.

Glover, K. and J. C. Willems (1974). Parameterizations of linear dynamical systems: Canonical forms and identifiability. *IEEE Transactions on Automatic Control* **19**(6), 640–646.

Grimstad, A., T. Mannseth and G. Naevdal (2003). Adaptive multiscale permeability estimation. *Computational Geosciences* **7**(1), 1–25.

Guyaguler, B. and R. N. Horne (2004). Uncertainty assessment of well-placement optimization. *SPE Journal (SPE 87663)* **7**(1), 24–32.

Handels, M., M. J. Zandvliet, D. R. Brouwer and J. D. Jansen (2007). Adjoint based well placement optimization under production constraints. In *SPE Reservoir Simulation Symposium (SPE 105797)*, Houston.

Heijn, T., R. Markovinovic and J. D. Jansen (2004). Generation of low-order reservoir models using system-theoretical concepts. *SPE Journal (SPE 88361)* **9**(2), 202–218.

Heinberg, R. (2003). *The Party's Over - Oil, War and the Fate of Industrial Societies*. New Society Publishers.

Hinrichsen, D. and A. J. Pritchard (1990). An improved error estimat for reduced-order models of discrete-time systems. *IEEE Transactions on Automatic Control* **35**(3), 317–320.

Hoyland, L. A., P. Papatzacos and S. M. Skjaeveland (1989). Critical rate for water coning: Correlation and analytical solution. *SPE Journal (SPE 15855-PA)* **4**(4), 495–502.

Hubbert, M. K. (1956). Darcy's law and the field equations of the flow of underground fluids. *Petroleum Transactions AIME (749-G)* **207**, 222–239.

Isidori, A. (1983). *Nonlinear Control Systems - An Introduction*. Springer-Verlag.

Jacquard, P. and C. Jain (1965). Permeability distribution from field pressure data. *SPE Journal (SPE 1307)* (December), 281–294.

Jafarpour, B. and D. B. McLaughlin (2007a). Efficient permeability parameterization with the discrete cosine transform. In *SPE Reservoir Simulation Symposium (SPE 106453)*, Houston.

Jafarpour, B. and D. B. McLaughlin (2007b). History matching with an ensemble kalman filter and discrete cosine parameterization. In *SPE Reservoir Simulation Symposium (SPE 108761)*, Houston.

Jahns, H. O. (1966). A rapid method for obtaining a two-dimensional reservoir description from well pressure response data. *SPE Journal (SPE 1473-PA)* **6**(4), 315–327.

Jansen, J. D. (2007). Model-based control of subsurface flow. In *8th International Symposium on Dynamics and Control of Process Systems (DYCOPS)*, Cancun.

Jansen, J. D., D. R. Brouwer, G. Naevdal and C. P. J. W. van Kruijsdijk (2005). Closed-loop reservoir management. *First Break* **23**, 43–48.

Kallrath, J. (2000). Mixed integer problems in the chemical process industry: Experience, potential and future perspectives. *Trans IChemE* **78**(Part A), 809–822.

Kalman, R. E. (1960). A new approach to linear filtering and prediction problems. *Transactions of the ASME - Journal of Basic Engineering* **82**(Series D), 35–45.

Kalman, R. E. (1963). Mathematical description of linear dynamical systems. *SIAM Journal of Control* **1**(2), 152–192.

Kapteijn, P. K. A. and S. Muessig (2003). Smart fields: How to generate more value from hydrocarbon resources. *Oil Gas European Magazine* **3**, OG1–OG6.

Kawski, M. (2003). High-order maximum principles. In *New Trends in Nonlinear Dynamics and Control*, pp. 313–326. Springer-Verlag.

Kirk, D. E. (1970). *Optimal Control Theory - An Introduction*. Prentice-Hall.

Kosmala, A., S. I. Aanonsen, A. Gajraj, V. Biran, Brusdal. K., A. Stokkenes and R. Torrens (2003). Coupling of a surface network with reservoir simulation. In *SPE Annual Technical Conference and Exhibition (SPE 84220)*, Denver.

Kosmidis, V. D., J. D. Perkins and E. N. Pistikopoulos (2005). A mixed integer optimization formulation for the well scheduling problem on petroleum fields. *Computers & Chemical Engineering* **29**(7), 1523–1541.

Kraaijevanger, J. F. B. M., P. J. P. Egberts, J. R. Valstar and H. W. Buurman (2007). Optimal waterflood design using the adjoint method. In *SPE Resevoir Simulation Symposium (SPE 105764)*, Houston.

Krener, A. J. (1973). The high order maximum principle. In *Geometric Methods in System Theory*, pp. 174–184. D. Reidel.

Ledzewicz, U. and H. Schattler (2002). Optimal bang-bang controls for a two-compartment model in cancer chemotherapy. *Journal of Optimization Theory and Applications* **114**(3), 609–637.

Li, R., A. C. Reynolds and D. S. Oliver (2003). History matching of three-phase flow production data. *SPE Journal (SPE 87336)* **8**(4), 328–340.

Ljung, L. (1999). *System Identification - Theory for the User (2nd Edition)*. Prentice-Hall.

Lucas, S. K. and C. Y. Kaya (2001). Switching-time computation for bang-bang control laws. In *IEEE American Control Conference*, Arlington, pp. 176–181.

Luenberger, D. G. (1967). Canonical forms for linear multiviarable systems. *IEEE Transactions on Automatic Control* **June**, 290–293.

Luenberger, D. G. (1973). *Linear and Nonlinear Programming*. Addison-Wesley.

Luenberger, D. G. (1981). *Introduction to dynamic systems: Theory, models and applications*. John Wiley & Sons.

Maciejowski, J. M. (2002). *Predictive Control with Constraints*. Prentice Hall.

Markovinovic, R., E. L. Geurtsen, T. Heijn and J. D. Jansen (2002). Generation of low-order reservoir models using pod, empirical gramians and subspace identification. In *8th European Conference on the Mathematics of Oil Recovery*, Freiberg.

Maurer, H., C. Buskens, J.H.R. Kim and C.Y. Kaya (2005). Optimization methods for the verification of second order sufficient conditions for bang-bang controls. *Optimal Control Applications and Methods* **26**, 129–156.

Mayne, D. Q., J. B. Rawlings, C. V. Rao and P. O. M. Scokaert (2000). Constrained model predictive control: stability and optimality. *Automatica* **36**, 789–814.

Meier, L. and A. E. Bryson (1990). Efficient algorithm for time-optimal control of a two-link manipulator. *Journal of Guidance, Control and Dynamics* **13**(5), 859–866.

Mohler, R.R. (1973). *Bilinear Control Processes*. Academic Press.

Montes, G., P. Bartolme and A. L. Udias (2001). The use of genetic algorithms in well placement optimization. In *SPE Latin American and Caribbean Petroleum Engineering Conference (SPE 69439)*, Buenos Aires.

Moore, B. C. (1981). Principal component analysis in linear systems: Controllability, observability, and model reduction. *IEEE Transactions on Automatic Control* **26**(1), 17–32.

Muskat, M. (1937). *Flow of Homogeneous Fluids Through Porous Media*. McGraw-Hill.

Naevdal, G., D. R. Brouwer and J. D. Jansen (2006). Waterflooding using closed-loop control. *Computational Geosciences* **10**(1), 37–60.

Naevdal, G., L. M. Johnsen, S. I. Aanonsen and E. H. Vefring (2005). Reservoir monitoring and continuous model updating using ensemble kalman filter. *SPE Journal (SPE 84372)* **10**(1), 66–74.

Narayanan, K., A. S. Cullick and M. Bennett (2003). Better field development decisions for multi-scenario, interdependent reservoir, well, and facility simulations. In *SPE Reservoir SImulation Symposium (SPE 79703)*, Houston.

Nikolaou, M., A. S. Cullick and L. Saputelli (2006). Production optimization - a moving-horizon approach. In *SPE Intelligent Energy Conference and Exhibition (SPE 99358)*, Amsterdam.

Nyhavn, F., F. Vassenden and P. Singstad (2000). Reservoir drainage with down hole permanent monitoring and control systems. In *SPE Annual Technical Conference and Exhibition (SPE 62937)*, Dallas.

Ozdogan, U. and R. N. Horne (2006). Optimization of well-placement optimization under time-dependent uncertainty. *SPE Journal (SPE 90091)* **9**(2), 135–145.

Parry, P., V. Davidson, A. Clark and Z. Guilford (2006). Labour and skills crisis could stall oil and gas boom. Technical report, BoozAllenHamilton.

Peaceman, D. W. (1977). *Fundamentals of Numerical Reservoir Simulation*. Elsevier Scientific.

Peaceman, D. W. (1978). Interpretation of well-block pressures in numerical reservoir simulation. *SPE Journal (SPE 6893-PA)* (June), 183–194.

Pontryagin, L. S., V. G. Boltyanskii, R. V. Gamkrelidze and E. F. Mishchenko (1962). *The Mathematical Theory of Optimal Processes*. John Wiley & Sons.

Ramirez, W. F. (1987). *Applications of Optimal Control Theory to Enhanced Oil Recovery*. Elsevier Science Publishers.

Reynolds, A., M. Zafari and G. Li (2006). Iterative forms of the ensemble kalman filter. In *10th European Conference on the Mathematics of Oil Recovery*, Amsterdam.

Reynolds, A. C., N. He, L. Chu and D. S. Oliver (1996). Reparameterization techniques for generating reservoir descriptions conditioned to variograms and well-test pressure data. *SPE Journal (SPE 30588-PA)* **1**(4), 413–426.

Rommelse, J. R., O. Kleptova, J. D. Jansen and A. W. Heemink (2006). Data assimilation in reservoir management using the representer method and the ensemble kalman filter. In *10th European Conference on the Mathematics of Oil Recovery*, Amsterdam.

Ruppen, D., C. Benthack and D. Bonvin (1995). Optimization of batch reactor operation under parametric uncertainty – computational aspects. *Journal of Process Control* **5**(4), 235–240.

Samsatli, Nouri J., Lazaros G. Papageorgiou and Nilay Shah (1998). Robustness metrics for dynamic optimization models under parameter uncertainty. *AIChE Journal* **44**(9), 1993–2006.

Saputelli, L., M. Nikolaou and M. J. Economides (2006). Real-time reservoir management: A multiscale adaptive optimization and control approach. *Computational Geosciences* **10**(1), 61–96.

Sarma, P., K. Aziz and L. J. Durlofsky (2005). Implementation of adjoint solution for optimal control of smart wells. In *SPE Reservoir Simulation Symposium (SPE 92864)*, Houston.

Sarma, P., W. H. Chen, L. J. Durlofsky and K. Aziz (2006a). Production optimization with adjoint models under nonlinear control-state path inequality constraints. In *SPE Intelligent Energy Conference and Exhibition (SPE 99959)*, Amsterdam.

Sarma, P., L. J. Durlofsky, K. Aziz and W. H. Chen (2006b). Efficient real-time reservoir management using adjoint-based optimal control and model updating. *Computational Geosciences* **10**(1), 3–36.

Sarma, P., L. J. Durlofsky, K. Aziz and W. H. Chen (2007). A new approach to automatic history matching using kernel pca. In *SPE Reservoir Simulation Symposium (SPE 106176)*, Houston.

Shah, P. C., G. R. Gavalas and J. H. Seinfeld (1978). Error analysis in history matching: The optimum level of parameterization. *SPE Journal (SPE 6508-PA)* **18**(3), 219–228.

Simmons, M. R. (2005). *Twilight in the Desert*. John Wiley and Sons.

Spall, J.C. (1992). Multivariate stochastic approximation using a simultaneous perturbation gradient approximation. *IEEE Transactions on Automatic Control* **37**(3), 332–341.

Srinivasan, B., D. Bonvin, E. Visser and S. Palanki (2002a). Dynamic optimization of batch processes: Ii. role of measurements in handling uncertainty. *Computers & Chemical Engineering* **27**(1), 27–44.

Srinivasan, B., S. Palanki and D. Bonvin (2002b). Dynamic optimization of batch processes: I. characterization of the nominal solution. *Computers & Chemical Engineering* **27**(1), 1–26.

Stengel, R. F. (1986). *Stochastic Optimal Control: Theory and Application*. John Wiley & Sons.

Sudaryanto, B. and Y. C. Yortsos (2000). Optimization of fluid front dynamics in porous media using rate control 1. equal mobility fluids. *Physics of Fluids* **12**(7), 1656–1670.

Sudaryanto, B. and Y. C. Yortsos (2001). Optimization of displacements in porous media using rate control. In *SPE Annual Technical Conference and Exhibition (SPE 71509)*.

Sussmann, H.J. (1979). A bang-bang theorem with bounds on the number of switchings. *SIAM Journal on Control and Optimization* **17**(5), 629–651.

Tarantola, A. (2005). *Inverse Problem Theory and Methods for Model Parameter Estimation*. SIAM.

Tavassoli, Z., J. N. Carter and P. R. King (2004). Errors in history matching. *SPE Journal (SPE 86883)* **9**(3), 352–361.

Terwiesch, Peter, Mukul Agarwal and D. W. T. Rippin (1994). Batch unit optimization with imperfect modelling: a survey. *Journal of Process Control* **4**(4), 238–258.

Terwiesch, P., D. Ravemark, B. Schenker and D. W. T. Rippin (1998). Semi-batch process optimization under uncertainty: Theory and experiments. *Computers & Chemical Engineering* **22**(1-2), 201–213.

van den Berg, J. (2005). *Model Reduction for Dynamic Real-Time Optimization of Chemical Processes*. Ph. D. thesis, Delft University of Technology.

Van Doren, J. F. M., R. Markovinovic and J. D. Jansen (2006). Reduced-order optimal control of water flooding using proper orthogonal decomposition. *Computational Geosciences* **10**(1), 137–158.

Van Doren, J. F. M., P. M. J. Van den Hof, J. D. Jansen and O. H. Bosgra (2008). Determining identifiable parameterizations for large-scale physical models in reservoir engineering. In *Proceedings of the 17th IFAC World Congress*, Seoul.

van Essen, G. M., M. J. Zandvliet, P. M. J. Van den Hof, O. H. Bosgra and J. D. Jansen (2006a). Robust optimization of oil reservoir flooding. In *Proceedings of the 2006 IEEE International Conference on Control Applications*, Munich.

van Essen, G. M., M. J. Zandvliet, P. M. J. Van den Hof, O. H. Bosgra and J. D. Jansen (2006b). Robust waterflooding optimization of multiple geological scenarios. In *SPE Annual Technical Conference and Exhibition (SPE 102913)*, San Antonio.

van Essen, G. M., M. J. Zandvliet, P. M. J. Van den Hof, O. H. Bosgra and J. D. Jansen (2007). Robust waterflooding optimization of multiple geological scenarios. *submitted to SPE Journal*.

van Hessem, D. (2004). *Stochastic inequality constrained closed-loop model predictive control*. Ph. D. thesis, Delft University of Technology.

Virnovsky, G. A. (1991). Water flooding strategy design using optimal control theory. In *European IOR Symposium*, Stavanger.

Voss, S. and T. Patel (2007). *Total, Shell Chief Executives Say "Easy Oil" Is Gone*. www.bloomberg.com.

Yeten, B. (2003). *Optimum Deployment of Nonconventional Wells*. Ph. D. thesis, Stanford.

Yeten, B., D. R. Brouwer, L. J. Durlofsky and K. Aziz (2004). Decision analysis under uncertainty for smart well deployment. *Journal of Petroleum Science and Engineering* **44**, 175–191.

Zakirov, I. S., S. I. Aanonsen, E. S. Zakirov and B. M. Palatnik (1996). Optimization of reservoir performance by automatic allocation of well rates. In *5th European Conference on the Mathematics of Oil Recovery*, Leoben.

Zandvliet, M. J., O. H. Bosgra, J. D. Jansen, P. M. J. Van den Hof and J. F. B. M. Kraaijevanger (2007). Bang-bang control and singular arcs in reservoir flooding. *Journal of Petroleum Science and Engineering* **58**, 186–200.

Zandvliet, M. J., O. H. Bosgra, P. M. J. Van den Hof, J. D. Jansen and J. F. B. M. Kraaijevanger (2006). Bang-bang control in reservoir flooding. In *10th European Conference on the Mathematics of Oil Recovery*, Amsterdam.

Zandvliet, M. J., M. Handels, D. R. Brouwer, J. D. Jansen and G. M. van Essen (2008a). Adjoint based well placement optimization under production constraints. *accepted for publication in SPE Journal*.

Zandvliet, M. J., J. F. M. Van Doren, O. H. Bosgra, J. D. Jansen and P. M. J. Van den Hof (2008b). Controllability, observability and identifiability in reservoir engineering. *submitted to Computational Geosciences*.

Zhang, F. and A. C. Reynolds (2002). Optimization algorithms for automatic history matching of production data. In *8th European Conference on the Mathematics of Oil Recovery*, Freiberg.

Zhang, F., J. A. Skjervheim, A. C. Reynolds and D. S. Oliver (2005). Automatic history matching in a bayesian framework, example applications. *SPE Journal (SPE 84461)* **8**(3), 214–223.

Zhou, K., J. C. Doyle and K. Glover (1996). *Robust and Optimal Control*. Prentice Hall.

List of Symbols

$\mathbf{A_{11}}, \mathbf{A_{21}}, \mathbf{B_1}, \mathbf{B_2}$	functions defining $\mathbf{f}_1, \mathbf{f}_2$
$\mathbf{A}, \mathbf{B}$	matrices defining $\dot{\mathbf{p}}(t)$
$\mathbf{C}, \mathbf{D}$	matrices defining $\mathbf{y}(t)$
c	compressibility
$\mathcal{C}_k$	controllability matrix
d	discount factor
$\mathbf{d}$	improving direction
f_{w}	fractional flow rate of water
$\mathbf{f}_1, \mathbf{f}_2$	functions defining $\dot{\mathbf{x}}(t)$
$\mathbf{G}$	transfer function
$\hat{\mathbf{G}}$	reduced order transfer function
$\mathbf{g}$	vector of inequality constraints
$\mathbf{h}$	vector of equality constraints
H	Hamiltonian
H_∞	worst case energy norm
J	performance measure
$\bar{J}$	robust performance measure
J_{con}	minimal required input energy
J_{obs}	maximal produced output energy
k	absolute permeability
k_r	relative permeability
$l_1, \mathbf{l}_2, \psi$	functions defining J
$\mathcal{L}^1_m$	space of m-valued absolute-integrable functions
L	number of regularized parameters
M	number of uncertain physical parameters
n	number of time-steps in history matching
N	total number of grid blocks
N_x	number of grid blocks in x-direction
N_y	number of grid blocks in y-direction
$\mathcal{N}$	set of grid block indices
$N_{\max}$	maximum number of identifiable parameters
$N_{\mathbf{u}}$	number of manipulated inputs
$N_{\mathbf{y}}$	number of measured outputs
$\mathcal{O}_k$	observability matrix
p	pressure

p^j	pressure in grid block j
$\mathbf{p}$	vector of grid block pressures
$\mathbf{p}_k$	vector of grid block pressures at time-step k
$\hat{\mathbf{p}}_k$	transformed vector of grid block pressures at time-step k
$\mathbf{P}_\mathbf{y}, \mathbf{P}_{\boldsymbol{\theta}}$	weighting matrices
$\mathcal{P}$	controllability Gramian
$\mathcal{Q}$	observability Gramian
q	source / sink term
r	cost per unit volume
r_w	wellbore radius
S	saturation
s^j	water saturation in grid block j
$\mathbf{s}$	vector of grid block water saturations
t	time
T	terminal time
$\mathbf{T}$	transformation matrix
$\bar{u}$	superficial velocity
$\mathbf{u}$	vector of manipulated inputs
$\mathbf{u}_k$	vector of manipulated inputs at time-step k
$\mathcal{U}$	set of allowable controls
v	grid block volume
V	history match cost function
w	well index
$\mathbb{X}^\mathrm{con}$	controllable subspace
$\mathbb{X}^\mathrm{unobs}$	unobservable subspace
$\mathbf{x}$	state vector
$\mathbf{y}$	vector of measured outputs
$\mathbf{y}_k$	vector of measured outputs at time-step k
$\mathbf{z}$	well configuration (vector of well locations)
$\mathcal{Z}$	set of possible well configurations

$_\mathrm{av}$	average
$_\mathrm{bhp}$	bottom-hole pressure
$_\mathrm{init}$	initial
$_\mathrm{inj,\,prod}$	injection, production
$_\mathrm{min,\,max}$	minimum, maximum
$_\mathrm{no}$	nominal
$_\mathrm{npv}$	net present value
$_\mathrm{o,\,w}$	oil, water
$_\mathrm{opt}$	optimization
$_\mathrm{re}$	reactive
$_\mathrm{rf}$	recovery factor
$_\mathrm{ro}$	robust
$_\mathrm{up}$	updated
$_\mathrm{val}$	validation
$_\mathrm{wc}$	worst-case

α	valve setting
$\boldsymbol{\alpha}$	vector of regularized parameters
$\boldsymbol{\beta}$	vector of switching functions
δ^k	step size at iteration k
ϵ	scaling factor
θ_i	uncertain physical parameter
$\boldsymbol{\theta}$	vector of uncertain physical parameters
Θ	set of realizations
λ	eigenvalue
$\boldsymbol{\lambda}$	adjoint vector
μ	viscosity
ρ	density
σ_k	k^{th} Hankel singular value
$\boldsymbol{\tau}$	bang-bang vector of switching times
ϕ	porosity
$\boldsymbol{\Phi}$	regularization matrix
φ	function defining $\bar{J}$
Δt	discretization time-step
$\nabla\cdot$	divergence operator
∇	gradient operator

List of Publications

Accepted and submitted journal papers

van Essen, G. M., Zandvliet, M. J., Van den Hof, P. M. J., Bosgra, O. H., and Jansen, J. D. (2007). Robust waterflooding optimization of multiple geological scenarios. *submitted to SPE Journal*.

Zandvliet, M. J., Bosgra, O. H., Jansen, J. D., Van den Hof, P. M. J., and Kraaijevanger, J. F. B. M. (2007). Bang-bang control and singular arcs in reservoir flooding. *Journal of Petroleum Science and Engineering* **58**, 186–200.

Zandvliet, M. J., Handels, M., Brouwer, D. R., Jansen, J. D., van Essen, G.M. (2008a). Adjoint based well placement optimization under production constraints. *accepted for publication in SPE Journal*.

Zandvliet, M. J., Van Doren, J. F. M., Bosgra, O. H., Jansen, J. D., and Van den Hof, P. M. J. (2008b). Controllability, observability and identifiability in reservoir engineering. *submitted to Computational Geosciences*.

Technical reports

van Essen, G. M., and Zandvliet, M. J. (2007). St. Joseph Waterflooding Optimization Study. *Shell Internation Exploration and Production*, Technical report EP-2007-5030 (restricted).

Conference proceedings

Handels, M., Zandvliet, M. J., Brouwer, D. R., and Jansen, J. D. (2007). Adjoint based well placement optimization under production constraints. In *SPE Reservoir Simulation Symposium (SPE 105797)*, Houston.

van Essen, G. M., Zandvliet, M. J., Van den Hof, P. M. J., Bosgra, O. H., and Jansen, J. D. (2006). Robust optimization of oil reservoir flooding. In *IEEE International Conference on Control Applications*, Munich.

van Essen, G. M., Zandvliet, M. J., Van den Hof, P. M. J., Bosgra, O. H., and Jansen, J. D. (2006). Robust waterflooding optimization of multiple geological scenarios. In *SPE Annual Technical Conference and Exhibition (SPE 102913)*, San Antonio.

Zandvliet, M. J., Scherer, C. W., Hol, C. W. J., and van de Wal, M. M. J. (2004). Multi-objective $\mathcal{H}_\infty$ control applied to a wafer stage model. In *IEEE Conference on Decision and Control*, Bahamas.

Zandvliet, M. J., Bosgra, O. H., Van den Hof, P. M. J., Jansen, J. D., and Kraaijevanger, J. F. B. M. (2006). Bang-bang control in reservoir flooding. In *10^{th} European Conference on the Mathematics of Oil Recovery*, Amsterdam.

Summary

The coming years there is a need to increase production from petroleum reservoirs, and there is an enormous potential to do so by increasing the recovery factor. This is possible by making better use of recent technological developments, such as horizontal wells, downhole valves and sensors. However, actually making better use of these improved capabilities is difficult because of many open problems in reservoir management and production operations processes. Consequently, there is significant scope to increase the recovery factor of oil and gas fields by tailoring tools from the systems and control community to *efficiently* perform dynamic optimization of wells (*e.g.* number, locations) and their production settings (*e.g.* bottom-hole pressures, flow rates, valve settings) based on uncertain reservoir models, in the sense that they lead to good decisions while requiring limited time from the user. This thesis aims at developing these tools, and the main contributions are as follows.

Optimal control of production settings

Many production setting optimization problems can be written as optimal control problems that are linear in the control. If the only constraints are upper and lower bounds on the control, these problems can be expected to have pure bang-bang optimal solutions. In situations where the optimal solutions are not purely bang-bang but also smooth (*i.e.* containing so-called singular arcs), it is shown that pure bang-bang solutions exist which are only slightly suboptimal. This has obvious practical implications, since bang-bang solutions can be implemented with simple on-off control valves.

Robust control of production settings

The adjoint method to derive gradients of a cost function with respect to production settings can be combined with robust optimization to efficiently compute settings that are robust against uncertainty in reservoir models. A water flooding application demonstrates that production settings can be found that are robust against uncertainty as defined by an entire class of models within a geological structure, by optimizing over one set of 100 realizations of the permeability distribution, and validating over a second set of 100 realizations.

Optimal well placement

The type of production settings (*e.g.* reactive versus constant) significantly effect the well placement problem, in that a well configuration that is optimal when the wells are operated with one type of settings may be far from optimal when the wells are operated with another type of settings. Furthermore, the gradients used in production setting optimization can be used to efficiently compute directions in which to iteratively improve upon an initial well configuration by surrounding the to-be-placed wells by pseudo wells (*i.e.* wells that operate at a negligible rate).

Controllability, observability and identifiability of reservoir models

The most controllable and observable pressures in single-phase flow reservoir models can be computed by performing an eigenvalue decomposition of the controllability and observability Gramians. By projecting the eigenvectors corresponding to the largest absolute eigenvalues of the Gramians onto the model grid, we can interpret how the reservoir model's controllability and observability properties vary over space. It turns out that pressures near wells in which we can control the flow rate or bottom-hole pressure are controllable, whereas pressures near wells in which we can measure the flow rate or bottom-hole pressure are observable. Furthermore, the controllability and observability properties are determined by the well configuration (*i.e.* the number and location of wells) and to a lesser extent by the heterogeneity of the reservoir at hand. The Hankel singular values of single-phase flow reservoir models decrease rapidly, indicating that they behave as models of much lower order. This severely limits the number of identifiable parameters. From the systems and control literature an upper bound $N_{\max}$ for the maximum number of identifiable parameters is given. It is shown that if the vector of to-be-estimated parameters contains the N grid block permeabilities, then $N_{\max} \ll N$ and the model structure is not identifiable. Furthermore, by inspecting how the controllable and observable part of a reservoir model depends on permeability, it is shown that the relevant spatial patterns of permeability strongly resemble the relevant spatial patterns of pressure. Consequently, a new method of regularization is to re-parameterize permeability through a linear combination of the most relevant spatial patterns of pressure. A history matching example shows that this controllability and observability-based regularization leads to good results.

Samenvatting

De behoefte bestaat om in de komende jaren de productie van petroleum reservoirs te vergroten. Een belangrijke mogelijkheid hiertoe wordt geboden door het toepassen van recente technologische ontwikkelingen, zoals horizontale putten en ondergrondse kleppen en sensoren, voor het verhogen van de winningsfactor. Deze toepassing wordt echter beperkt door vele open vraagstukken in reservoir management en productie-optimalisatie. Zodoende kan de winningsfactor significant verbeterd worden door het efficiënt toepassen van meet- en regeltechnieken op onzekere modellen met betrekking tot het dynamisch optimaliseren van putten (bijvoorbeeld aantal en locatie) en bijbehorende productiestanden (bijvoorbeeld drukken, debieten, en kleppen). Optimalisatie-tools moeten de mogelijkheid creëren om de juiste beslissingen te nemen binnen een beperkte tijd. Dit proefschrift heeft het doel om deze tools te ontwikkelen. De belangrijkste bevindingen worden hieronder beschreven.

Optimale aansturing van productiestanden

Het optimaliseren van productiestanden kan vertaald worden naar een 'optimal control' probleem, dat lineair is in de aansturing. Als de enige beperkingen onderen bovengrenzen op de aansturing zijn, kan men verwachten dat voor een dergelijk probleem de optimale oplossing zuiver 'bang-bang' (aan-uit) is. In de gevallen waar de optimale oplossing niet zuiver bang-bang is, maar zogenaamde 'singular arcs' bevat, kunnen we een zuivere bang-bang oplossing vinden, die slechts zeer beperkt suboptimaal is. Dit biedt concrete toepassingsmogelijkheden, aangezien bang-bang oplossingen met simpele aan-uit kleppen kunnen worden gerealiseerd.

Robuuste aansturing van productiestanden

De adjoint-methode voor het bepalen van de gradiënten van een kostenfunctie met betrekking tot productiestanden kan gecombineerd worden met robuuste optimalisatie, om zo productiestanden te vinden die robuust zijn tegen onzekerheid in reservoirmodellen. Een 'waterflooding' voorbeeld laat zien dat productiestanden kunnen worden gevonden, die robuust zijn tegen modelonzekerheid, wanneer deze gedefinieerd wordt door een verzameling modellen binnen een geologische structuur. Hiertoe is geoptimaliseerd over een verzameling van hon-

derd realisaties van de permeabiliteit en gevalideerd over een tweede verzameling van honderd realisaties.

Optimale plaatsing van putten

Het type productiestanden (bijvoorbeeld reactief versus constant) heeft significante invloed op de optimale plaatsing van putten; een putconfiguratie kan optimaal zijn voor het ene type standen, maar verre van optimaal voor het andere. Daarnaast kunnen de gradiënten voor het optimaliseren van productiestanden gebruikt worden om richtingen te bepalen voor het iteratief verbeteren van een initiële putconfiguratie. De te plaatsen putten worden hiertoe omringt door zogenaamde pseudoputten, dat wil zeggen putten met een verwaarloosbaar debiet.

Regelbaarheid, waarneembaarheid en identificeerbaarheid van reservoirmodellen

De meest regelbare en waarneembare drukken in één-fase reservoirmodellen kunnen worden berekend door een eigenwaarden-decompositie van de regelbaarheids- en de waarneembaarheids-Gramiaan. Door de eigenvectoren van de grootse absolute eigenwaarden van de Gramianen te projecteren op het modelraster, kan men interpreteren hoe de regelbaarheids- en waarneembaarheidseigenschappen van een reservoirmodel verschillen in de ruimte. Het blijkt dat drukken regelbaar zijn in de buurt van putten, waar men de debieten of drukken kan aansturen. Bovendien blijkt dat drukken waarneembaar zijn in de buurt van putten, waar men drukken of debieten kan meten. Daarnaast worden de regelbaarheids- en waarneembaarheidseigenschappen bepaald door de putconfiguratie en, in mindere mate, door de heterogeniteit van het betreffende reservoir. De Hankel singuliere waarden van één-fase reservoirmodellen nemen snel af, waardoor zij zich als modellen van een veel lagere orde gedragen. Dit beperkt in grote mate het aantal identificeerbare parameters. Vanuit de meet- en regeltechniek wordt een bovengrens $N_{\max}$ voor het aantal identificeerbare parameters gegeven. Het wordt aangetoond dat $N_{\max} \ll N$ en dat het modelstructuur niet identificeerbaar is, waarneer de vector van te schatten parameters de N gridblok permeabiliteiten bevat. Door de afhankelijkheid van het regelbare en waarneembare deel van een reservoirmodel ten opzichte van de permeabiliteit te analyseren, kan worden aangetoond dat de relevante ruimtelijke patronen van permeabiliteit sterk overeenkomen met de relevante ruimtelijke patronen van drukken. Zodoende bestaat er een methode voor regularisatie door het opnieuw parametriseren van de permeabiliteit in de vorm van een lineaire combinatie van de meest relevante ruimtelijke patronen van drukken. Een 'history matching' voorbeeld toont aan dat deze op regelbaarheid en waarneembaarheid gebaseerde regularisatie tot goede resultaten leidt.

About the author

Maarten Johan Zandvliet was born on February 12, 1978 in Washington D.C., USA. He finished his pre-university school (VWO) in 1996 at the Vrijzinnig-Christelijk Lyceum in The Hague. In August 1996 he started his study Mechanical Engineering at Delft University of Technology, where he graduated in September 2003 in Systems and Control. From December 2003 to January 2008 he was a PhD student jointly at the Delft Center for Systems and Control and the Department of Petroleum Engineering, where he conducted his research within the sponsored VALUE and ISAPP projects. The results of this research are reported in this thesis. In February 2008 he started working as a reservoir engineer at the well and reservoir management department of Shell International Exploration and Production.